UNIVERSITAT DE BARCELONA

CPEB2 in mammary gland homeostasis and breast cáncer

Rosa Pascual Domingo

UNIVERSITAT DE
BARCELONA

Universitat de Barcelona
Facultat de Farmàcia
IRB Barcelona
Programa de Doctorat en Biomedicina

CPEB2 in mammary gland homeostasis and breast cancer

Aquesta tesi ha estat realitzada per Rosa Pascual Domingo sota la direcció del Dr. Raúl Méndez de la Iglesia, Professor d'Investigació ICREA a l'Institut de Recerca Biomèdica (IRB) Barcelona. Es presenta aquesta memòria per optar al títol de doctor per la Universitat de Barcelona en el Programa de Doctorat en Biomedicina.

Raúl Méndez de la Iglesia	Antonio Zorzano Olarte	Rosa Pascual Domingo
Director de tesi	Tutor de tesi	Doctoranda

Barcelona, 2018

A mons pares,

Index

Abbreviations

APA	alternative polyadenylation
CK	cytokeratin
CPE	cytoplasmic polyadenylation element
CPEBs	cytoplasmic polyadenylation binding proteins
CPSF	cleavage and polyadenylation specific factor
CTD	C-terminal domain
DMBA	7,12-dimethylbenz(a)anthracene
DSE	downstream sequence element
ECM	extracellular matrix
eIFs	eukaryotic initiation factors
EMT	epithelial-mesenchymal transition
Eph	ephrin receptor
ER	estrogen receptor α
ES cells	embryonic stem cells
FC	fold change
HER2	human epidermal growth factor receptor 2
HR	homologous recombination
IGV	integrated genomic viewer
IHC	immunohistochemistry
IRES	internal ribosomal entry sites
KO	*knock-out*
MaSC	mammary stem cell
MECs	mammary epithelial cells
MMPs	matrix metalloproteinases

MPA	medroxyprogesterone
mRNA	messenger RNA
mRNPs	ribonucleoprotein particles
MRUs	mammary repopulating units
mTOR	mammalian target of rapamycin
NTD	N-terminal domain
OPG	osteoprotegerin
PABP	poly(A) binding protein
PAS	polyadenylation signal
PCA	principal component analysis
PR	progesterore receptor
Pre-mRNA	precursor messenger RNAs
RANK	receptor activator of nuclear factor-κB
RBP	RNA Binding protein
RIP	RNA-immunoprecipitation
RNAP II	RNA polymerase II
RRMs	RNA-recognition motifs
TIC	tumor-initiating cell
TNBC	triple-negative breast cancers
uORFs	upstream open reading frames
UPR	unfolded protein response
UTRs	unstranslated regions
VEGF	vascular endothelial growth factor
vs.	*versus*
WT	*wild-type*

Abstract

The mammary gland develops postnatally and is remodeled, during each estrous cycle and pregnancy, through very dynamic expansions and involutions of the polarized epithelial tree. Thus, the mammary gland requires a fine-regulated balance between proliferation and differentiation, which is disrupted in breast tumors. How translational control contributes to mammary gland homeostasis and tumorigenesis remains largely unexplored. The CPEB-family (Cytoplasmic Polyadenylation Element Binding) of RNA-binding proteins regulates, temporarily and spatially, the translation and subcellular localization of CPEB-bound mRNAs, accounting for up to 25 % of the genome.

Herein we present a systematic study of the four members of the CPEB-family (CPEB1-4) in the context of the adult mammary gland, using *knock-out* (KO) models for all four CPEBs. We found that the lack of CPEB2 results in defects in mammary gland branching and lineage specification. Interestingly, CPEB2 depletion also has consequences for breast tumorigenesis. Moreover, were able to identify the target mRNAs bound by CPEB2 in mammary epithelial cells and to establish a molecular mechanism by which CPEB2 regulates mammary gland homeostasis and breast cancer development.

Altogether, this work unravels a novel translational mechanism regulating cell fate in the mammary gland and breast tumor development.

Introduction

1 Post-transcriptional regulation of gene expression

The cell is an exquisite set of complex gears that are tightly coordinated to allow proper performance. Which are the mechanisms ensuring correct functioning at the cellular, tissue and organism levels? How is the cellular machinery able to sense and adapt to environmental cues? These are long-standing and fascinating questions in biology and the central dogma of molecular biology (Crick, 1958, 1970) provided a framework to answer such questions, describing the flow of genetic information from genes to proteins that still prevails nowadays (Figure 1).

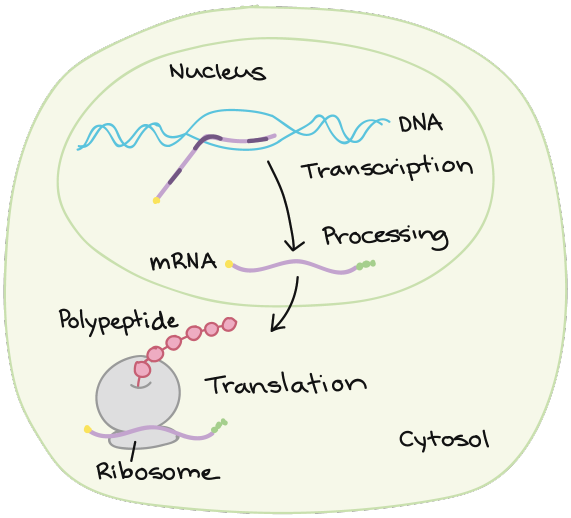

Figure 1: Simplification of the central dogma of molecular biology. This image shows how genes are transcribed to mRNA in the nucleus, processed for nuclear export and then translated in the cytoplasm (cytosol). From *khanacademy.org*.

To cope with physiological and environmental demands, the program of gene expression is a network that is heavily interconnected and tightly regulated at many levels, from transcription to translation (Moore, 2005; Orphanides, 2002). However, for historical reasons, much more effort has been devoted to the study of transcription and complex transcriptional regulatory circuits have been described in the context of development, physiology and malignancy (Ihmels et al., 2002; Segal et al., 2003). Nevertheless, potent global approaches to study post-transcriptional gene regulation have been emerging in the last years; consequently, integration of this data allowed the identification of RNAs bound by specific RNA-biding proteins (RBPs) as well as the analysis of the translation status of each messenger RNA (mRNA) (Halbeisen et al., 2008). In addition, the number of RBPs has greatly expanded thanks to recent proteome-wide studies (Hentze et al., 2018). Accordingly, RBPs, which modulate every step in the life of an mRNA, have arisen as major

regulators of gene expression with paramount functions in physiological and pathological processes. Moreover, each single RBP can bind hundreds of mRNAs, forming extensive networks in which functionally related genes may be co-regulated, representing "RNA regulons" (Morris et al., 2010). In this section we will introduce concepts related to mRNA processing and translation that are helpful for a better comprehension of the molecular mechanism of the CPEB-family of RNA-binding proteins.

1.1 The journey of the mRNA from the nucleus to the cytoplasm

As soon as the precursor messenger RNA (pre-mRNA) is formed, it is bound by RBPs forming ribonucleoprotein particles (mRNPs) that will mediate diverse processing reactions to obtain a competent mRNA. The mature mRNA consists of a polynucleotide chain that contains the coding sequencing (CDS), that determines the aminoacid sequence of the coded protein, flanked by the 3' and 5' unstranslated regions (UTRs) which are encoded by exons but do not codify for proteins (Figure 2).

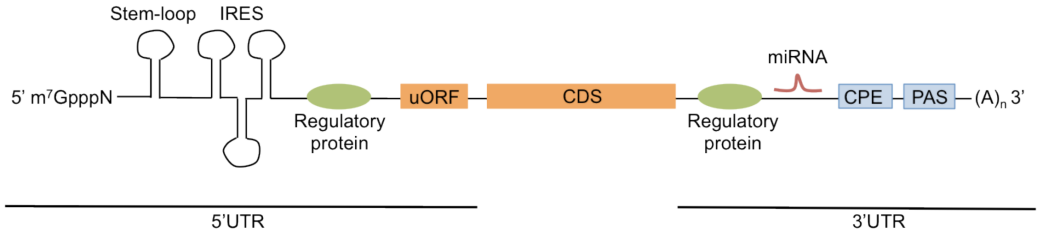

Figure 2: General structure of a mature messenger RNA (mRNA) and its *cis*-regulatory elements (see section 1.2.1). In the 5'UTR we can find the cap structure (m^7GpppN or m^7G cap), a stem-loop that can negatively affect translation, an IRES that mediate cap-independent translation as well as uORFs that in normal conditions reduce translation of the main coding sequence (CDS). Both the 5' and the 3' UTRs can contain *cis*-acting elements that will be bound by RBPs (in green) that regulate mRNA fate. The 3'UTR can be targeted by microRNAs (miRNAs) that repress translation. Cytoplasmic polyadenylation elements (CPEs), the poly(A) signal (PAS) and the poly(A) tail are also depicted. IRES, internal Ribosomal Entry Site; uORFs, upstream Open Reading Frames. From Jordina Guillén-Boixet, a former PhD student at Raúl Méndez laboratory.

Protein-coding genes are transcribed by RNA polymerase II (RNAP II) and they are modified co-transcriptionally by 5'end capping, splicing as well as 3'end cleavage and polyadenylation. The C-terminal domain (CTD) of the largest subunit of RNAP II acts as a loading platform for factors involved in pre-mRNA processing (Aguilera, 2005). Moreover, the nascent RNA is coated with RBPs that give specificity to the processing and ensure mRNA integrity, export and downstream cytoplasmic steps. If mRNPs are not properly assembled, the mRNA will be retained in the nucleus and degraded.

First, as soon as nascent mRNA reaches a length of 22-25 nucleotides, 5'end capping occurs. Three consecutive enzymatic reactions on the pre-mRNA results in a mature methylated cap structure in the 5'end (so-called 7-methylguanosine or m^7G cap) (Topisirovic et al., 2011). Importantly, this modification is required for nuclear export, prevention of 5' to 3' exonucleotide degradation as well as being essential for cap-dependent translation (see section 1.2).

Additionally, splicing is also essential for a pre-mRNA to become a functional and mature mRNA. Thus, a ribonucleoprotein complex called the spliceosome mediates the removal of the introns and the ligation of the flanking exons together. As a result, several protein isoforms can be obtained from a single gene by inclusion or exclusion of different exons, hence expanding the genomic information density and increasing the regulatory possibilities of gene expression. This procedure is named alternative splicing and its importance is underlined by the fact that more than 90 % of human genes are alternative spliced (Papasaikas & Valcárcel, 2016).

Last but not least, eukaryotic pre-mRNAs (with exception of canonical histone mRNAs) experience 3'end cleavage and polyadenylation before transcripts are exported from the nucleus to the cytoplasm. This processing takes place in a two-step reaction that involves an endonucleolytic cleavage of the pre-mRNA followed by the addition of a polyadenosine stretch at the 3'end (Di Giammartino et al., 2011; Wahle & Rüegsegger, 1999). The reaction depends on the presence of three sequences; the Poly(A) signal (PAS or hexanucleotide, A(A/U)UAAA) located 10-30 nucleotides upstream of the cleavage site, the cleavage site itself and the U/GU rich downstream sequence element (DSE) (Proudfoot, 2011). These elements harbored by the pre-mRNA are bound by RBPs that act cooperatively to accomplish 3'end cleavage and polyadenylation. Thus, the PAS is bound by the cleavage and polyadenylation specific factor (CPSF) and the DSE is recognized by the cleavage stimulation factor (CstF). These proteins, together with the cleavage factor I and II (CFI and CFII), form a complex that specify and catalyze the cleavage. Then, CPSF recruits the poly(A) polymerase that synthesize a poly(A) tail of approximately 250 adenosines, which is coated with poly(A) binding proteins (PABP) in order prevent degradation and to promote both nuclear export and translation (Proudfoot, 2011).

Furthermore, similar to alternative splicing, also alternative polyadenylation (APA) can occur in the nucleus (Di Giammartino et al., 2011). Accordingly, a single gene can encode

for multiple RNA transcripts that have the same coding sequence but differ on their 3'UTR. More than half of the human genes undergo APA and, from an evolutionary point of view, it is clear that more complex organisms have enhanced post-transcriptional regulation by 3'UTR elements (Mayr, 2016). Multiple UTRs create another layer of regulation by including or excluding *cis*-acting elements in 3'UTRs that will result in changes in mRNA stability, translation efficiency, mRNA localization or protein-protein interaction (Bava et al., 2013; Berkovits & Mayr, 2015; Mayr, 2016).

Finally, mature transcripts are exported through nuclear pores to the cytoplasm where they may undergo localization to subcellular regions, degradation by decay pathways or translation. The aforementioned mRNA fates are mostly determined by regulatory elements clustered in the UTRs (see section 1.2.1).

1.2 Translation initiation and formation of the closed-loop mRNP

Protein synthesis is mainly regulated at the initiation step (rather than during elongation or termination); this means that recruitment of the ribosomal machinery is basically the limiting step of translational efficiency. The relevance of translation initiation is underscored by the fact that, while the elongation and termination phases are assisted by a limited set of dedicated factors, translation initiation in eukaryotes is a complex event that is assisted by more than 25 polypeptides (Gebauer & Hentze, 2004).

Translation of most eukaryotic mRNAs occurs in a cap-dependent fashion, meaning that it is initiated by ribosome recruitment through the m^7G cap structure and then followed by ribosome scanning towards a start codon. The first step of translation initiation is the assembly of the trimeric eukaryotic initiation factors 4F (eIF4F) complex at the 5'cap; the eIF4F complex is composed of the DEAD-box RNA helicase eIF4A, the cap-binding protein eIF4E and the scaffolding protein eIF4G. The helicase eIF4A is thought to be crucial for unwinding RNA secondary structures and therefore preparing a clear path for ribosome scanning (Parsyan et al., 2011). Through its interaction with eIF3, eIF4G recruits the 43S pre-initiation complex (Figure 3 step 1), which consists of the aforementioned eIF3, the 40S small ribosomal subunit, eukaryotic initiation factors (eIF1, eIF1A, eIF5, eIF3) and the ternary complex of GTP-bound eIF2 plus the initiator methionine transfer RNA ($Met\text{-}tRNA_i^{Met}$) (Gebauer & Hentze, 2004; Gray & Wickens, 1998; Leppek et al., 2017; Sonenberg & Hinnebusch, 2009).

Importantly, the PABP bound to the 3' poly(A) tail interacts with eIF4G at the cap, thereby circularizing the mRNA (Sachs et al., 1997; Tarun & Sachs, 1995). This conformation, known as the closed-loop, enhances ribosome recycling, as well as mRNA stability and translation (Amrani et al., 2008; Uchida et al., 2002). Therefore, a deadenylated mRNA becomes translationally inactive and it is prone to degradation.

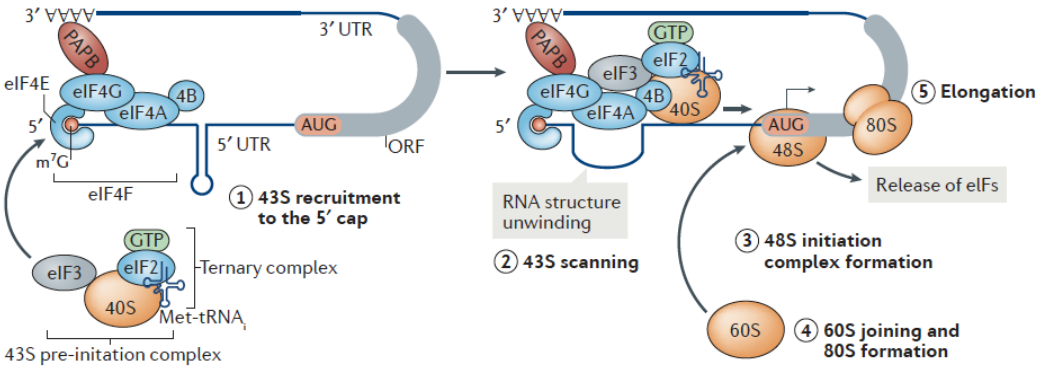

Figure 3: Mechanism for canonical cap-dependent translation initiation. The main steps of translation initiation are depicted in this illustration from (Leppek et al., 2017). Step 1, 43S pre-initiation complex recruitment to the 5' cap thanks to the interaction with the scaffolding protein eIF4G that also interacts with PABP thereby circularizing the mRNA (closed-loop model). Step 2, 43S scanning along the 5' UTR until the start codon. Step 3, 48S initiation complex formation. Step 4, generation of the elongation competent 80S ribosome by the joining of the 60S large subunit. Step 5, elongation of the polypeptide while the assembled ribosome travels through the CDS (also called ORF, open reading frame).

Once the 43S pre-initiation complex has bound the mRNA near the cap, it scans in a 5' to 3' direction until reaching the initiation codon in an ATP-dependent manner (Figure 3 Step 2). Stable binding of the 43S complex at the start codon yields the formation of the 48S initiation complex (Figure 3 Step 3) and triggers GTP hydrolysis, release of eIFs and subsequent joining of the 60S large ribosomal subunit to the 48S subunit in order to form the elongation-competent 80S ribosome, which proceeds to translation elongation (Figure 3 Steps 4 and 5) (Gebauer & Hentze, 2004; Gray & Wickens, 1998; Leppek et al., 2017; Sonenberg & Hinnebusch, 2009). Then, the assembled ribosomes travel through the coding region aided by elongation factors (eEFs) while synthesizing the encoded polypeptide. At the termination codon, peptide chain-releasing factors (eRFs) are required to release the polypeptide from the ribosome (Dever & Green, 2015).

1.2.1 Regulation of translation by *cis*-acting element

As briefly mentioned earlier, elements present in the UTRs can greatly influence the translation efficiency of mRNAs (Figure 2). On the one hand, in the 5'UTR we can find specific binding sites for regulatory proteins and also secondary RNA structures that hinder cap-dependent translation (Gray & Wickens, 1998). Moreover, some cellular mRNAs harbor internal ribosomal entry sites (IRES) that enable them to be translated in a cap-independent fashion; IRES-containing mRNAs can be favored for translation when cap-dependent translation is diminished (Leppek et al., 2017). In a similar way, 5'UTRs can also contain upstream open reading frames (uORFs). Despite the fact that, in general, uORFs prevent translation from the main start codon by recruiting ribosomes more upstream, they aid translation of the main ORF under stress conditions where eIF2α gets phosphorylated and the ternary complex cannot be assembled (Sonenberg & Hinnebusch, 2009). On the other hand, the 3'UTR contains both microRNAs binding sites, which can repress translation, as well as specific binding sites for RBPs that can affect stability, localization or efficiency of translation (Gebauer & Hentze, 2004). This thesis focuses on the study of a family of RNA-binding proteins named CPEBs that bind a specific element in the 3'UTR present in certain mRNAs; whereby regulating cytoplasmic polyadenylation and, thus, translation of those mRNAs.

1.3 CPEBs: cytoplasmic polyadenylation element binding proteins

The cytoplasmic polyadenylation element binding (CPEB) proteins are sequence-specific mRNA-binding proteins that regulate cytoplasmic polyadenylation. Even though we have seen that the addition of a poly(A) tail seems to happen by default in the nucleus, this structure is very dynamic and its length is tightly regulated in the cytoplasm. Specifically, length of the poly(A) tail can be modified post-transcriptionally by non-canonical poly(A) polymerases and deadenylases. Considering that the poly(A) tail acts synergistically with the 5'cap facilitating translation initiation through stabilization of the closed-loop mRNP (see section 1.2), the modulation of the poly(A) tail contributes to the stability, transport and translation of mature mRNAs. Notably, some deadenylated mRNAs may not be degraded but stored in a translationally dormant state instead. Then, in response to cellular cues, they may undergo cytoplasmic polyadenylation which enhances translation. Therefore, cytoplasmic polyadenylation is a fast and reversible mechanism for regulating translation, allowing for quick responses to environmental changes (Weill et al., 2012).

Cytoplasmic polyadenylation requires two *cis*-acting sequences in the 3'UTR: the cytoplasmic polyadenylation element (CPE, consensus sequence UUUUUA$_{1-2}$U) recognized by the CPEBs, and the PAS (the conserved hexanucleotide A(A/U)UAAA) bound by CPSF. These elements must be closer than 100 nucleotides for cytoplasmic polyadenylation to take place, being the optimal distance 25 nucleotides (Piqué et al., 2008). Remarkably, CPEBs can potentially regulate 25 % of the human genome (Belloc & Méndez, 2008; Piqué et al., 2008).

1.3.1 The CPEB-family of proteins

The CPEB-family of RNA-binding proteins is composed of four members in vertebrates (CPEB1-4); differentially, in *Drosophila Melanogaster*, there are two CPEB orthologs (Orb and Orb2) (Fernández-Miranda & Méndez, 2012; Ivshina et al., 2014) (Figure 4). Within the CPEB-family, there are two subfamilies based on sequence identity of the RNA recognition motifs: CPEB1 and CPEB2-4 (Figure 4). CPEB proteins share the same RNA-binding C-terminal domain (CTD), while they differ on their unstructured regulatory N-terminal domain (NTD) (Figure 5). This fact has two significant implications: CPEBs can bind overlapping target mRNAs by recognizing CPEs in the 3'UTR (Afroz et al., 2014); however, they are regulated by different post-transcriptional modifications at the NTD that will be triggered by distinct signaling pathways. Therefore, CPEB proteins could compete against one another for the binding, act sequentially on the same target mRNA or even compensate the loss of one member of the CPEB-family (Drisaldi et al., 2015; Mendez et al., 2000a,b; Theis et al., 2003; Guillén-Boixet et al., 2016; Igea & Méndez, 2010). Also, there are alternatively spliced isoforms for the CPEBs but their biological relevance is unkown.

Two RNA-recognition motifs (RRMs) in tandem followed by a zinc-binding domain (ZZ-domain) form the highly conserved CTD that confers RNA-binding properties to the CPEBS. Even so, it has been suggested that the higher structured CTD of CPEB1 enables the recognition of "non-consensus" CPEs with higher affinity (Afroz et al., 2014). In contrast, the NTD is highly variable and it is modified by different enzymes and upon different stimuli for each CPEB (Figure 5). Notably, CPEBs play a dual role in mRNA translational regulation, being able to either promote or prevent polyadenylation (and subsequent mRNA translation) depending on the recruited partners. Post-transcriptional modifications in the NTD will determine the activation/repression status of the CPEBs. Historically, meiotic progression

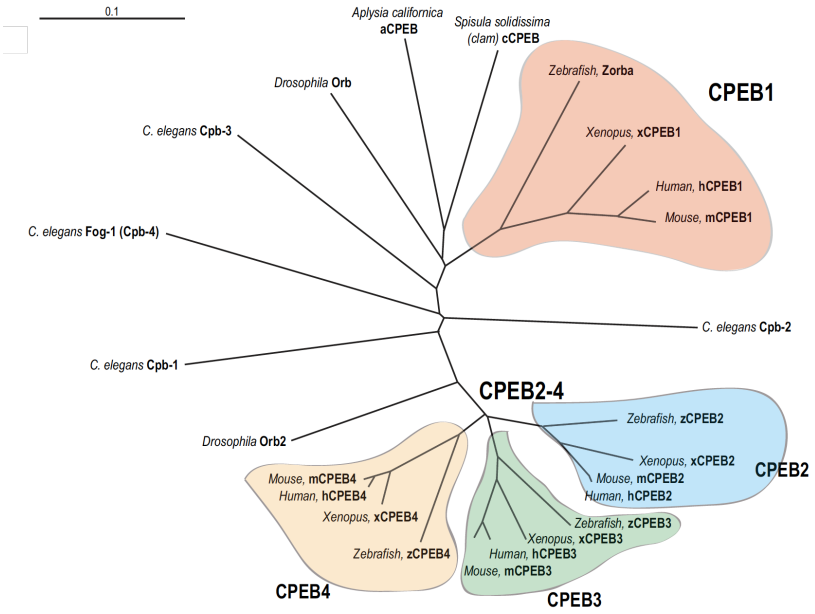

Figure 4: Unrooted phylogenetic tree of the most representative CPEB proteins. CPEB1 vertebrate orthologs (red balloon) are the most distant members of the family; whereas vertebrates CPEB2 (blue), CPEB3 (green) and CPEB4 (yellow) are closer. From (Fernández-Miranda & Méndez, 2012).

of *Xenopus laevis* oocytes has been during years the framework for identifying such modifications and studying their effect on CPEB-target mRNAs (Mendez & Richter, 2001).

1.3.2 Regulation and functions of the CPEBs

In the case of CPEB1, its phosphorylation status determines whether it activates or represses the translation of a given target mRNA. When unphosphorylated, CPEB1 represses translation by recruiting a complex that promotes poly(A) tail shortening. The identity of these partners remains poorly defined since the three suggested models are mutually exclusive. In these models, CPEB could either recruit the deadenylase PARN outcompeting the action of the cytosolic poly(A)-polymerase Gld2 (Figure 6 Model 1) (Kim & Richter, 2006) or inhibit ribosomal recruitment by bringing either Maskin (Figure 6 Model 2) or eIF4E-T (Figure 6 Model 3), which are both eIF4E binding proteins that would hamper the formation of the eIF4F complex (Stebbins-Boaz et al., 1999). The activating mechanism of CPEB1 occurs upon progesterone stimulation in *Xenopus laevis* oocytes; a single phosphorylation by Aurora A kinase remodels the CPEB1-complex allowing Gld2 to extend the poly(A) tail (Kim & Richter, 2006; Mendez et al., 2000a,b). Further phosphorylation of CPEB, by both Cdk1 and PlK1, targets it for degradation through a PEST-box domain (Mendez et al., 2002; Reverte et al., 2001) (Figure 5).

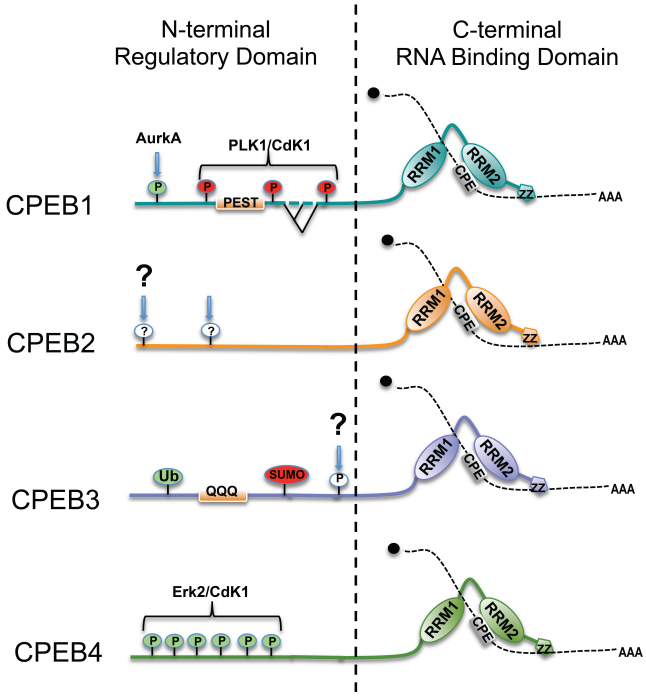

Figure 5: Schematic view of the CPEB family of RNA-binding proteins. The protein domains of the CPEBs, the known post-transcriptional modifications (P, phosphorylation; Ub, ubiquitination; SUMO, SUMOylation; QQQ, poly-glutamine stretch) as well as the responsible kinases are depicted in this picture. The mRNA is illustrated as a dashed black line with a 5' cap (black dot) and a 3' poly(A) tail (AAA).

Besides controlling mRNA-specific translation, CPEB1 is also crucial in order to transport mRNAs to specific subcellular locations. For instance, in dendrites, the CPEB-containing complex is bidirectionally transported along microtubules by kinesin and dynein; upon synapse stimulation, mRNAs in such complex (like CaMKII mRNA) are activated by cytoplasmic polyadenylation in the vicinity of a dendritic spine (Huang et al., 2003). Therefore, CPEBs have the ability to control translation not only in time but also in space. In this regard, CPEB1 is also crucial to localize CPE-containing mRNAs at the meiotic and mitotic spindles enabling local translation and facilitating cell cycle progression (Eliscovich et al., 2008) (Segura-Morales C.*, Pascual R.* et al; under revision). Interestingly, in addition to its role in the cytoplasm, it has been demonstrated that CPEB1 also mediates alternative 3'UTR processing in the nucleus (Bava et al., 2013).

Although the molecular mechanisms of activation and repression are not so well-defined for the other members of the CPEB family, recent work nicely demonstrated that the activation of CPEB4 also depends on its phosphorylation status. For CPEB4, hyperphosphory-

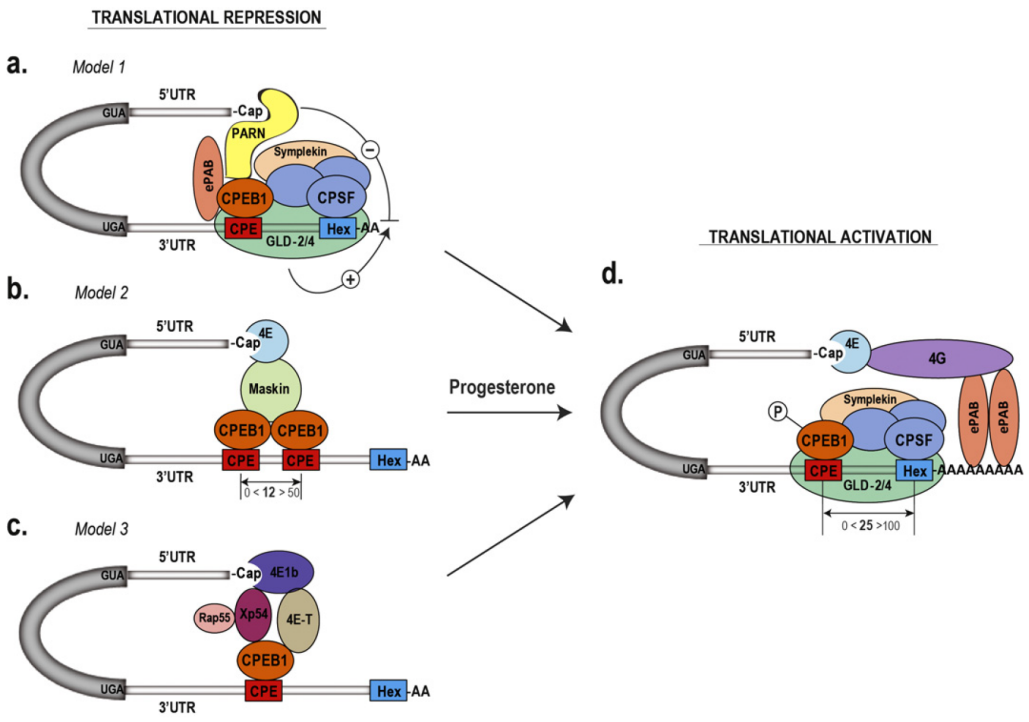

Figure 6: Mechanism for CPEB1-meditaed translational control. Schematic representation of CPEB1 repression (a-c) and activation (d) complexes. (a) Repression complex mediated by CPEB1 interaction with PARN deadenylase. (b) Repression mediated by the interaction between CPEB1 and Maskin, which binds to eIF4E. (c) Repression complex mediated by CPEB interaction with Xp54/ROCK, eIF4E-T and eIF4E1b, a decoy isoform of eIF4E. (d) Upon progesterone stimulation, CPEB is phosphorylated (P), the activation complex is formed and polyadenylation is driven by GLD2/4 polymerase. This picture also shows that two CPEs separated by an optimal distance of 12 nucleotides seem to be necessary for CPEB1-mediated repression—most probably because they favor the formation of a dimer (Piqué et al., 2008). ePAB, embryonic poly(A)-binding protein. AA indicates short poly(A) and AAAAAAAAA indicates long poly(A) tail. From (Fernández-Miranda & Méndez, 2012).

lation by ERK and Cdk1 defines its active state; while unphosphorylated CPEB4 phase separates into inactive liquid-like droplets through its intrinsically disordered regions in the NTD (Guillén-Boixet et al., 2016). CPEB4 acts as a translational activator in many scenarios such as oocyte maturation (Igea & Méndez, 2010), mitotic cell-cycle progression (Novoa et al., 2010) or angiogenesis (Calderone et al., 2016). In addition, as a consequence of harboring uORFs, *Cpeb4* mRNA translation is favored in stress conditions; upon endoplasmic reticulum stress CPEB4 coordinates hepatic unfolded protein response (UPR) by activating CPE-containing transcripts related to endoplasmic reticulum homeostasis (Maillo et al., 2017). Similar to CPEB1, CPEB4 can accumulate in the nucleus too. Nuclear localization of CPEB4 can occur in conditions of hypoxia or glucose depravation (Kan et al., 2010) but the mechanisms and functions of this localization remain still elusive.

Alternatively, the NTD of CPEB3 is rich in glutamines and forms amyloid-like aggregates that are regulated by SUMOylation and monoubiquitination (Drisaldi et al., 2015; Pavlopoulos et al., 2011). CPEB3 activation has been related to its prion-like oligomerization capacity (Stephan et al., 2015). Additionally, CPEB3 has been suggested to promote mRNA degradation (Hosoda et al., 2011) and also inhibition of transcription in the nucleus (Peng et al., 2010). Described functions for CPEB3 include those involved in learning and memory (Chao et al., 2013; Fioriti et al., 2015) and thermosensation (Fong et al., 2016).

Finally, post-transcriptional modifications that regulate the activity of CPEB2 remain to be elucidated. Together with CPEB1, CPEB2 has been shown to regulate HIF-1α (*Hif1a*) mRNA translation following insulin stimulation (Hägele et al., 2009). Moreover, recent work demonstrated that CPEB2 promotes translation by binding its target mRNAs and that it was required for long-term memory consolidation (Lu et al., 2017b). Regarding its inhibitory activities, it has been suggested that CPEB2 interacts with the elongation factor eEF2 slowing down peptide elongation to negatively regulate HIF-1α translation (Chen & Huang, 2012).

2 The mammary gland

The mammary gland produces and delivers milk from the mother to the newborn. Being the only organ after which an entire class of animals has been named, the mammary gland and the process of lactation is credited for the evolutionary success of mammals not only for the nutritional and antimicrobial properties of milk but also because the extended period of contact between mothers and offspring probably gives the opportunity for a lengthened period learning (Peaker, 2002).

2.1 From the anlage to the milk-producing organ

In all mammals, mammary glands arise from a localized thickening of the ectoderm that create the mammary placode. This thickening occurs at day 10-11 of embryonic development in mouse and at week 4 in human, and it takes place with little proliferation and it is mainly due to cell migration. However, later on, from embryonic day 16 to 21 (birth), great proliferation of the epithelial cells leads to the appearance of the mammary bud. In fe-

males, this creates a small ductal tree that consists of 10-20 canalized branches arising from a single duct attached to each nipple. The formation of the epithelial bud is also accompanied by dramatic changes in the mesoderm that will form both the mammary mesenchyme aligned around the epithelial bud, and the fat pad precursors (Cowin & Wysolmerski, 2017; Hovey et al., 2002) (Figures 7 and 8).

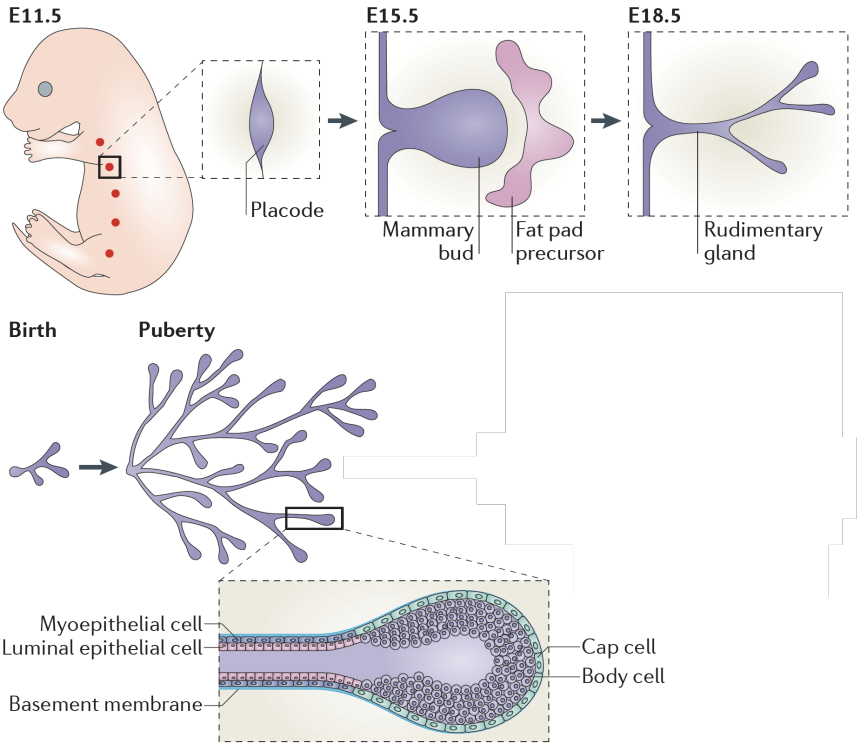

Figure 7: Mammary gland development. Scheme of mammary gland embryonic development; by embryonic day 18.5 (E18.5), a rudimentary gland is evident (upper part). During puberty, hormonal cues trigger the formation of the terminal end buds (inset). Adapted from (Gjorevski & Nelson, 2011).

After birth, the mammary gland is still a rudimental ductal tree that grows in an isometric manner; it is not until puberty that, by the action of hormones and growth factors, it fully matures and expands. Thus, the mammary gland is the only organ that it is mostly developed postnatally and, moreover, it is subjected to a lot of remodeling in every estrus cycle or in case of pregnancy (Hovey et al., 2002).

2.1.1 Pubertal mammary gland

When females are around 3-4 weeks of age, ovarian hormones, such as estrogen, impinge on the mammary gland promoting ductal elongation and lateral branching. The epithelial

ductal tree is enveloped by a basement membrane and embedded within a complex stroma (the mammary fat pad) which contains fibroblasts, adipocytes, blood vessels, nerves and various immune cells (Polyak & Kalluri, 2010). The tips of pubertal growing ducts enlarge forming spoon-shaped multilayered epithelial structures called terminal end buds (TEBs), where cells proliferate at a high rate to invade the fat pad. In the TEBs there are two morphologically distinct cell types that are the precursors of the two main lineages in the adult mammary gland: cap cells that form the outer layer and will give raise to myoepithelial cells, and the body cells that are located in the center and are the ancestors of luminal cells. Therefore, the mature mammary duct consists of an outer layer of myoepithelial cells, so-called basal cells, and an inner layer of luminal epithelial cells that surround a hollow lumen (Brisken & O'Malley, 2010; Gjorevski & Nelson, 2011) (Figure 7).

The main trigger of the dramatic remodeling during puberty is estrogen, that is the most potent mitogenic stimulus at that time (Macias & Hinck, 2012). It was already demonstrated thirty years ago that exogenous 17β-estradiol, the predominant form of estrogen in the human body, was enough to rescue pubertal mammary expansion in ovariectomized mice (Daniel et al., 1987). Therefore, pubertal ductal elongation is elicited via signaling through estrogen receptor α (ERα, herein called ER). Downstream paracrine mediators, such as Amphiregulin (*Areg*), are also essential drivers of the massive epithelial cell proliferation characteristic of puberty (Bocchinfuso & Korach, 1997; Ciarloni et al., 2007). Regarding lateral branching, computational models integrating data from organotypic cultures, as well as results from transgenic models, suggest that lateral branching could be explained by concentration gradients of TGF-β that might specify sites of branch initiation and maintain ductal spacing *in vivo* (Jahchan et al., 2010; Nelson et al., 2006). Moreover, the non-canonical Wnt ligand Wnt5a was shown to be required for TGF-β-mediated inhibition of ductal growth (Roarty & Serra, 2007). Beyond TGF-β signaling; mechanical stress, extracellular matrix (ECM) deposition or localization of matrix metalloproteinases (MMPs) are other pathways suggested to regulate mammary ductal branching (Gjorevski & Nelson, 2010; Khokha & Werb, 2011).

2.1.2 Adult mammary gland

In humans, each menstrual cycle comprises two phases determined by changes in ovarian hormones triggered by the hypothalamic-pituitary axis. There is a first pre-ovulatory fol-

licular phase distinguished by an estrogen peak, followed by a post-ovulatory luteal phase during which the body prepares for a potential pregnancy. The luteal phase is characterized by high levels of progesterone, which induces proliferation of mammary epithelial cells (Joshi et al., 2015); progesterone levels will rise further in case of pregnancy (Brisken, 2013). In rodents, the reproductive cycle (called estrus cycle) lasts 4-5 days approximately and, similar to humans, peaks of estrogen and progesterone also determine follicular (pro-estrus /estrus) and luteal (met-estrus/di-estrus) phases, respectively (Fata et al., 2001).

In the mammary gland, progesterone is not only crucial for adult proliferation and branching but also for alveoli formation in each estrus cycle, that will differentiate into milk-producing secretory alveoli in case of pregnancy (Brisken, 2013). In contrast, estrogen elicit little proliferation in adult mammary gland; nevertheless, it triggers the synthesis of progesterone receptor (PR), which signaling induces potent downstream proliferation of mammary epithelial cells (MECs).

The proliferative response of mammary epithelial cells to progesterone is exerted in both autocrine and paracrine manners. It has been shown that the autocrine response, where luminal PR^+ cells proliferate in a cyclin D1-dependent manner, takes places 24 hours after progesterone injection. Later on, 48 hours post-progesterone, sustained growth is stimulated by paracrine mediators; hence, PR^+ cells become non-proliferative and signal to the neighboring PR^- cells (both luminal and myoepithelial) leading to a greater long-term proliferation (Beleut et al., 2010). This will explain why in earlier studies in humans and rodents, few proliferating mammary epithelial cells expressing ER and PR were observed (Clarke et al., 1997; Russo et al., 1999). The most potent paracrine-mediator of progesterone-driven proliferation is RANK ligand that is secreted by PR^+ MECs and bound by the RANK receptor present in the PR^- MECs (see section 2.5). Beyond RANKL, other paracrine factors involved in progesterone-driven proliferation in adult mammary gland are the aforementioned Amphiregulin (*Areg*), Wnt4 and Calcitonin (*Calca*); these mediators are ligands for epidermal growth factor, Frizzled or calcitonin receptors, respectively (Brisken et al., 2000; Ciarloni et al., 2007; Ismail et al., 2004; Rajaram et al., 2015).

Notably, mammary stem cells (MaSCs) (section 2.2) are highly responsive to steroid hormones. It has been nicely illustrated how ovariectomy markedly diminishes the MaSC pool and the outgrowth potential *in vivo*; whereas treatment with estrogen plus progesterone increases the MaSC activity (Asselin-Labat et al., 2010). Furthermore, in physiolog-

ical conditions, the MaSC subset increases 14-fold during maximal progesterone levels at the mouse luteal diestrus phase (Joshi et al., 2010).

Additionally, also prolactin (*Prl*), that binds the prolactin receptor, is critical for alveolar differentiation and function (Brisken et al., 1999). During lactation, the mammary epithelium develops into an elaborate network of branched ducts that maximize the surface and the release of milk into the ducts occurs by contraction of the myoepithelium upon oxytocin action (Forsyth & Neville, 2009) (Figure 8).

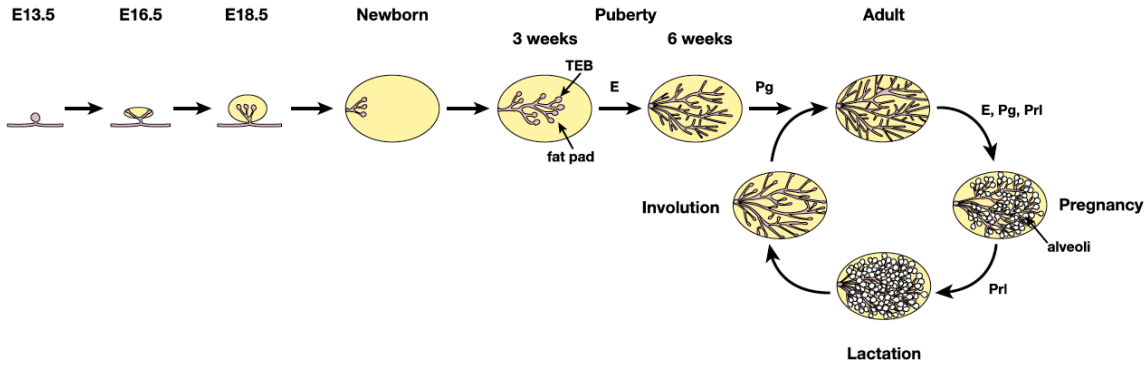

Figure 8: Schematic diagram of the main stages of the mammary gland in the embryo and adult. Development from mouse embryonic day 13.5 (E13.5) to E18.5 is depicted, newborns have a small arborized rudimentary gland invading the fat pad. At puberty, profound morphogenesis occurs, largely under the control of estrogen (E). In the adult mammary gland, progesterone (Pg) regulates branching, as well as alveolar expansion together with Prolactin (Prl) and estrogen (E). In the late stages of pregnancy and during lactation, prolactin plays a key role in establishing the secretory state. After lactation, the gland involutes and returns to a state that resembles the virgin gland. From (Visvader & Stingl, 2014).

Later on, when milk-producing alveolar cells are not longer required, up to 80 % of the epithelium is removed in a process named involution (Figure 8). Notably, most of the secretory epithelium is removed within 6 days after weaning by massive cell death through apoptosis. Two main phases have been described in the involution process: a first reversible phase regulated by local factors (48h after weaning), and a second phase that initiates a remodeling program which relies on both circulating factors and specific MMPs (Watson, 2006). This remodeling of the epithelial compartment restores a simple ductal structure like that of the virgin state . Remarkably, the mammary gland maintains its ability to perform this dramatic reshaping for the pregnancy-lactation-involution cycle during several decades is humans.

2.2 Epithelial differentiation hierarchy in the mammary gland

Over fifty years ago, it was nicely demonstrated that the mammary tree can be completely replenished by transplanting fragments of the mammary epithelium from any stage of postnatal development (Daniel et al., 1968; DeOme et al., 1959; Kordon & Smith, 1998). Now we know, thanks to transplantation studies, that a single mammary stem cell (MaSC) can repopulate the entire gland, and that MaSCs reside within the myoepithelial compartment (Shackleton et al., 2006; Stingl et al., 2006). Moreover, these studies also identified the markers for the MaSCs, also called mammary repopulating units (MRUs). They established that MaSC are characterized by the expression of high levels of CD29 (β1integrin) and CD49f (α6integrin), which are both stem cell markers in the skin, as well as being positive for CD24 (heat-stable antigen). Moreover, CD24 marker allows to distinguish between luminal ($CD24^{high}$) and myoepithelial ($CD24^{+}$) populations (Sleeman et al., 2005). Nevertheless, it has been shown that the use of EpCAM (CD326) instead of CD24, as a marker for mammary epithelial cells, is recommended for some mice strains, such as C57BL/6 (Prater et al., 2012).

Therefore, transplantation studies suggested the existence of a common bipotent stem cell in the mammary gland, because the transplanted cell contributed to both luminal and myoepithelial lineages. However, the first lineage-tracing study in the mammary gland showed, using luminal- and myoepithelial-specific cytokeratin promoters, that each compartment was maintained by their own long-lived lineage-restricted unipotent stem cells (Van Keymeulen et al., 2011). Then, it was argued that transplantation studies might not reflect the physiological circumstances and they might mimic a regenerative state (Van Amerongen et al., 2012; Van Keymeulen et al., 2011). Nonetheless, these findings were challenged by a clonal cell-fate mapping study combined with three-dimensional imaging strategy, which provided evidence for the existence of bipotent MaSCs together with long-lived progenitors (Rios et al., 2014). Consequently, there is a lot of controversy in the field and it is still under debate whether luminal stem cells exist or luminal progenitors come from a bipotent MaSC (Figure 9).

2.2.1 The luminal mammary compartment

The luminal population of the mammary epithelium is a heterogeneous compartment whose two main populations are ductal and alveolar cells, which are hormone-sensing and milk-

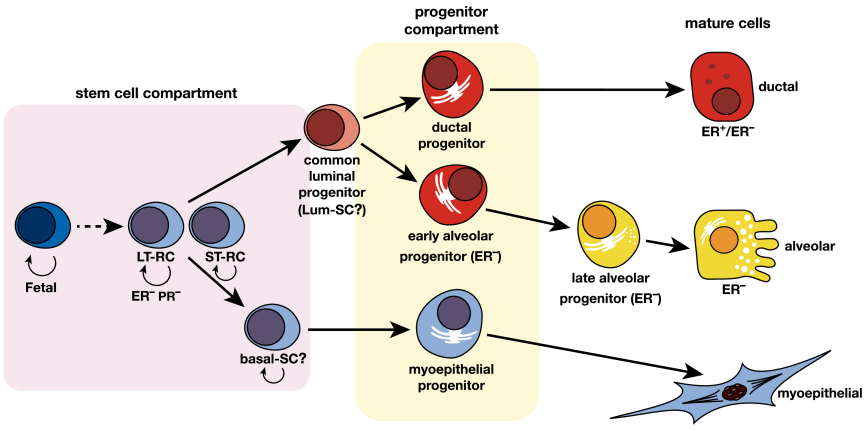

Figure 9: Hypothetical model of the mammary epithelial hierarchy. A multipotent fetal MaSC is depicted in this picture. In adult mammary gland, the stem cell (SC) compartment comprises multipotent both long-term and short-term repopulating cells (LT-RCs and ST-RCs, respectively). These cells give rise to committed progenitor cells for the myepithelial and luminal (ductal and alveolar) epithelial lineages. There may be a common luminal progenitor for the ductal and alveolar sublineages. In addition, two types of unipotent cells (lum-SC and myo-SC) might exist *in vivo*. From (Visvader & Stingl, 2014).

producing cells, respectively (Asselin-Labat et al., 2007; Sleeman et al., 2007). These lineages have their own progenitors (Giraddi et al., 2015; Van Keymeulen et al., 2017; Shehata et al., 2012); therefore, in the non-pregnant mouse we can find of at least three luminal cell types that can be distinguished by their expression of Sca1 (Ly6A/E) and CD49b (α2-integrin). The former has proven to be a useful marker for luminal subpopulations, since Sca1 expression identifies a subset of luminal cells that express high levels of the luminal differentiation proteins like ER or cytokeratins 8 and 18 (CK8/18) (Shehata et al., 2012; Sleeman et al., 2007). Additionally, CD49b is a surface marker for luminal progenitors (Shehata et al., 2012).

The largest of these three luminal populations in virgin adult mammary gland has a Sca1$^+$CD49b$^-$ phenotype and is devoid of any colony-forming potential *in vitro* or engrafting capacity *in vivo*, and thus they are termed non-clonogenic luminal (NCL) cells. These NCL cells are the ductal differentiated (DD) cells and most of them (around 80 %) express ER and other markers of luminal differentiation (Shehata et al., 2012; Sleeman et al., 2007).

Alongside NCLs, two further populations with *in vitro* colony-forming capacity can also be detected in the luminal compartment. On the one hand, Sca1$^+$CD49b$^+$ luminal progenitors (so-called ductal or Sca1$^+$ progenitors) that are the ancestors of ductal differentiated cells. Ductal progenitors express high levels of luminal cell differentiation markers, such

as ER, PR, Gata3 or Foxa1 (Asselin-Labat et al., 2007; Kouros-Mehr et al., 2006; Shehata et al., 2012). On the other hand, $Sca1^{-}CD49b^{+}$ progenitors (also termed alveolar or $Sca1^{-}$ progenitors) will give rise to alveolar milk-producing cells at lactation. Alveolar progenitors are characterized by a low expression of luminal differentiation markers and high expression of transcripts related to milk production including *Lalba* and *Mfg-e8* (Maningat et al., 2009; Shehata et al., 2012).

Comparable luminal cell subpopulations have also been identified in the human mammary epithelium. Shehata et al demonstrated that the $ALDH^{+}$ subpopulation in the human mammary gland is analogous to the ER^{-} population in the mouse, since both populations contain the highest proportion of progenitors and express high levels of alveolar-associated genes (such as *Elf5*, *Mfg-e8* or *Aldh1a3*) (Shehata et al., 2012). In addition, luminal progenitors that express high levels of luminal cell differentiation markers have also been described for human breast (Lim et al., 2009, 2010; Stingl et al., 2001). The transcription factor Elf5, while being enriched in alveolar progenitors (Oakes et al., 2008), is also expressed in ductal progenitors (Shehata et al., 2012), and together with the tyrosine kinase Kit appear to be defining markers of luminal progenitor cells in both mouse and human (Lim et al., 2010).

In summary, in mice, luminal progenitors can be discriminated from differentiated luminal cells using a variety of cell surface markers, including CD49b (Shehata et al., 2012), CD61 (Asselin-Labat et al., 2007), CD14 (Asselin-Labat et al., 2011; Shehata et al., 2012) and c-Kit (Asselin-Labat et al., 2011; Regan et al., 2012). Nevertheless, these markers are not functionally interchangeable because some of them are expressed by all luminal progenitors, whereas others have more restricted expression patterns; this is the case for CD49b and CD61, respectively. It should be also noted that the utility of these markers is also strain-dependent; for instance, CD61 (β3-integrin) effectively mark luminal progenitors form FVB/N mice but not C57BL/6 (Asselin-Labat et al., 2011; Shehata et al., 2012). A better understanding of the luminal hierarchy in the mammary gland is essential for identifying breast cancer cells of origin that are still elusive (see section 2.6).

2.3 Breast cancer subtypes

Cancer is a multistep process where normal cells gradually accumulate alterations that allow them to surpass its homeostatic control and divide aberrantly (Hanahan & Weinberg, 2011). Breast cancer is the most common type of cancer amongst women worldwide (Desantis et al., 2014), and it is a highly heterogeneous disease in terms of histology, dissemination patterns to distant sites, therapeutic response and outcome of the patients. Global gene expression analyses using high-throughput technologies have helped to explain much of this heterogeneity and provided relevant classifications of cancer patients. Therefore, breast cancer has been stratified into at least five definitive molecular subtypes, despite subgroups within subtypes have been identified (Bruna et al., 2016; Curtis et al., 2012). The five stablished breast cancer intrinsic subtypes are luminal A, luminal B, HER2-positive, basal-like and claudin-low (Prat & Perou, 2011; Visvader & Stingl, 2014). In this section, main features and treatment options for each subtype of breast cancer are discussed.

Moreover, it is also worthy to mention that there is clinical evidence of distinct patterns of metastasis in the different breast cancer subtypes. Although bone is the most common metastatic site in all subtypes with the exception of basal-like tumors; HER-2 tumors has increased metastatic potential in brain, lung and liver compared to luminal A/B. On the contrary, basal-like tumors are more prone to metastasize to brain, lung and distant lymph nodes rather than to liver or bone (Kennecke et al., 2010).

2.3.1 HER2 positive breast cancer

The HER2 subtype refers to tumors with an $ER^{-}PR^{-}HER2^{+}$ phenotype. The human epidermal growth factor receptor 2 (HER2, *Erbb2*) is a proto-oncogene that is activated through gene amplification in approximately 20 % of human breast cancers (Gradishar, 2012). Targeted therapies, such as the anti-HER2 monoclonal antibody trastuzumab (Herceptin; Roche) or the small-molecule inhibitor lapatinib (Tykerb; GlaxoSmithKline) are available for cancers bearing HER2 over-expression. Unfortunately, not all HER2 over-expressing patients respond to these molecularly targeted therapies; for instance, PTEN loss has been implicated in trastuzumab resistance (Nagata et al., 2004). Targeted therapies against HER2 cancer cells are administered alongside a chemotherapy agent, yet this subtype holds a poor prognosis derived from a higher risk of early relapse, similar to what occurs in basal-like

tumors (Dai et al., 2015).

2.3.2 Luminal breast cancer

Luminal tumors are characterized by being positive for the hormone receptors ER and PR, as well as by having expression profiles reminiscent of luminal epithelial cells (including expression of CK8/18 and genes associated with ER activation such as *Ccnd1*) (Perou et al., 2000). Remarkably, luminal breast cancer holds the best prognosis and is the most common subtype in breast cancer; nearly 80 % of breast cancer tumors express hormone receptors (Syed, 2015).

As mentioned earlier, within the luminal tumors, two subtypes exist: luminal A and luminal B tumors. As an approximation it is defined that luminal A tumors are ER^+PR^+ but $HER2^-$, whereas luminal B subtype expresses hormone receptors as well as the proto-oncogene HER2 ($ER^+PR^+HER2^+$). Nevertheless, this equivalence does not always hold, because only part of the luminal B tumors expresses HER2 (Cheang et al., 2009). Consequently, it is more accurate to differentiate between luminal A and luminal B subtypes according to their proliferation status; since luminal B tumors express higher levels of proliferation genes and are enriched for $Ki67^+$ cells ($\geq$14 %) (Cheang et al., 2009; Perou et al., 2000; Senkus et al., 2015; Feeley et al., 2014). Notably, and likely associated to the aforementioned enhanced proliferation, luminal B tumors possess poorer prognosis than luminal A. Concomitantly, luminal A patients do not require chemotherapy, while some luminal B patients might benefit from it (Cheang et al., 2009; Perou et al., 2000; Senkus et al., 2015).

All patients with detectable ER expression (defined as $\geq$1 % of invasive cancer cells positive for ER) will be treated with endocrine therapy (also termed hormone therapy) (Senkus et al., 2015). Endocrine therapy, mainly selective estrogen receptor modulators (SERMs) and aromatase inhibitors, aim to modulate the binding of estrogen receptor and block the estrogen production, respectively. The best-known example of SERM is tamoxifen, which has been used for more than 30 years to treat hormone receptor positive breast cancer (Tremont et al., 2017). New therapies are being developed for luminal tumors that recur on standard therapies, such as the mTOR inhibitor everolimus (Afinitor; Novartis) or palbociclib (Ibrance; Pfizer), a cyclin-dependent kinases CDK4/6 inhibitor.

Additionally, there is also a small number of breast cancer tumors that fall into the normal-like subgroup. These are tumors that display a $ER^{+}PR^{+}HER2^{-}$ phenotype (similar to the luminal A subtype), but have a normal breast tissue profiling (Perou et al., 2000). An explanation why normal-like tumor samples group with true normal breast samples in terms of expression might be because of the low cellularity of these tumors; then, the normal-like expression profiling might be an artifact from having high percentage of normal tissue in the sample (Parker et al., 2009).

2.3.3 Triple-negative breast cancer

Basal-like tumors are the majority of the triple-negative breast cancers (TNBCs), which are heterogeneous and account for about 12 % of all breast cancer patients (Syed, 2015). Thus, the basal subtype is composed of $ER^{-}PR^{-}HER2^{-}$ tumors with expression profiles similar to that of normal breast myoepithelial cells. Such pattern includes high expression of basal markers (such as CK5 or CK4) as well as proliferation related genes (Perou et al., 2000). Basal-like tumors are more probable to have low BRCA1 expression and to harbor *Tp53* mutations (see section 2.4). For TNBC the prognosis is discouraging and no targeted agents are available to supplement the standard chemotherapy options. Only bevacizumab (Avastin; Roche), which was the first monoclonal antibody against vascular endothelial growth factor (VEGF), is approved for this disease in Europe, but the US Food and Drug Administration (FDA) revoked the use for breast cancer in 2010 (Syed, 2015).

Another breast cancer intrinsic subtype included in TNBC, known as Claudin-low, was identified in mouse and human tumors approximately ten years ago (Herschkowitz et al., 2007). Clinically, Claudin-low tumors are poor prognosis $ER^{-}PR^{-}HER2^{-}$ invasive ductal carcinomas that account for around 7 % of all invasive breast cancers (Dias et al., 2017). This subtype shares some expression features with basal-like tumors, such as low expression of luminal genes like *Gata3*, *Krt8* and *Krt18* (CK8/18); but remarkably, they are characterized by low expression of genes involved in tight junctions and epithelial cell-cell adhesion, including the claudin genes (Herschkowitz et al., 2007; Prat & Perou, 2011). Furthermore, claudin-low tumors are enriched in attributes linked to MaSCs (Lim et al., 2009).

2.4 Etiology of breast cancer

2.4.1 Gene mutations in breast cancer

Although most breast cancers are sporadic in origin, approximately 5–10 % of them are inherited through gene mutations (Van Der Groep et al., 2006). Among these inherited breast cancer cases, the majority is caused by mutations in the tumor-suppressor genes breast cancer 1 (*Brca1*) or breast cancer 2 (*Brca2*), both related to DNA repair. Nevertheless, is still unclear why *Brca1/2*-mutation carriers predominantly develop breast or ovarian cancers. Gene-expression profiling approaches have classified *Brca1/2* mutated tumors as basal-like breast tumors. Furthermore, tumors arising in *Brca1/2* mutation carriers lack expression of the non-mutated *Brca* allele, maybe by inactivation via somatic mutation or epigenetic silencing; presumably, this induces genomic instability fostering cancer progression (Turner et al., 2004). Consistent with this, *Tp53* mutation appears in a higher frequency in this context (Crook et al., 1998). Another frequently mutated gene in breast cancer is *Pik3ca* that, on the contrary, is more commonly mutated in luminal tumors and bears activating mutations in cancer. Interestingly, it was recently showed that oncogenic mutation in *Pik3ca* activates a multipotent genetic program that could explain intratumoral heterogeneity (Koren et al., 2015; Van Keymeulen et al., 2015). Nevertheless, the presence of mutations in breast epithelial cells is not always enough to trigger breast carcinogenesis. Thus, additional factors must determine whether genetically altered cells progress to the state during which they provoke clinically manifest disease.

2.4.2 Hormone function in breast cancer

As mentioned earlier, the mammary epithelium is highly sensitive to the effects of the ovarian steroid hormones estrogen and progesterone; being critical for puberty, estrus cycling and pregnancy (see section 2.1). Similarly, it has been also appreciated that ER and PR are decisive prognostic markers and therapeutic targets in breast cancer. Still, the crosstalk between ER and PR in cancer might be more complex than expected since recent work showed that PR is not merely an ER-induced gene target, yet PR can modulate ER behavior by potentially acting as a proliferative brake in ER^+PR^+ tumors (Mohammed et al., 2015).

For all types of mammary tumors, the probability of suffering breast cancer positively correlate with number of menstrual cycles a woman experiences in a lifetime; hence, the

exposure time of the mammary epithelium to ovarian hormones influences breast cancer risk (Brisken, 2013). Epidemiological studies revealed that pregnancy is one of the most significant factors to influence breast cancer risk; strikingly, one early full-pregnancy is highly protective against luminal breast cancer (Schedin, 2006). One possible explanation links this fact to the MaSC activity, owing that a single early pregnancy is enough to alter the Wnt/Notch signaling ratio leading to decreased proliferative potential of the MaSCs (Meier-Abt et al., 2013).

2.5 RANKL in mammary gland homeostasis and breast cancer

The Tumor Necrosis Factor (TNF) family member RANK ligand (herein called RANKL, also known as TRANCE, *Tnfsf11*) is likely to be the most potent paracrine mediator of progesterone-induced proliferation, since ectopically expressed RANKL rescue mammary epithelial proliferation in PR *knock-out* (KO) mouse (Mukherjee et al., 2010). RANKL was discovered in bone as a regulator of osteoclast differentiation; under physiological conditions, RANKL produced by osteoblasts binds to RANK receptor (*Tnfrsf11a*) on the surface of osteoclasts precursors, recruiting TRAF6 and leading to NF-κB activation (Boyce & Xing, 2007). In the mammary gland, RANKL secreted by PR^+ luminal cells binds to membrane RANK receptor present in PR^- cells, mediating growth by activating the IKKα/IκBα–NFκB–cyclinD1 signaling pathway (Cao et al., 2001). Furthermore, RANKL stimulates Wnt signaling pathway through R-spondin1 (*Rspo1*) and it is also involved in stem cell activation during pregnancy (Asselin-Labat et al., 2010; Joshi et al., 2015).

RANKL also contributes to mammary gland tumorigenesis. First evidences of the participation of RANKL in the development of mammary tumors come from hormone-induced breast cancer models (Gonzalez-Suarez et al., 2010; Schramek et al., 2010), that combine the synthetic progestin medroxyprogesterone acetate (MPA) with a carcinogen (Aldaz et al., 1996). In this model, authors showed that deletion, in mammary epithelial cells, of RANK receptor or IKKα dramatically delayed mammary tumor development; indicating that the RANKL/RANK pathway relays on signals through IKKα to mediate progestin-driven mammary cancer (Schramek et al., 2010). Remarkably, selective inhibition of RANKL using the recombinant antagonist RANK-Fc attenuates breast tumorigenesis not only in a hormone-induced model, but also in a transgenic spontaneous breast cancer model (Gonzalez-Suarez et al., 2010). Furthermore, in this spontaneous tumor model, RANK signaling blockade

might reduce tumor recurrence by inducing tumor cell differentiation (Yoldi et al., 2016). In accordance, RANK signaling has been suggested to regulate mammary cell commitment and self-renewal of mammary cancer stem cells (Pasquale et al., 2013; Schramek et al., 2010).

In various mouse models, it has been shown that estrogen signaling synergize with *Brca1* loss to promote tumorigenesis (Rao et al., 2017); this observation has prompted the investigation of the contribution of RANKL in *Brca1*-mutated breast cancers. In this regard, it has been proposed that BRCA1-deficient luminal progenitors accumulate DNA damage and display aberrant proliferation due to a persistent activation of the RANKL/NFκB pathway (Sau et al., 2016). Accordingly, inhibition of RANKL abrogated the occurrence of neoplastic lesions in genetically modified mice carrying both *Brca1* and *Tp53* mutations (Sigl et al., 2016). In three-dimensional breast organoids derived from *Brca1* mut/+ patients, inhibition of RANKL signaling, with the human monoclonal antibody denosumab (Kostenuik et al., 2009), declined proliferation (Nolan et al., 2016). Notably, denosumab has already been demonstrated to have a positive benefit-risk profile in the treatment of osteoporosis in post-menopausal women (Lacey et al., 2012). This fact allowed the authors to perform a small pilot experiment where *Brca1*-mutated patients were treated with denosumab and Ki67 expression was scored. Results of this test showed a substantial reduction in Ki67 staining in subjects treated with the RANKL-blocking antibody (Nolan et al., 2016). Thus, RANKL could have a double benefit effect in breast cancer patients by reducing breast cancer risk as well as protecting bone health, which is usually at stake in these women.

In addition, RANKL may be a useful biomarker to identify subgroups at high risk of breast cancer. Indeed, increased progesterone and RANKL serum levels stratify a subgroup of postmenopausal women who exhibit increased risk of developing breast cancer but without known genetic predispositions (Kiechl et al., 2017). Similarly, higher concentrations of soluble RANKL are positively associated with an increased risk of luminal breast cancer (Sarink et al., 2017). Also serum levels of OPG (osteoprotegerin), the decoy receptor for RANKL, are deregulated in breast cancer (Widschwendter et al., 2015). Altogether, these data suggest that RANKL inhibition could be a new weapon against breast cancer (González-Suárez & Sanz-Moreno, 2016; Rao et al., 2017).

2.6 The cell of origin in breast cancer

Comparative studies, between breast cancer expression signatures and those from healthy epithelial populations, have suggested that distinct cells of origin may give rise to the different breast cancer subtypes (Visvader & Stingl, 2014) (Figure 10).

In 2009, a study showed that the luminal progenitor signature was very alike to that of basal-like breast tumors and that *Brca1*-mutated tissues showed an aberrant expansion of a luminal progenitor subpopulation (Lim et al., 2009). This experimental data was the first evidence that breast cancer intrinsic subtypes may reflect cell states along the differentiation hierarchy of the normal breast. Corroborating these results, deleting *Brca1* in luminal progenitors, but not in the basal compartment, produces tumors that phenocopy human *Brca1*-mutated breast cancers and most of sporadic basal-like breast tumors (Molyneux et al., 2010). Similarly, luminal progenitors were regarded as key target population in patients bearing *Brca1* mutations (Nolan et al., 2016; Sau et al., 2016). In addition, $ALDH^{+}ER^{-}$ luminal progenitor cells in human breast tissue exhibit a signature that most strongly correlates with the basal-like subtype (Shehata et al., 2012). Conversely, the MaSC/basal signature is most closely related with the expression profile of the claudin-low subtype (Prat & Perou, 2011).

In summary, this data strongly suggests that luminal progenitors and MaSC give rise to basal-like and claudin-low tumors, respectively. Additionally, according to their expression profile (Shehata et al., 2012), we could speculate that a mature luminal cell is the tumor-initiating cells (TIC) for the luminal subtypes, and that the potential TIC for HER2-positive tumors is an partially differentiated luminal state (Figure 10). In this regard, it has been suggested that TICs in HER2/Neu tumors are potentially derived from luminal progenitors (Lo et al., 2012). Nevertheless, definitive evidences unveiling the cell of origin for these subtypes are still missing.

3 CPEBs in cancer

In recent years, it has become evident that post-transcriptional regulation plays a major role in cancer initiation and progression. Some examples are miRNAs (Lin & Gregory, 2015), splicing factors (Chabot & Shkreta, 2016), 3'UTR shortening (Mayr & Bartel, 2009), secondary structures in the 5'UTR like G-quadruplexes (Wolfe et al., 2014), as well as the

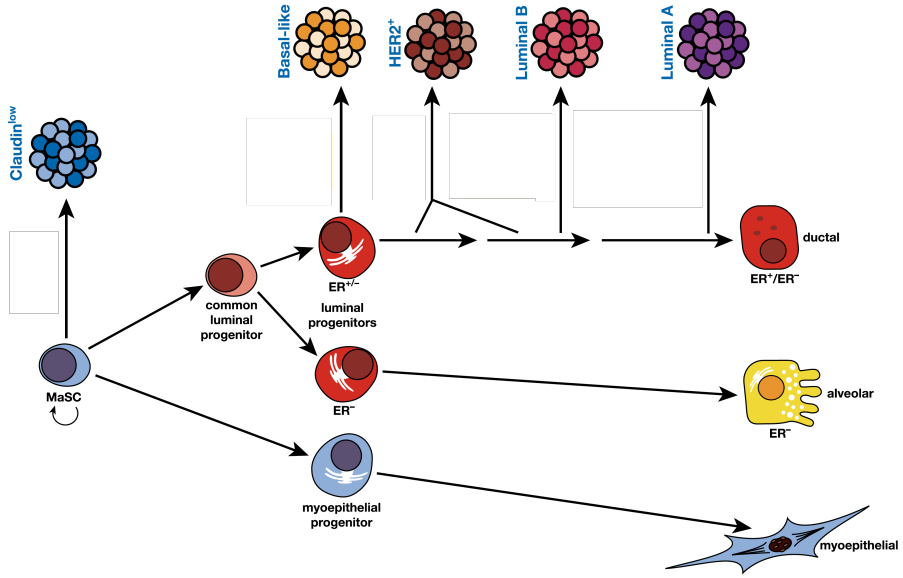

Figure 10: Schematic model of the human breast epithelial hierarchy and potential relationships with breast tumor subtypes. The five major breast cancer subtypes are shown linked to their closest normal epithelial counterpart based on gene expression profiling. Adapted from (Visvader & Stingl, 2014).

translation machinery itself (Sendoel et al., 2017; Truitt & Ruggero, 2016). Importantly, deregulation of translation is arising not only as a primary output of oncogenic signaling, but also as a central mediator of cancer resistance to several clinical therapies (Boussemart et al., 2014; Ilic et al., 2011). As a consequence, RNA-binding proteins, which can influence nearly every aspect of RNA metabolism (Glisovic et al., 2008), have recently emerged as critical players in cancer (Wurth et al., 2016; Wurth & Gebauer, 2015).

In this context, also the CPEB-family of RNA-binding proteins has been shown to contribute to cancer and metastasis. Generally speaking, CPEB1 seems to be downregulated in cancer suggesting a tumor suppressor function (Caldeira et al., 2012; D'Ambrogio et al., 2013; Hansen et al., 2009) ; while CPEB4 is mainly overexpressed in cancer and it could act as a tumor promoter gene (Chang, 2014; Lu et al., 2017a; Ortiz-Zapater et al., 2012; Sun et al., 2015; Zhong et al., 2015). Supporting this idea, CPEB1-KO mice show high sensitivity to papilloma formation (Burns & Richter, 2008), and primary mouse or human cells lacking CPEB1 have the ability to bypass sensence (Burns & Richter, 2008; Groisman et al., 2006; Groppo & Richter, 2011). Conversely, it has been described that CPEB4 promotes invasion and malignancy in pancreatic ductal adenocarcinomas (Ortiz-Zapater et al., 2012) as well as melanoma initiation (Pérez-Guijarro et al., 2016). Interestingly, high levels of CPEB4 in tumoral cells can generate oncoselectivity in viral anti-cancer therapies (Villanueva et al., 2017).

3.1 CPEBs in mammary gland and breast cancer

Although little is known about the role of CPEB proteins in the mammary gland physiology, they have been suggested to regulate translation and stability of milk protein transcripts, like the mRNA of β-casein (*Csn2*); such transcripts have been shown to be specifically enhanced upon insulin plus prolactin stimulation in cultured mouse epithelial cells. Notably, this response was mediated through cytoplasmic polyadenylation via the cytoplasmic polyadenylation element (CPE) present in the 3'UTR (Choi et al., 2004; Rhoads & Grudzien-Nogalska, 2007). Interestingly, the poly(A) tail length of the β-casein mRNA fluctuates in a way that it is shorter at weaning but longer at nursing (Kuraishi et al., 2000); indicating that milk-production is optimized with an increased translation of β-casein mRNA. Therefore, cytoplasmic polyadenylation modulation by CPEBs is likely to be responsible for both translation and mRNA stability of milk protein transcripts downstream certain hormones.

Regarding breast cancer, CPEBs have been related with epithelial-mesenchymal transition (EMT) and most experimental evidences come from breast cancer lines. Both CPEB1 and CPEB2 have been suggested to negatively regulate *Twist1* mRNA (Nairismägi et al., 2012). Moreover, CPEB1 and CPEB4 appear to have opposite roles also in breast cancer metastasis. It has been shown that CPEB1 loss causes an EMT-like phenotype and a drop in the number of metastasis (Nagaoka et al., 2015); whereas attenuation of CPEB4 expression results in decreased EMT, migration and invasion (Lu et al., 2017a). Additionally, the EMT-like phenotype in CPEB1-depleted cells might be caused in part by a loss of mammary epithelial cell polarity. In the mammary gland, CPEB1 appears to be essential for polarity integrity and tight-junction assembly by localizing zo-1 mRNA (*Tjp1*) to the apical part of the mammary epithelium (Nagaoka et al., 2012).

Furthermore, a specific human CPEB2 splicing variant has been described to be required for anoikis resistance in triple-negative breast cancer cell lines (Johnson et al., 2015). It has been suggested that human CPEB2 isoforms (with or without exon4) have opposite functions; whereby the inclusion of the exon4 upregulates pathways related to hypoxia and EMT that drive anoikis resistance and metastasis (DeLigio et al., 2017).

In addition to the aforementioned cancer-related roles, CPEB proteins are instrumental in cell proliferation (Giangarrà et al., 2015; Novoa et al., 2010) as well as in lineage-specification (Hu et al., 2014; Pérez-Guijarro et al., 2016). Therefore, the study of CPEBs in a hierarchically organized tissue undergoing a great deal of remodeling may shed light on novel functions of this family of RNA-binding proteins. The fact that the mammary gland harbors extraordinary proliferative and differentiation potential, plus the gap in knowledge regarding translational control in the mammary epithelium, motivated us to investigate the role of the CPEB-family in mammary gland homeostasis and breast cancer.

Objectives

The main goal of this study is to analyze *in vivo* the contribution of the four members of the CPEB-family of RNA-binding proteins in epithelial morphodynamics. To this aim, we focus our work on the mammary gland because it is highly polarized and hierarchically organized epithelia that is subject to great remodeling throughout adult life. Distinct transcriptional circuits orchestrating such finely-tuned processes have been described; however, translational regulation in the mammary gland remain basically unexplored. Therefore, we hypothesize that the CPE-family of proteins, which are activated by different external cues and control translation temporally and spatially, might be novel translational regulators of the mammary epithelia homeostasis.

Consequently, our specific objectives are:

1. To generate a CPEB2 *knock-out* model in order to complete the set of individual CPEB-KO models available in our laboratory.
2. To perform a systematic analysis of the functions of CPEB1-4 in mammary gland homeostasis *in vivo*.
3. To identify novel molecular mechanisms driven by the CPEB proteins occurring in mammary epithelial cells.
4. To explore a potential impact of modulating CPEBs in breast cancer.

Methods

Generation of constitutive and epithelial-specific CPEB2 *knock-out* mice

To generate a CPEB2 conditional knockout mouse (*Cpeb2*lox/lox), the vector (PRPGS00036-W-3-B04, Eucomm) was electroporated in mouse G4 embryonic stem (ES) cells (129S6/Sv and C57BL/6). Positive recombinant ES cells were identified by Southern blotting, transfected *in vitro* with the FlpO recombinase to remove the βgeo-cassette and microinjected in developing blastocysts. Resulting chimeric mice (*Cpeb2*lox/lox) were crossed with C57BL6/J mice, and mouse colony was maintained in a mixed background (129/Sv x C57Bl/6J). To obtain a ubiquitous and constitutive depletion of CPEB2, *Cpeb2*lox/lox mice were crossed with mice expressing DNA recombinase Cre under control of the Sox2 (SRY-box containing gene 2) promoter. Excision of exon 4 of the (*Cpeb2* gene leads to a frame shift in the mRNA generating premature stop codons and resulting in mice that are deficient in CPEB2 protein (CPEB2 *knock-out*, KO). Epithelial-specific CPEB2-KO mice were obtained by crossing *Cpeb2*lox/lox mice with C57BL/6J transgenic mice expressing Cre under control of the cytokeratin14 (CK14) promoter. Routine genotyping was performed by PCR (primer sequences are listed in Table 1, Appendix).

Southern Blotting

Agarose gels were incubated under soft agitation with depurination solution (0.25 M HCl; 15 min), denaturation solution (1.5 M NaCl, 0.5 M NaOH; 45 min) and neutralization solution (0.5M Tris, 1.5 M NaCl; 30 min). After overnight transfer, DNA was cross-linked (254 nm; 0.12 J) to nylon membrane (0.45 mm; Pall Corporation, Port Washington, NY). The membrane was prehybridized with Church buffer for 3 hours at 65°C, hybridized with 32P-labeled probes for 12 hours, rinsed with washing buffer (standard saline citrate, 0.1 % SDS) and exposed to Phosphorimager screen.

Animal studies

Animals (*Mus musculus*, C57BL6/J-129S mixed background) were maintained under a standard 12-h light–dark cycle, at 23°C, with free access to food and water. Only female littermates between 10 and 12 weeks of age were used, unless otherwise stated. Mice were staged by histological analysis of the ovaries or vaginal cytology and selected for the follicular phase of the oestrous cycle (Bertolin & Murphy, 2014; Byers et al., 2012). For tumorigenesis experiments, mice were injected subcutaneously with MPA (medroxy-progesterone acetate, Depo-provera) at 6-7 weeks of age and then they were given DMBA (1 mg) by gavage weekly during the next 4 weeks (Aldaz et al., 1996; Wan et al., 2014). Tumors were detected

and monitored by manual palpation. Mice were sacrificed when a palpable mass exceeded 1 cm in diameter or at 19 weeks after MPA treatment. Endpoint tumors were classified according to previously identified pathological nomenclature (Cardiff et al., 2000). For experiments with MPA alone, MPA was injected subcutaneously at 7 weeks of age and mice were sacrificed 3 days later. All mice experiments were approved by the Animal Ethics Committee at the University of Barcelona.

Mammary Epithelial Cell isolation, Flow Cytometry and Cell sorting

Thoracic and inguinal mammary glands were dissected and mammary epithelial cells were prepared as previously described (Prater et al., 2012). Briefly, mammary glands were incubated with collagenase/hyaluronidase solution (STEMCELL Technologies), then red blood cells were lysed and cells were further dissociated with trypsin (Sigma), Dispase II (Sigma) and DNAse I (Sigma). FACS sorting was performed in FACS Aria Fusion sorter (BD Bioscience). Data was analyzed with the BD FACSDIVA software. Only in the case of 4-colour analysis the Gallios flow cytometer (Beckman Coulter) was used. The antibodies used were: EpCAM-PE (130-102-265), CD49f-APC (130-100-147), CD45-FITC (130-102-778), Ter119-FITC (130-102-257), CD31-FITC (130-102-970), CD49b-PE (130-102-778), EpCAM-APC/Cy7 (Biolegend, #118217) and Ly-6A/E (Sca1) PerCP/Cy5.5 (Biolegend, #108123). Antibodies were purchased from Miltenyi Biotec unless otherwise stated. Gating strategies were adjusted as previously described (Shehata et al., 2012). For 5-Ethynyl-2´-deoxyuridine (EdU) incorporation experiments, mice were injected intraperitoneal with EdU (80 mg/kg) and they were sacrificed 6 hours later (Giraddi et al., 2015). After isolation of the mammary epithelial cells samples were processed as indicated in the protocol Click-iT Plus EdU Flow Cytometry Assay (Invitrogen) using Pacific Blue picolyl azide.

Organoid culture

A number of 2,000 sorted cells were embedded in one drop of BME (Cultrex) and cultured for 15 days in uncoated 24-well glass plates (#242-20 zell-kontakt). Culture protocol was adapted from (Jamieson et al., 2017); advanced DMEM/F12 media was supplemented with Penicilin/Streptomycin (Gibco), Glutamax (Gibco), Hepes (Gibco), Insulin (Sigma), Hydrocortisone (Biolonza), B27 (Thermofisher), N-Acetylcyteine (Sigma), EGF (Sigma), FGF2 (Sigma), FGF10 (Peprotech), Wnt3a (in house), Heparin (STEMCELL Technologies), Y-27632 (Rock inhibitor, Tocris) and R-spondin1 (in house). ROCK inhibitor was added for the first week and the medium was refreshed every 3-5 days. Full drops were scanned with an Olympus IX81

inverted microscope at 10x magnification (ScanR software). Bright-field Z-stacks of each field were projected in a single image and then the full drop was digitally reconstructed by stitching the different image projections using an ImageJ custom-made macro developed for this purpose at the IRB Advanced Digital Microscopy Facility.

For branching experiments, organoids were cultured following the protocol from (Nguyen-Ngoc et al., 2014) with 40 ng/ml FGF2 in uncoated 24-well glass plate (100 organoids embedded in one drop of matrigel). Organoids were imaged at 4x magnification with an Olympus IX81 inverted microscope (ScanR software) and images were processed using the aforementioned custom-made macro. Then, as suggested by (Nguyen-Ngoc et al., 2014), organoids with 3 or more elongated buds were scored as branched. This classification was done manually using Cell Counter macro of ImageJ.

Immunohistochemistry and wholemounts

For mammary gland wholemounts, inguinal mammary glands were placed on a slide and fixed immediately with Carnoy's solution overnight. Then the tissue was hydrated, stained with carmine alum (Sigma, #C1022, #A7167), dehydrated, cleared with xylene and mount with Leica CV Mount (14046430011). Images from wholemounts were acquired with Olympus Macroscope (zoom 1.6) and joint with the MosaicJ tool from ImageJ (Thévenaz & Unser, 2007). For junction quantification, images were processed using a ImageJ custom-made macro developed for this purpose and analyzed using AngioTool (Zudaire et al., 2011). For histology and immunohistochemistry, inguinal mammary glands were fixed in 10 % neutral buffered formalin solution and embedded in paraffin. Paraffin-embedded tissue sections (3 μm in thickness) were air dried and further dried at 60°C over-night. Immunohistochemistry was performed using an Autostainer Plus (Dako - Agilent). Prior to immunohistochemistry, for Ki67 sections were dewaxed as part of the antigen retrieval process using the low pH EnVision FLEX Target Retrieval Solutions (Dako, Burlington) for 20min at 97°C using a PT Link (Dako – Agilent). For caspase 3 samples were dewaxed and antigen retrieval treatment was performed with citrate buffer pH6 for 20 min at 121°C with an autoclave. Quenching of endogenous peroxidase was performed by 10 min of incubation with Peroxidase-Blocking Solution (Dako REAL S2023). Primary antibodies rabbit polyclonal anti-Ki67 (ab15580, Abcam) and rabbit polyclonal anti-cleaved caspase 3 (Cell signaling, 9661S) were diluted 1:1000 and 1:300 with EnVision FLEX Antibody Diluent (K800621, Dako, Agilent) and incubated for 60 and 120 min, respectively at room temperature. The

secondary antibody used was a BrightVision Poly-HRP-Anti Rabbit IgG Biotin-free, ready to use (Immunologic, DPVR-110HRP). For ER (Dako, M7047 clone 1D5) and RANKL (R&D AF462) immunohistochemistry was performed as previously described (Mohammed et al., 2015; Gonzalez-Suarez et al., 2010). Antigen–antibody complexes were reveled with 3-3′-diaminobenzidine (K3468, Dako), with the same time exposure per antibody (3 and 5 min respectively). Sections were counterstained with hematoxylin (Dako, S202084) and mounted with Mounting Medium, Toluene-Free (CS705, Dako) using a Dako CoverStainer. Bright-field images were acquired with a NanoZoomer-2.0 HT C9600 scanner (Hamamatsu). All images were visualized with a gamma correction set at 1.8 in the image control panel of the NDP.view software (Hamamatsu, Photonics, France). Image analysis was performed using TMARKER software (Wild et al., 2013).

Immunoblotting

Beads homogenized tissue or mammary epithelial cells (EasySep, STEMCELL Technologies) were lysed in ice-cold RIPA lysis buffer (with phosphatase and protease inhibitors). Lysates were then sonicated for 5 min at high or low intensity, respectively (Standard Bioruptor Diagenode). Cellular debris was pelleted (15,700g, 15 minutes, 4°C) and protein concentration was determined by DC Protein assay (Bio-Rad). Equal amounts of proteins were separated by SDS-polyacrylamide gel electrophoresis. After transfer onto nitrocellulose membranes (GE10600001, Sigma), membranes were blocked for 1h in 5 % milk and specific proteins were labeled with the corresponding primary antibodies against Vinculin (Abcam, ab18058), PBX1 (Cell Signaling, 1674342S), Stat5a (Santa Cruz, sc-166479), Cyclin D1 (Santa Cruz, sc-8396), CPEB2 (kindly provided by Dr. Yi-Shuian Huang laboratory). Secondary HRP antibodies were also diluted in 5 % milk and proteins were revealed using ECL Western blot- ting detection reagents (GE Healthcare).

RNA analysis

Total RNA was extracted either by TRIzol reagent (Invitrogen), One microgram of RNA was reverse-transcribed with oligodT and random primers using SuperScript IV (ThermoFisher) or RevertAid (ThermoFisher) following the manufacturer's recommendations. Quantitative real-time PCR was performed in a LightCycler 480 (Roche) using PowerUp SYBR Green Master Mix (Roche). Primer sequences are listed in Table 2 (Appendix). RNA quantifications were normalized to GAPDH as endogenous control. For microarrays, samples from sorted cellls from WT and CPEB2-KO animals (two animals of each genotype) were

processed at IRB Barcelona Functional Genomics Core Facility following standard procedures. Affymetrix MG-430 PM strip data for DD, DP, AP and Myo cell population samples in WT and CPEB2KO in biological duplicates was processed with Bioconductor (Gentleman et al., 2004) using RMA background correction, quantile normalization and RMA summarization to obtain probeset expression estimates (Carvalho & Irizarry, 2010). Afterwards, we used limma 3.22.7 (Ritchie et al., 2015) to identify differentially expressed genes between CPEB2KO and WT in all 4 cell populations using a pvalue threshold of 0.01 and a |FC|>2. Additionally, we assessed differences between WT samples across the 4 cell populations, selecting as candidate genes those ones showing a |FC|>3. Finally, we used the GSEA pre-ranked algorithm (Subramanian et al., 2005) to identify significantly enriched and depleted gene sets in Gene Ontology, KEGG and Broad Hallmarks categories, using the annotation from the org.Mm.eg.db Bioconductor package (October 2014) and human-mouse homology information when necessary (ENSEMBL August 2016).

RNA-immunoprecipitation-sequencing analysis

Mammary epithelial cells (EasySep, STEMCELL Technologies) were isolated from WT or CPEB2-KO animals (two animals were pool per sample and two samples of genotype were processed). Pellets were washed twice with cold HBSS, lysed with RIPA buffer (50mM Tris-Cl pH8, 150mM NaCl, 1 mM MgCl2, 1 % NP-40, 1mM EDTA, 0.1 % SDS, protease inhibitor cocktail and RNase inhibitors) and then sonicated for 5 min at low intensity with Standard Bioruptor Diagenode. After centrifugation (10 min, 4°C), supernatants were collected, precleared, and immunoprecipitated (4h, 4°C) with 10 μg of anti- CPEB2 antibody (kindly provided by Dr. Yi-Shuian Huang laboratory) bound to 50μl of Dynabeads Protein G (Invitrogen). Beads were washed and split for either protein or RNA extraction. For RNA isolation, beads were resuspended in 100 μl Proteinase K buffer with 70 μg of Proteinase K (Roche) and incubated 30 min at 42°C and 30 min at 65°C. RNA was extracted following standard phenol/chloroform protocol. Samples were processed at IRB Functional Genomics Facility following standard procedures. First, Illumina 50bp bp single-end RIP-Seq data for WT and CPEB2KO as well as their respective Input samples of mammary epithelial cells in biological duplicates were aligned against the *Mus musculus* UCSC mm10 rRNA genome using Bowtie1 0.12.9 (Langmead et al., 2009) with 2 mismatches and default options, in order to identify and remove from downstream analysis reads coming from potential rRNA contamination. Curated non-rRNA reads were then aligned against the *Mus musculus* mm10 reference genome using Bowtie2 2.2.2 (Langmead & Salzberg, 2012), allowing for 1 mismatch

and reporting best alignment site per read. Duplicated reads potentially arising from amplification artifacts were detected and removed with the sambamba software version 0.5.1 using default options. An interaction analysis of CPEB2 WT vs KO samples using their respective Input controls was performed using DESeq2 (Love et al., 2014) to identify potential RNA binding sites using sample counts at 3'UTR level (longest 3'UTR per gene, ENSEMBL March 2017), and removing multihit alignments with MAPQ=0. Candidate 3'UTRs were selected using a Benjamini-Hochberg adjusted p-value of 0.1 (high confidence RIP-target genes) (Table 3, Appendix). Gene Ontology enrichment analysis was performed using Gene ontology enrichment analylsis was performed using Enrichr (Chen et al., 2013; Kuleshov et al., 2016).

Statistics and reproducibility

Data is expressed as mean ± standard error of the mean (s.e.m.) and statistics were analyzed using the GraphPad Prism software. Comparisons between groups were carried out with the non-parametric Mann-Whitney test (*$p<0.05$ **$p<0.01$), unless otherwise stated. We estimated sample variance based on previously published data and calculated the sample size with the 'Sample Size Calculation' tool from the Center for Clinical Research and Biostatistics (CCRB). For animal studies, the same sample size calculations were applied. Experiments were done following a randomized-block design. Besides, littermates kept in the same cage since weaning were used whenever possible. The experiment was blinded until the conclusion of the experimental analysis.

Results

1 Generation of CPEB2 constitutive and conditional KO mouse model

In order to unveil novel functions of the CPEB-proteins related to proliferation and differentiation *in vivo*, the first step was to generate a genetically engineered loss-of-function mouse model for CPEB2. Regarding other CPEBs, the *knock-out* (KO) models for CPEB1 and CPEB4 were described before (Calderone et al., 2016; Maillo et al., 2017), and CPEB3-KO mice were obtained from a consortium and further validated in our laboratory (data not shown). In the case of CPEB2, as described in Methods, the exon 4 was targeted for excision; this deletion creates of a premature termination codon that would result in the loss of the CPEB2 protein (Figure 11A). Correct integration of the insert in mouse embryonic stem (ES) cells was assessed by southern-blotting using radioactive probes against both ends of the HR arms (Figure 11A) (see Appendix). Besides, we used a neomycin probe to check that only one insertion had occurred. Southern-blot analysis ended with five *Cpeb2*loxfrt positive clones (5B7, 5D11, 5D12, 5G1, 5H3) (Figure 11B). After karyotype analysis, clones 5D12 and 5H3 were selected for transfection *in vitro* with the DNA recombinase Flippase (Flp) in order to excise the Neomycin cassette, thus obtaining the *Cpeb2*lox allele (Figures 11A and 11C). Then, *Cpeb2*lox mice were mated with animals expressing the DNA recombinase Cre under control of the Sox2 promoter to obtain ubiquitous and constitutive CPEB2-KO (*Cpeb2*(-)) mice (Figures 11A and 11C). Once the *Cpeb2*(-) allele was obtained, Sox2-Cre negative animals were used for subsequent experimental purposes. Routine genotyping was performed by PCR (primer sequences are listed in Table 1, Appendix) (Figure 11C). We confirmed a complete depletion of CPEB2 protein by western blot in several tissues from CPEB2-KO mice (Figures 12A and 12B), and we also observed a testis-specific isoform with a higher molecular weight, as previously described (Lai et al., 2016). CPEB2-KO mice were born at mendelian ratios (Figure 11D), indicating that absence of CPEB2 do not cause embryonic lethality. In a slightly different background and in distinct housing conditions, other phenotypes for CPEB2-KO mice have been observed (Lai et al., 2016). We used this CPEB2-KO model as well as the other individual CPEB-KO mice available in our laboratory to assess the roles of CPEB1-4 in mammary gland homeostasis. To our knowledge, this was the first time that the contribution of the four members of the CPEB-family is investigated *in vivo* in a given context.

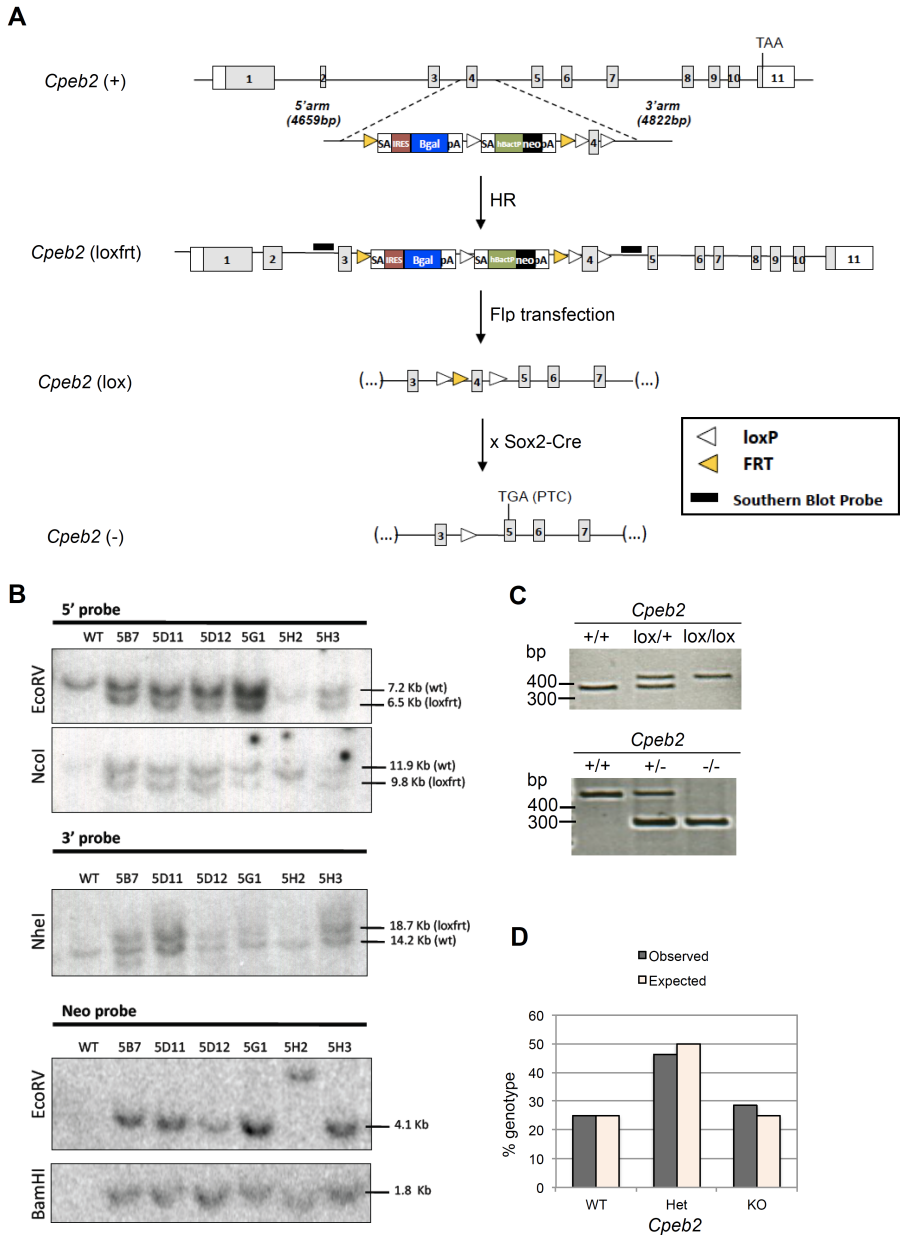

Figure 11: Generation of conditional and constitutive KO mouse models for CPEB2. (A) Schematic view of the targeting strategy by homologous recombination (HR) at the *Cpeb2* locus in mouse embryonic stem (ES) cells. The *Cpeb2* locus in *Mus musculus* contains 11 exons (boxes), including protein-coding (grey) and unstranlated (clear) sequences. Also loxP sites (white triangles) and FRT sites (yellow triangles) (that are recognized by the DNA recombinases Cre and Flp, respectively) are depicted. The neo cassette was deleted by expressing the Flp recombinase *in vitro*. To obtain the excision of exon4 and loss of CPEB2 ubiquitously, mice were crossed with Sox2-Cre mice. hBactP, promotors. Bgal, β-galactosidase. Neo, neomycin. PTC, premature termination codon. IRES, internal ribosome entry site. SA, splicing acceptor. pA, polyA sequence. (B) ES clones that underwent HR assessed by southern-blotting. DNA was digested with the indicated restriction enzymes and hybridized with the 5', 3' or Neo probes indicated in (A). (C) PCR amplification for either conditional (upper panel) or null (lower panel) *Cpeb2* alleles. (D) Observed and expected genotypes of the offspring from heterozygous mattings.

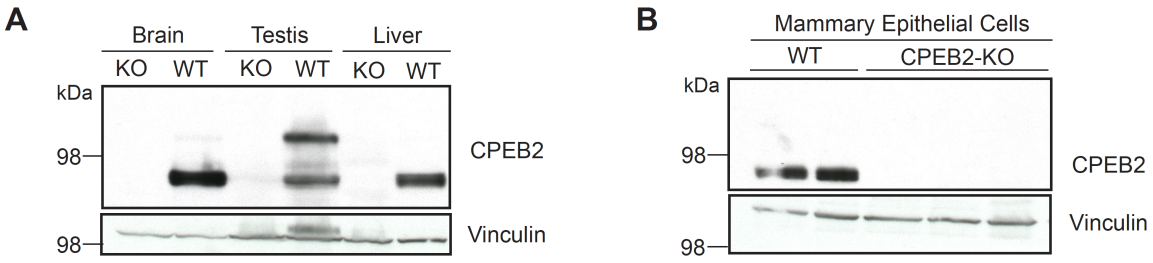

Figure 12: CPEB2 is effectively deleted in CPEB2-KO mice. Extracts from (A) whole tissues or (B) isolated mammary epithelial cells from WT and constitutive CPEB2-KO mice were assessed by western-blotting for CPEB2 and Vinculin as a control.

2 Expression of the CPEB-family in the mammary gland

The mammary gland is a highly polarized tissue composed of two main epithelial cell types: luminal and myoepithelial cells. Luminal and myoepithelial populations can be isolated taking advantage of the differential expression of EpCAM and CD49f (α6-integrin). While luminal cells are epithelial cells that express high levels of EpCAM; myoepithelial cells (also named basal cells) are characterized by lower levels of EpCAM and higher levels of integrins, since they are in contact with the extracellular matrix (Figure 13). Moreover, the mammary gland is a highly dynamic organ that undergoes profound morphological changes during distinct post-natal stages. Development and remodeling of the mammary gland is evident in carmine-stained mammary wholemounts (Figure 14A). Briefly, at puberty, the mammary gland consists of a rudimentary tree of ducts, whose tips enlarge forming the terminal end buds (TEBs). After, adult mammary epithelial ducts fill the whole mammary fat pad and exhibit secondary and tertiary branching. Upon pregnancy alveoli are formed, that will differentiate into milk-producing units during lactation. Massive remodeling occurs after weaning, where the mammary gland comes back to a virgin-like state by a process called involution. As a starting point, we measured mRNA levels of *Cpeb1-4* in pubertal, adult, pregnant, lactating and involuted mammary gland. We observed that in adult virgin mice the levels of *Cpeb2* were higher compared to other CPEBs, followed by *Cpeb2*. Interestingly, *Cpeb2* expression was peaking at lactation (Figure 14B).

In order to investigate whether there was any change in expression between the two major epithelial cell types, we evaluated *Cpeb1-4* mRNAs levels in sorted luminal and myoepithelial cells. Indeed, our results indicated that *Cpebs* are differentially expressed in these two epithelial populations of the mammary gland; interestingly, *Cpeb1* and *Cpeb2* are

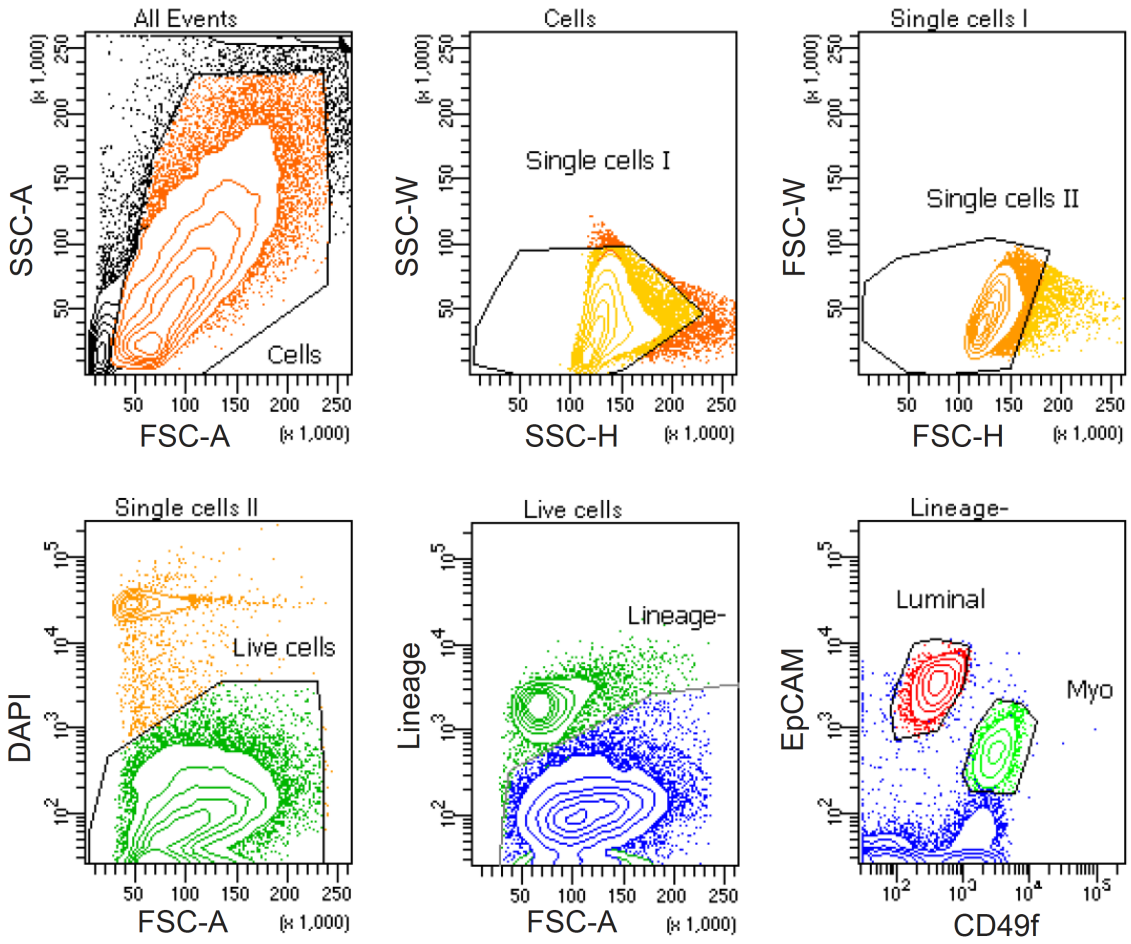

Figure 13: FACS strategy. Representative FACS plots showing the gating strategy for isolation and analysis of luminal ($EpCAM^{high}CD49f^{low}$) and myoepithelial ($EpCAM^{low}CD49f^{high}$) populations of the mammary tissue. Lineage staining is used to discard immune ($CD45^{+}$), endothelial ($CD31^{+}$) and erythroid ($Ter119^{+}$) cells.

the most abundant CPEBs in the myoepithelial and luminal compartments, respectively (Figure 14C).

3 CPEB2 regulates adult mammary gland homeostasis

We started the phenotypic characterization of the mammary tissue from single CPEB-KO mice by analyzing mammary gland wholemounts for each genotype (Figure 15A). This technique allowed us to have a complete view of the whole mammary gland and to assess epithelial branching as a read-out of proliferation and differentiation. In order to quantify epithelial branching in an unbiased and automatic way, we made use of the AngioTool software developed to quantify ramifications of blood vessels (see Methods) (Figure 15B). Our results showed that both CPEB1-KO and CPEB2-KO females had a defect in epithelial branching (Figure 15C).

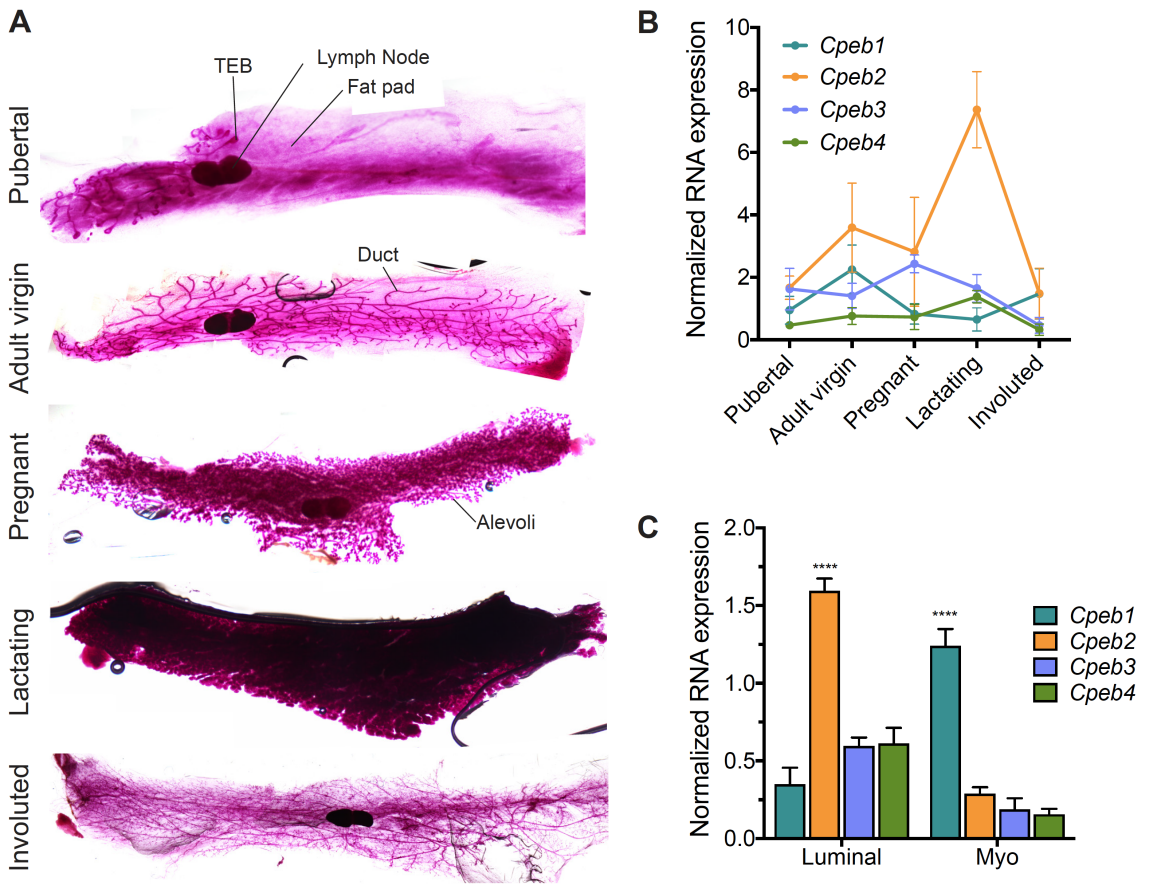

Figure 14: *Cpeb1-4* mRNA expression in the mammary gland. (A) Carmine-stained mammary wholemounts of the various post-natal stages of the mammary gland: puberty (5 weeks old), adult nulliparus (10 weeks old), mid-pregnancy (day 12 of gestation), lactation (2 weeks of lactation) and involution (6 days after weaning). (B) mRNA levels of *Cpeb1-4* normalized to *Gapdh* in whole tissue mammary gland (n=2, except for adult that n=4). (C) mRNA levels of *Cpeb1-4* normalized to *Gapdh* in sorted cells from adult virgin mammary gland (n=3, 2way ANOVA, ****p<0.0001). Myo, myoepithelial.

Nevertheless, it has been previously published that CPEB1-KO females do not develop functional ovaries (Tay & Richter, 2001). Consequently, CPEB1-KO females do not secrete normal levels of reproductive hormones that are needed for mammary gland elongation and branching (Nagaoka et al., 2012); this is not the case for CPEB2-KO females. Therefore, we reasoned that the branching phenotype would be rescued by an epithelial-specific KO in the case of CPEB1 but not for CPEB2. For this purpose, we crossed *Cpeb1*lox/lox or *Cpeb2*lox/lox animals with a transgenic mice expressing the recombinase Cre under the control of the promoter of CK14, which is expressed by all mammary epithelial cells during embryonic development (Van Keymeulen et al., 2011). Indeed, while CPEB1-KO$^{CK14-Cre}$ had the same number of junctions than WT$^{CK14-Cre}$, CPEB2-KO$^{CK14-Cre}$ still presented de-

creased branching (Figures 15D and 15E). These results show that CPEB2 regulates mammary gland branching in an epithelial cell-autonomous manner. Nonetheless, we were not able to reproduce in 3D culture assays the branching defects in absence of CPEB2 (Figures 16A and 16B).

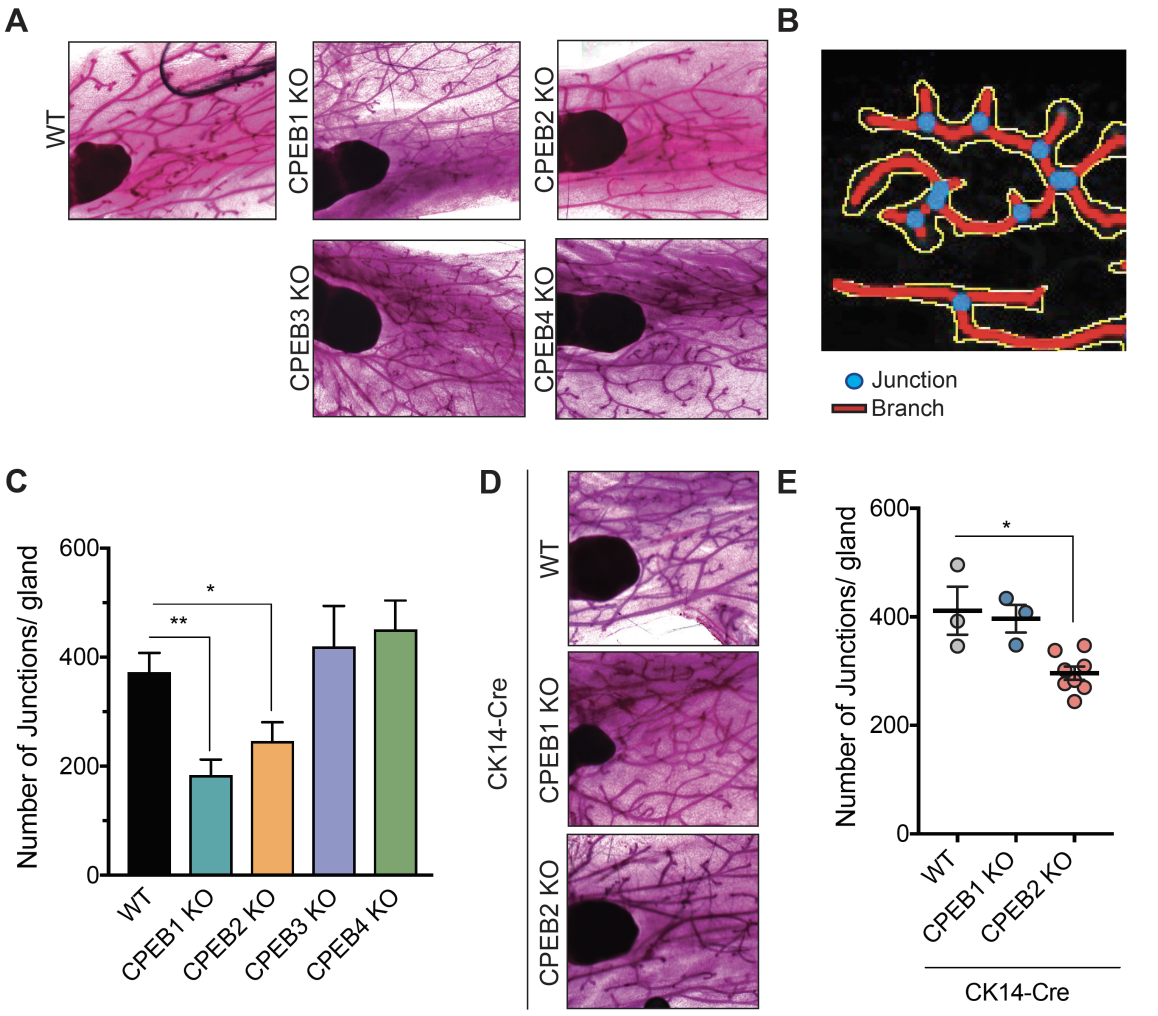

Figure 15: CPEB2-KO females show defects in mammary epithelial branching. (A) Representative carmine-stained mammary wholemounts from adult virgin WT and constitutive CPEB1-KO, CPEB2-KO, CPEB3-KO and CPEB4-KO mice. (B) Example of an output image from AngioTool software (Methods). (C) Results from automatic quantification of the number of junctions in the adult virgin mammary gland constitutive models (WT n=11, CPEB1-KO n=4, CPEB2-KO n=10, CPEB3-KO n=5, CPEB4-KO n=4). (D) Representative mammary wholemounts from adult virgin epithelial-specific WT$^{CK14-Cre}$, CPEB1-KO$^{CK14-Cre}$ and CPEB2-KO$^{CK14-Cre}$. (E) Results from automatic quantification of the number of junctions in epithelial-specific models (WT $^{CK14-Cre}$ n=3, CPEB1-$^{CK14-Cre}$ n=3, CPEB2-$^{CK14-Cre}$ n=8).

In addition to morphology and branching, another very relevant aspect in the biology of the mammary gland is the balance between luminal and myoepithelial (Myo) cells. In

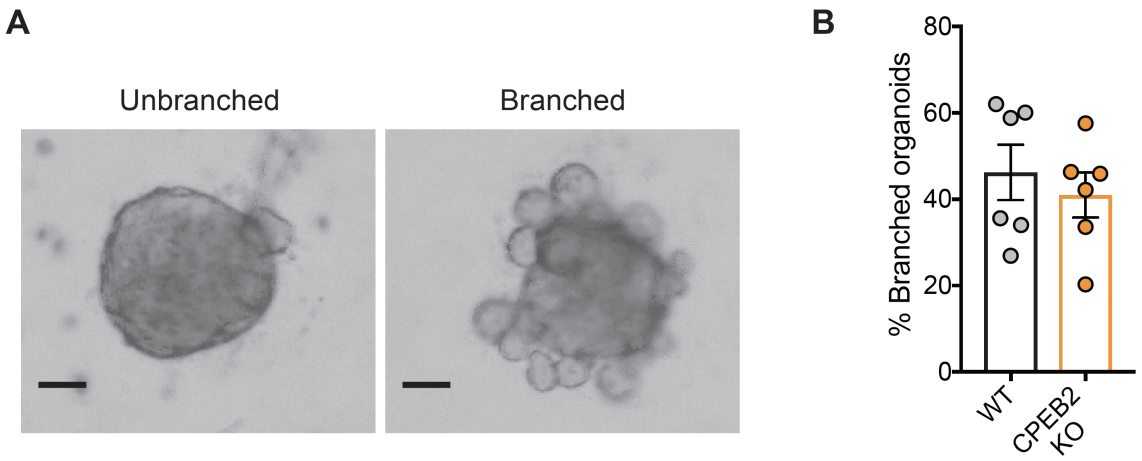

Figure 16: Figure 16. CPEB2 loss does not affect branching *in vitro*. (A) Images from organoids in 3D culture. Scale bar,50 μm. (B) Quantification of the percentage of branched organoids (an organoid was considered branched if it displayed $\geq$3 elongated buds).

fact, an unbalance between these populations could point to a problem in lineage specification. Therefore, we assessed the distribution of luminal and myoepithelial populations by FACS in the four single constitutive CPEB-KO mice (Figure 17A). Our results showed that only the absence of CPEB2 altered the ratio between these populations, favoring the accumulation of luminal over myoepithelial cells (Figure 17B).

4 Role of CPEB2 in pubertal and lactating mammary gland

Considering that deletion of CPEB2, but not of other CPEB-family members, led to defects in branching and populations homeostasis, we sought to examine phenotypes in CPEB2-KO mice at other stages of the mammary gland.

First, we analyzed pubertal mammary wholemounts and we found that CPEB2-KO females presented diminished invasion of the epithelial tree through the fat pad (Figures 18A and 18B). Since in adult mammary gland WT and CPEB2-KO ductal elongation was comparable and the only difference resided in the branching (Figure 15), this result indicates that CPEB2-KO females experience a delay in ductal expansion.

Moreover, we also explored potential problems at lactation by comparing WT and CPEB2-KO mammary wholemounts at mid-pregnancy, when lactogenic differentiation starts. Nevertheless, we did not discern any evident abnormality in these wholemounts (Figure 18C). Furthermore, we monitored the weight of heterozygous pups during breastfeeding and we

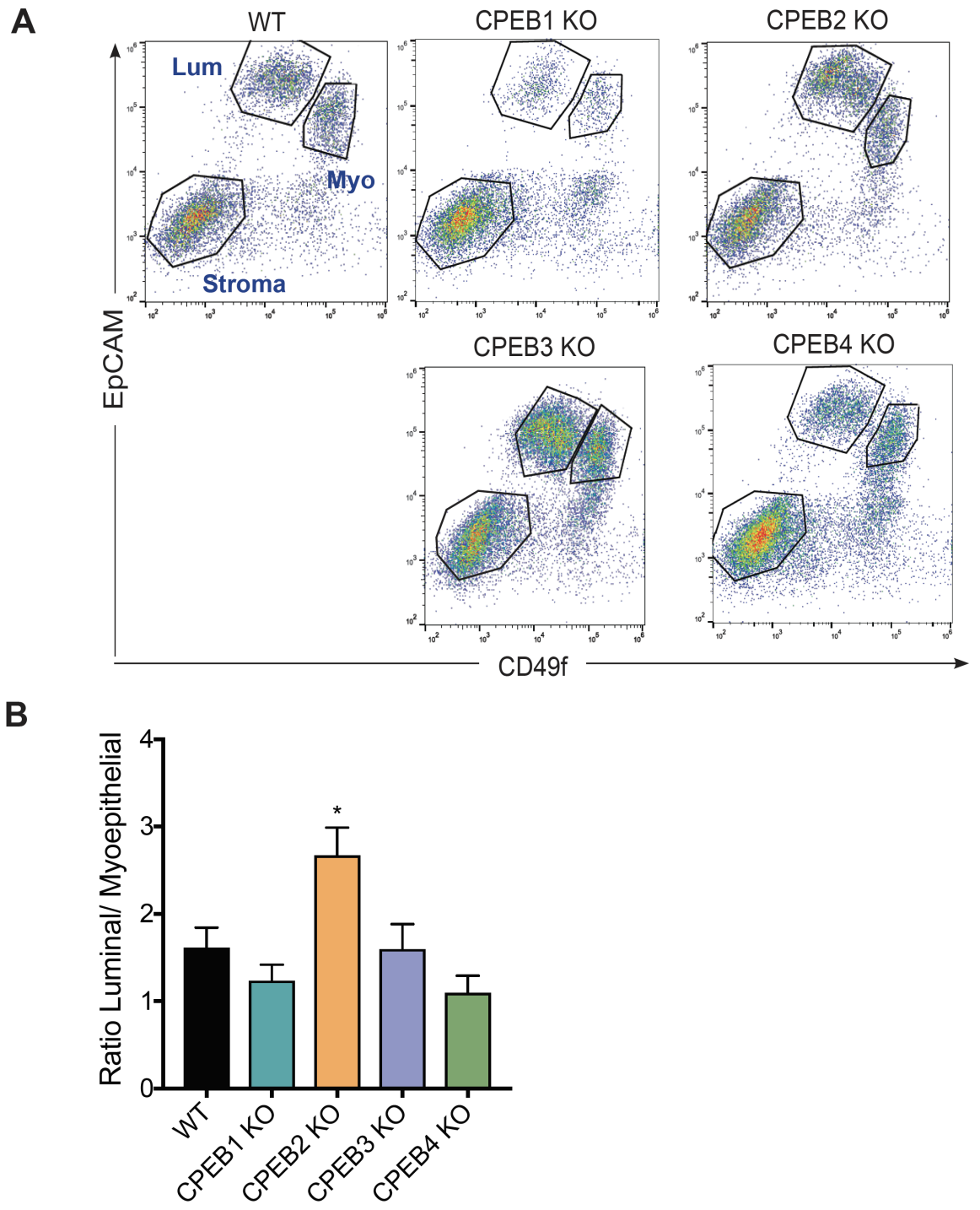

Figure 17: Lack of CPEB2 causes an unbalance in mammary epithelial populations. (A) Representative FACS plots for the indicated genotypes gated on lineage negative cells. Lum, luminal ($EpCAM^{high}CD49f^{low}$). Myo,myoepithelial ($EpCAM^{low}CD49f^{high}$). (B) Ratio between the percentage of luminal and myoepithelial cells gated on lineage negative (WT n=7, CPEB1-KO n=4, CPEB2-KO n=6, CPEB3-KO n=4, CPEB4-KO n=4).

did not observe any difference either (Figure 18D). Therefore, we concluded that CPEB2 is dispensable for lactogenic differentiation in the mammary gland. However, we were puzzled by this finding because *Cpeb2* mRNA levels were peaking at lactation, suggesting a

function for CPEB2 at this stage. Thus, we investigated the possibility of other CPEBs compensating for the lack of CPEB2 in this scenario. Indeed, we found that *Cpeb4* mRNA levels raised in CPEB2-KO mice only in the lactating stage but not in the adult virgin mammary gland (Figure 18E). Thus, CPEB4 could compensate the lack of CPEB2 during lactation. (See Discussion)

Therefore, we concluded that CPEB2 is important for pubertal mammary gland development, but it is replaceable in the process of lactation. In any case, we focused our study in the role of CPEB2 in adult virgin mammary gland encouraged by the phenotypes observed involving branching (Figure 15 and epithelial cell homeostasis (Figure 17.

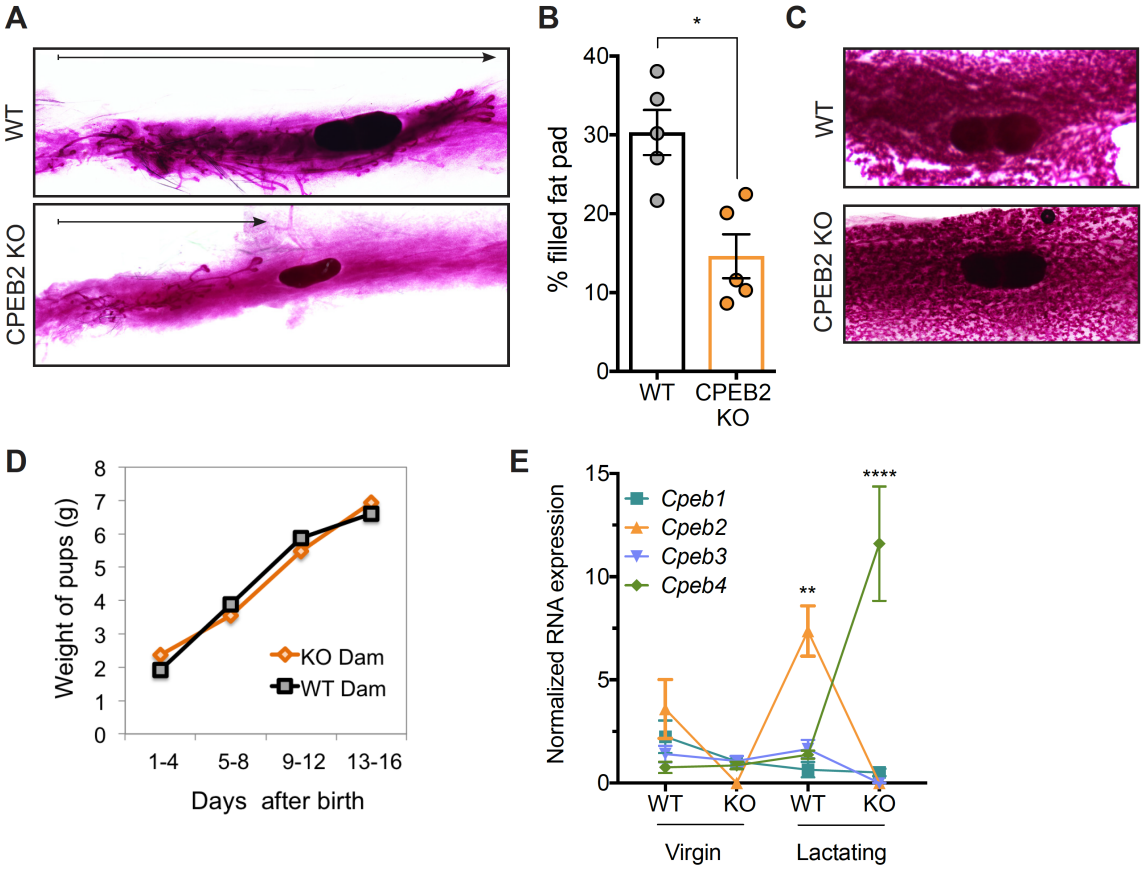

Figure 18: CPEB2 is important for mammary pubertal development but dispensable lactogenic differentiation. (A) Representative mammary wholemounts from pubertal WT and CPEB2-KO females (5 weeks old). (B) Quantification of the area of fat pad filled with epithelial ducts at puberty in WT and CPEB2-KO (n=5) (C) Mammary wholemounts from WT and CPEB2-KO females at mid-pregnancy. (D) Weight of heterozygous pups nursed by WT or CPEB2-KO dams. (E) mRNA levels of *Cpeb1-4* normalized to *Gapdh* in whole tissue mammary gland in adult (n=4) or lactating (n=2) WT and CPEB2-KO females. Statistics with 2way ANOVA, **p<0.01(WT virgin *versus* WT lactating)***p<0.001. KO, CPEB2-KO.

5 CPEB2 controls cell fate in the ductal luminal compartment

Since CPEB2 was highly expressed in the luminal compartment of the mammary gland (Figure 14C), we decided to study the virgin adult luminal population in CPEB2-KO females. When we first chose CD61 as a marker for luminal progenitors (Asselin-Labat et al., 2011), we did not observe any differences between WT and CPEB2-KO mammary epithelial cells (MECs) (Figure 19). Then, because CD49b has been shown to be a more selective marker than CD61 in C57BL/6 mice (Shehata et al., 2012), we switched to a panel with anti-CD49b plus anti-Sca1 antibodies to discern the three luminal populations present in adult virgin mammary gland; ductal differentiated (DD, $Sca1^{+}CD49b^{-}$), ductal progenitors (DP, $Sca1^{+}CD49b^{+}$) and alveolar progenitors (AP, $Sca1^{-}CD49b^{+}$) (Figure 20A) (Shehata et al., 2012).

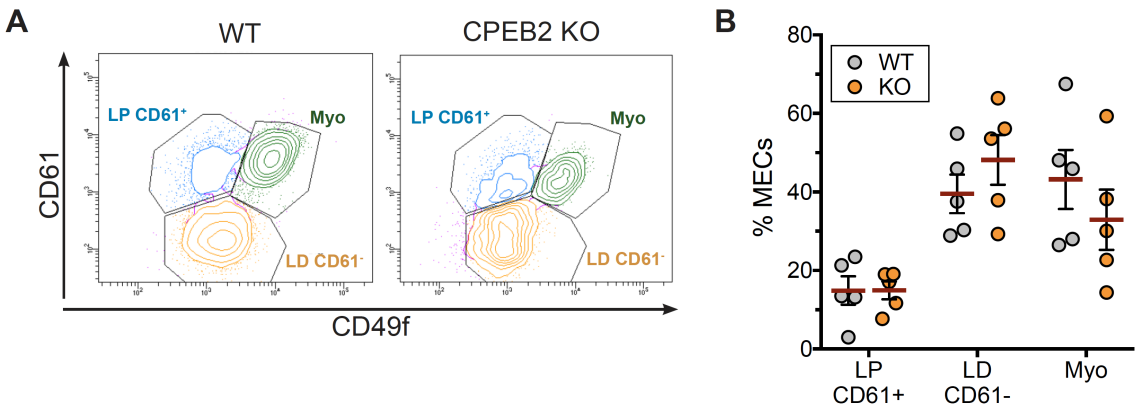

Figure 19: CPEB2-KO MECs do not display any difference compared to WT using CD61 as a luminal progenitor marker. (A) Representative FACS plots gated on mammary epithelial cells. (B) Quantification of Luminal Progenitors (LP, $CD61^{+}CD49f^{low}$), Luminal Differentiated (LD, $CD61^{-}CD49f^{low}$) and Myoepithelial (Myo, $CD61^{+}CD49f^{high}$).

Interestingly, using the latter strategy, we observed that absence of CPEB2 had a great impact on the ductal luminal lineage ($Sca1^{+}$) (Figure 20B), which are the epithelial hormone-sensing cells that express hormone receptors such as estrogen receptor α (ER). Specifically, in CPEB2-KO MECs we observed a significant increase in the percentage of cells included within the gate of ductal progenitors (Figures 20B and 20C) as well as a switch towards higher expression of Sca1 (Figures 20D and 20E). In contrast, alveolar progenitors remained unchanged; going in line with the observation that CPEB2-KO females did not show an obvious phenotype during lactation (Figures 18C and 18D).

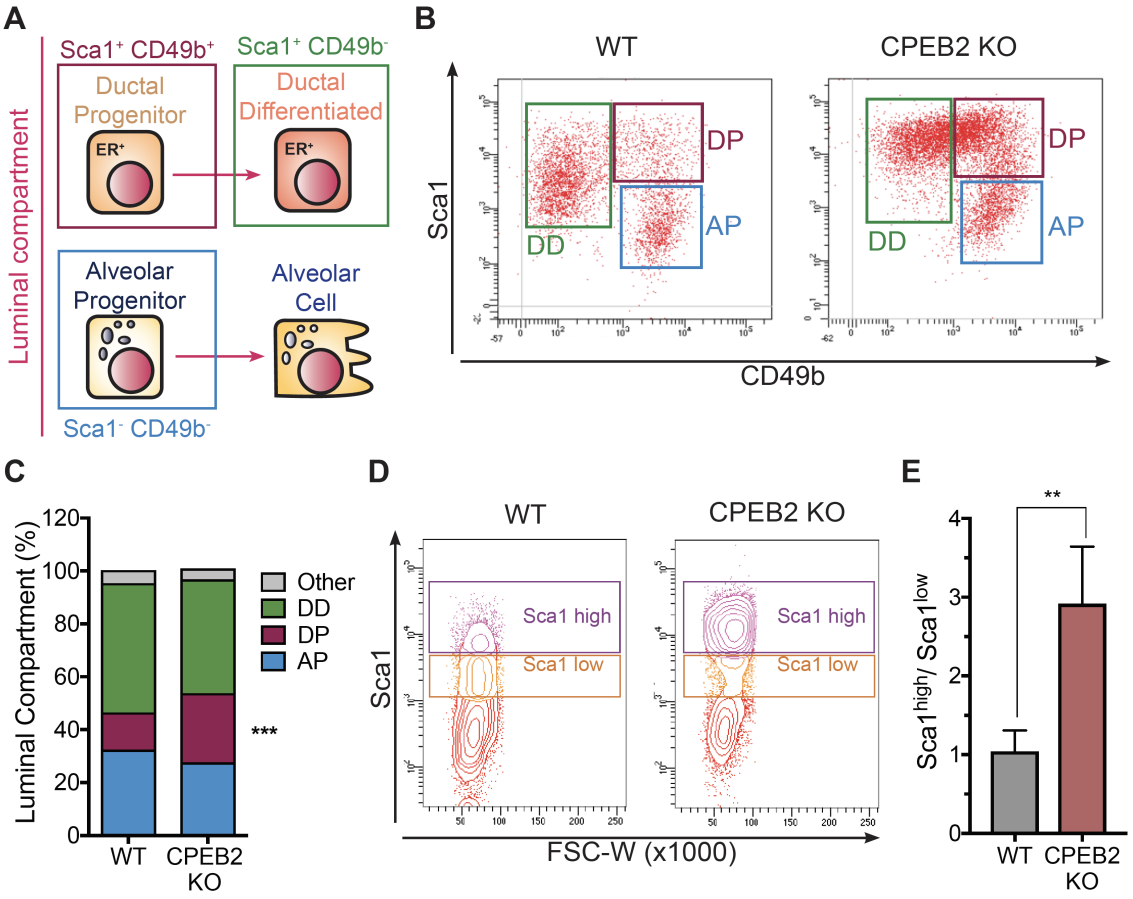

Figure 20: Lack of CPEB2 alters the ductal compartment of the mammary gland. (A) Graphical representation of the two main lineages in the luminal compartment: ductal (hormone-sensing lineage, Sca1^{+}) and alveolar (secretory lineage, Sca1^{-}). (B) Representative FACS plots gated on luminal cells. (C) Quantification of the luminal subpopulations: ductal differentiated (DD, Sca1^{+}CD49b^{-}), ductal progenitors (DP, Sca1^{+}CD49b^{+}) and alveolar progenitors (AP, Sca1^{-}CD49b^{+}). Statistics with 2way ANOVA, ***p<0.001 (n=17). (D) Representative FACS plots gated on luminal cells (E) Ratio of the percentage of Sca1^{high} and Sca1^{low} populations in luminal cells.

To further investigate the identity of these populations in CPEB2-KO mammary glands, we performed transcriptomic analysis of DP, DD, AP and Myo populations in WT and CPEB2-KO adult females using microarrays. Principal Component Analysis (PCA) plots revealed that samples cluster together by populations as expected (Figure 21A). Interestingly, WT and CPEB2-KO specimens seem to be more distant in ductal progenitors than in other populations (Figure 21A). As a quality control for the gating strategy and sample processing, we checked several markers for myoepithelial cells, luminal progenitors and the ductal lineage (Shehata et al., 2012; Visvader & Stingl, 2014). All the markers that we evaluated were expressed following the expected pattern (Figure 21B), indicating that our experimental setup was robust and trustable.

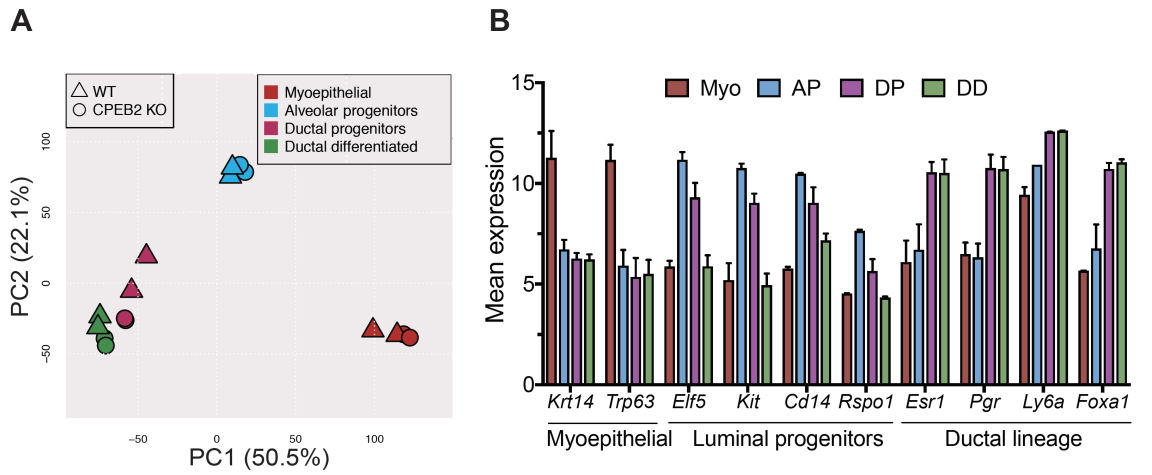

Figure 21: Microarray results confirm an accurate gating strategy. (A) Principal Component Analysis (PCA) for the microarray samples. (B) Mean expression of probes for markers of the various epithelial cell populations.

In addition, we assessed the expression of *Cpeb2* in myoepithelial cells as well as in luminal subpopulations. Our results, not only confirmed enhanced levels of *Cpeb2* mRNA in luminal cells (Figure 14C), but also defined the ductal compartment as the one with the highest *Cpeb2* expression (Figure 22A). In the same direction, ductal progenitors and ductal differentiated cells accumulated more transcriptomic changes (CPEB2-KO *vs.* WT) compared to the other populations (Figure 22B).

As our data so far pointed to a function of CPEB2 in the ductal compartment, we decided to interrogate our microarray data to ask whether CPEB2 could control cell fate in this lineage. To this aim, we generated signatures with differentially expressed genes in WT DP *vs.* WT DD (DP_UP=FC>3; DP_DOWN=FC<-1.5) and we observed that the signature DP_UP was clearly downregulated in CPEB2-KO DP (Figure 22C). Moreover, the expression of individual progenitor markers such as *Elf5*, *Kit*, *Cd14* and *Rspo1* was decreased in CPEB2-KO DP but not in CPEB2-KO AP; where all luminal progenitor markers expect for *Rspo1* remained unchanged in CPEB2-KO compared to WT (Figures 22D and 22E). This piece of data indicated that lack of CPEB2 causes an ER^+-specific phenotype in lineage commitment that did not affect to all luminal progenitors.

These results, coupled with the FACS data and the PCA (Figures 20B and 21A), suggested that, in absence of CPEB2, an intermediate ductal population between progenitors and differentiated ductal cells appears. This putative ductal intermediate population still pos-

sesses certain surface markers characteristic from DPs (such as CD49b), yet it displays attenuated expression of several progenitor markers. In sum, we hypothesized that sorted CPEB2-KO DPs are a mixed population that included, not only progenitors, but also a partially differentiated intermediate population. This hypothesis would explain why CPEB2-KO DPs (mixed-DPs) exhibit decreased expression of the ductal progenitor signature (Figure 22C) and single progenitor markers (Figure 22D). Further, the contribution of this intermediate population would also result in a drop in clonogenic potential of the CPEB2-KO mixed-DPs. Indeed, we clearly observed a diminished number of organoids originated from CPEB2-KO mixed-DPs compared to WT DPs (Figures 22F and 22G). As a negative control, we also plated DD cells that are devoid of clonogenic capacity (Shehata et al., 2012), and we did not observe any difference between WT and CPEB2-KO DD cells (Figure 22G).

6 Proliferation of MECs is decreased in absence of CPEB2

When performing Gene Set Enrichment Analysis (GSEA) with the microarray data, one of the most striking change in all mammary epithelial populations was a drop in categories related to cell cycle and proliferation in the CPEB2-KO; such as *G2M checkpoint* and *E2F targets* on top of the heatmap (Figure 23A). Corroborating the transcriptomic data, there were less Ki67+ proliferative cells in the mammary glands of adult CPEB2-KO females compared to WT (Figures 23B and 23C). As a definitive proof that proliferation was affected in CPEB2-KO MECs, we performed EdU incorporation experiments (see Methods). Briefly, EdU is a thymidine analogue that is incorporated into DNA when cells divide and it can be detected by FACS. After a 6-hours pulse, we observed that CPEB2-KO mammary epithelial cells incorporated almost no EdU (Figures 23D and 23E). Therefore, we found that all CPEB2-KO MECs displayed reduced proliferation, and this was not specific of ductal cells where CPEB2 is highly expressed (Figure 22A), suggesting a role of CPEB2 in the paracrine response to steroid hormones. Note that apoptosis was negligible in adult mammary gland both WT and CPEB2-KO (Figure 23F).

Additionally, we also investigated which pathways were upregulated in CPEB2-KO MECs compared to WT. In general lines, we observed that the category *TNFα signaling via NFκB* was common to all four populations and that DPs and DD display the same top five upregulated hallmarks (Figure 24A). In fact, it was quite puzzling for us to see *Estrogen response* as an upregulated category, given that estrogen triggers proliferation in the mammary gland, contrary to what we had observed in CPEB2-KO (Figure 23). To shed light on this issue, we

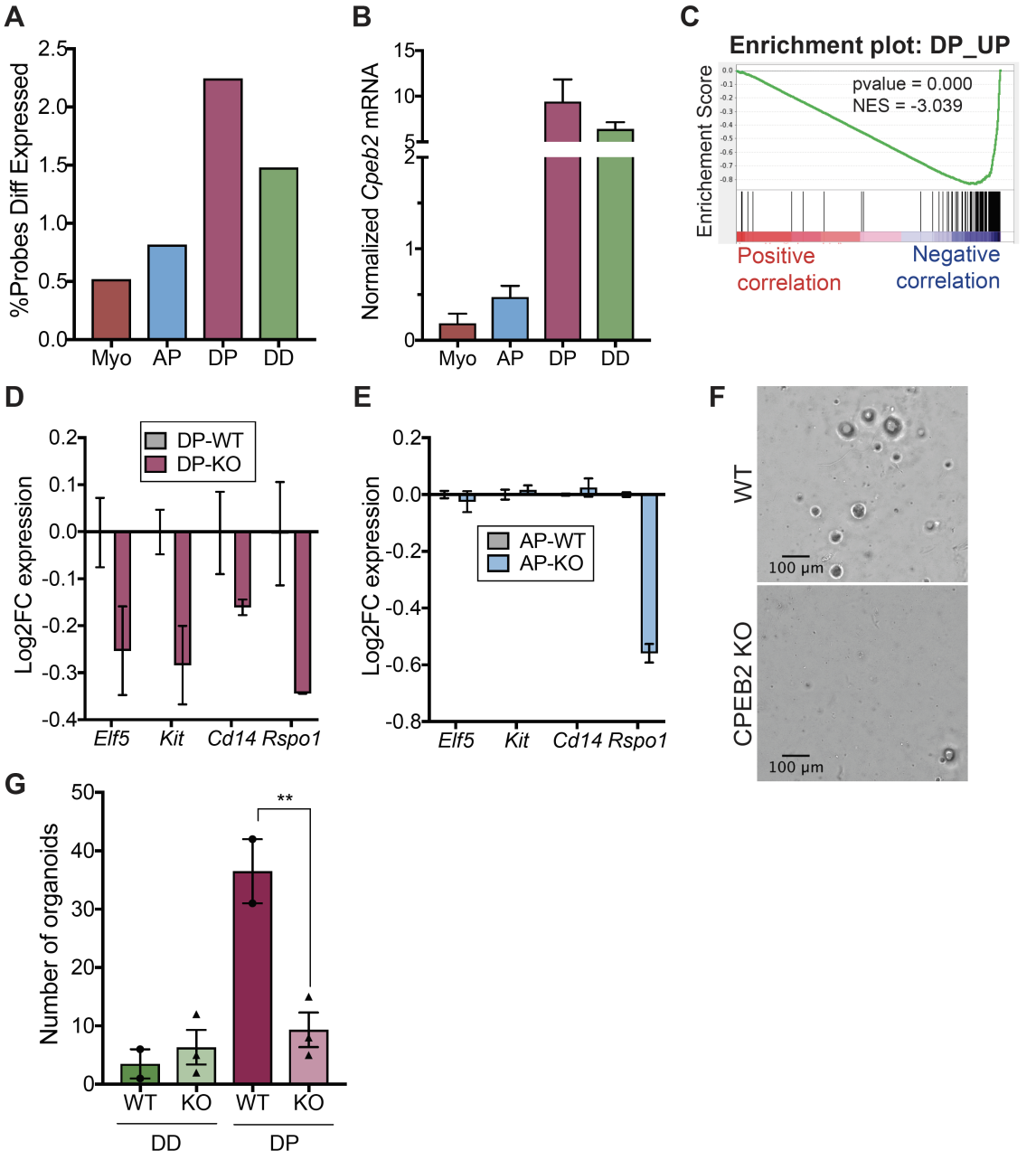

Figure 22: CPEB2 controls cell fate in the ductal lineage. (A) *Cpeb2* expression levels in the microarray samples. (B) Percentage of probes differentially expressed comparing CPEB2-KO and WT populations. (C) Gene Set Enrichment Analysis (GSEA) plot showing correlation between CPEB2-KO DP and signature of WT DP. NES, normalized enrichment score. (D) Expression of luminal progenitor markers in WT and CPEB2-KO ductal progenitors (DPs). (E) Expression of luminal progenitor markers in WT and CPEB2-KO alveolar progenitors (APs). (F) Representative images of organoids from sorted WT and CPEB2-KO DPs. (G) Automatic quantification of the number of organoids from sorted ductal differentiated (DD) or ductal progenitor (DP) cells. Throughout the figure, CPEB2-KO DP refers to the CPEB2-KO mixed-DP population found in absence of CPEB2.

examined by qPCR the levels of estrogen and progesterone receptors (*Esr1* and *Pgr*, respectively) as well as of effectors downstream the latter receptor, such as *Rankl*, *Wnt4*, *Ccnd1*

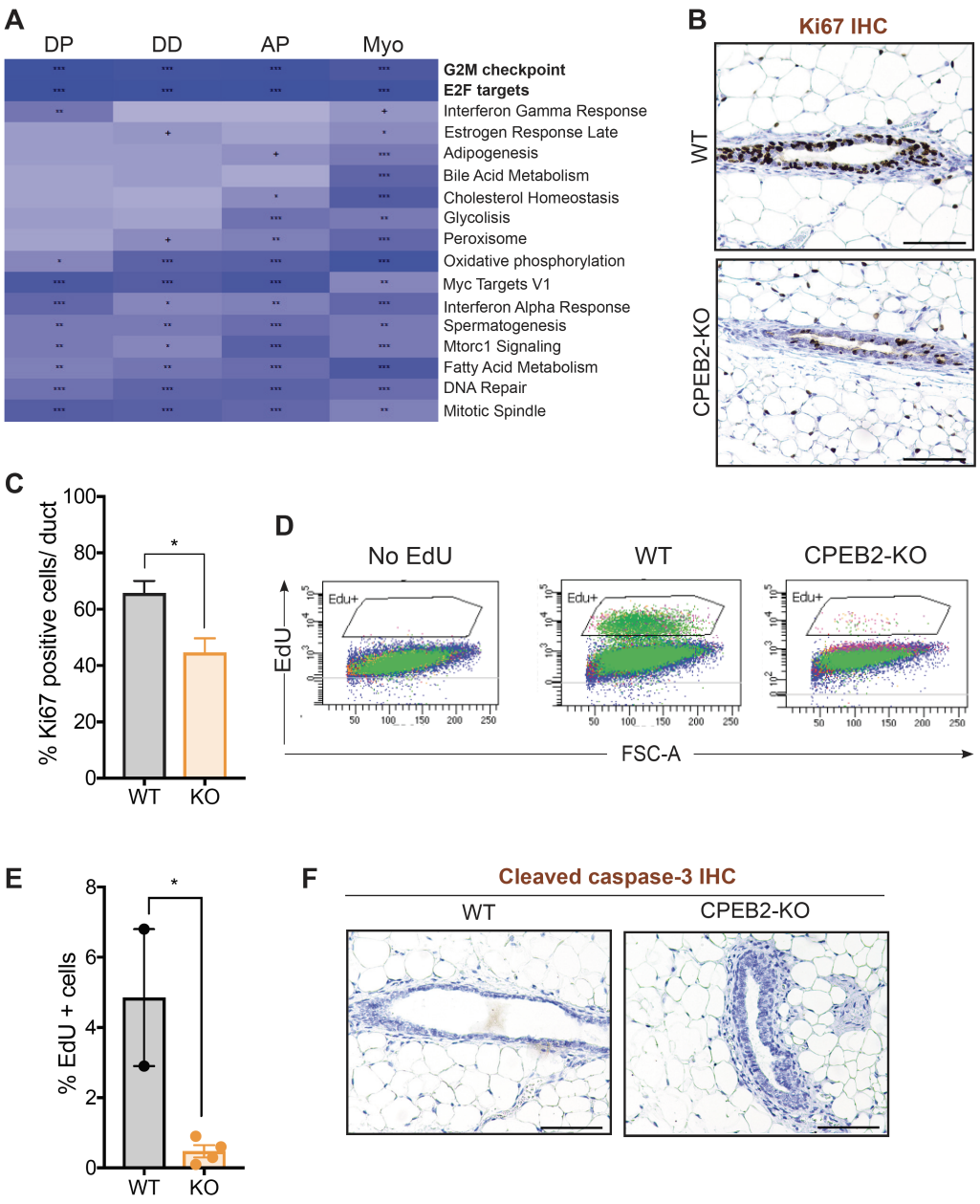

Figure 23: Mammary epithelial cells proliferate less in absence of CPEB2 (A) Heatmap illustrating expression changes from the microarray data. Specifically, hallmark gene sets (Broad Institute) downregulated in CPEB2-KO compared to WT are represented. FDR +/ */ **/ *** for 0.25/ 0.10/ 0.005/ 0.01. (B) Representative images of Ki67 positive cells by IHC in adult virgin mammary gland WT and CPEB2-KO. Scale bar, 50 μm. (C) Automatic quantification of Ki67 positive cells (n=7, average of 10 fields per animal). (D)Representative FACS plots (gated on Lineage negative) of EdU incorporation in not-injected (No EdU), WT or CPEB2-KO mice. (E) Percentage of EdU$^+$ cells within the Lineage negative population. Statistics with two-tailed unpaired Student's *t*-test, *p<0.05. (F) Representative fields of cleaved caspase-3 staining in the adult mammary glands with the indicated genotype.

(Cyclin D1), *Stat5a* and *Calca* (Calcitonin) (Grimm et al., 2016). Our results showed that both *Esr1* and *Pgr* as well as some progesterone-target genes like *Ccnd1* and *Stat5a* were indeed

upregulated, but this was not the case for all of them and, in any case, not at the same extent as progesterone receptor (Figure 24B).

Further, we decided to validate some of these results at the protein levels. Interestingly, we confirmed an increased number of ER positive cells in CPEB2-KO mammary ducts (both constitutive and epithelial-specific) compared to WT (Figures 24C and 24D). This piece of data fits with our previous result of more cells expressing higher levels of Sca1 in CPEB2-KO MECs (Figures 20D and 20E). However, we could not corroborate higher protein levels of progesterone-driven genes like Stat5a (Figure 24E). Hitherto, our results suggested that, in CPEB2 KO MECs, increase of ER expression does not correlate with enhanced ER downstream signaling. Thus, we believe that CPEB2 may be required for correct proliferation downstream hormone receptors and that the enhancement of the *Estrogen response* pathway at the transcriptomic level in CPEB2-KO may be a compensation mechanism to try to counterbalance the lack of proliferation. In order to investigate the molecular mechanisms by which CPEB2 controls proliferation as well as cell-fate and hormone response in the ductal ER^+ compartment, we aimed to identify the mRNAs recognized by CPEB2 in MECs.

7 CPEB2-bound mRNAs in mammary epithelial cells

Since CPEB2 is an RNA-binding protein that regulates translation of its targets, the transcriptomic data alone is not enough to understand the function of CPEB2 in mammary epithelial cells. For this reason, in order to identify the mRNAs bound by CPEB2, we performed RNA-immunoprecipitation (RIP) with a specific anti-CPEB2 antibody, followed by Illumina sequencing in WT MECs. In parallel, as a negative control, same conditions were used in CPEB2-KO MECs. Western blot results showed a clean immunoprecipitation (IP) of endogenous CPEB2 only in WT conditions (Figure 25A); conversely, CPEB2-KO IP determined the background noise of mRNAs that might be bound by the anti-CPEB2 antibody.

Considering that there were not major transcriptomic changes in the Inputs, our first approach to identify RIP target genes was to measure overall RIP 3'UTR signal enrichment in WT *vs.* CPEB2-KO RIP samples (DESeq2, BHpvalue<0.05 and FC>2); this analysis returned a list of 279 CPEB2-bound mRNAs in MECs (RIP targets). Further, results from an interaction analysis taking into account the corresponding Input samples (DESeq2, interaction BH-pvalue<0.1) resulted in a reduced list of 169 high-confidence CPEB2-target

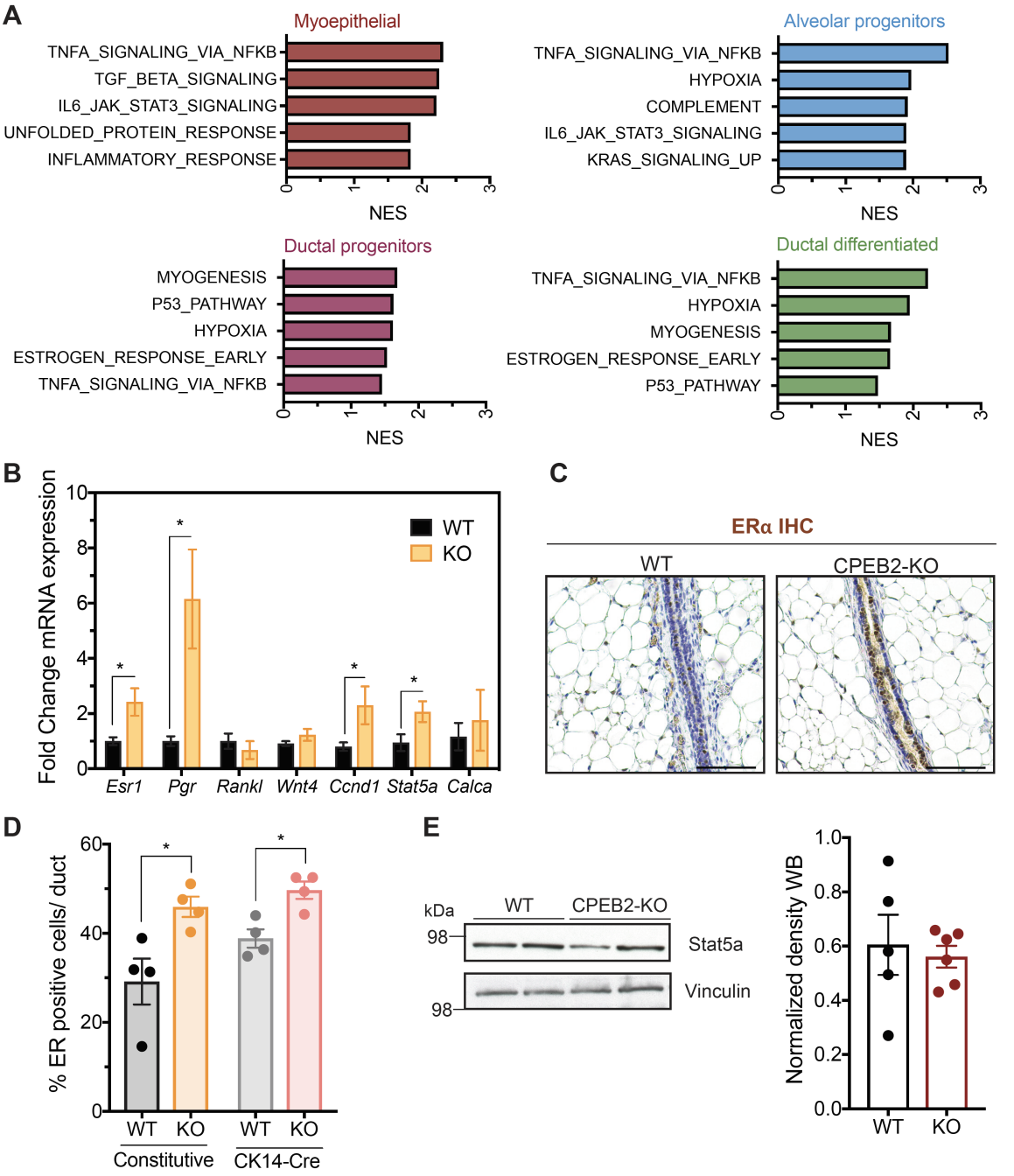

Figure 24: Upregulation of the *Estrogen response* pathway at the transcriptomic level in CPEB2-KO ducal cells might be a compensation mechanism (A) Normalized enrichment score of hallmark gene sets (Broad institute) upregulated in CPEB2-KO *vs.* WT in the different epithelial populations. Only top five categories with the highest enrichment scores and p-value<0.05 are depicted. (B) mRNA levels in total adult mammary gland homogenates normalized to *Gapdh* and to the WT values (n=6). (C) Representative images of ERα positive cells by IHC in adult virgin mammary gland WT and CPEB2-KO. Scale bar, 50 μm. (D) Automatic quantification of ERα positive cells in the constitutive and epithelial-specific models (n=4, average of 10 fields per animal). (E) Western Blot image and quantification for Stat5a and Vinculin as a control. Same amounts of protein lysates from isolated mammary epithelial cells from the indicated genotypes were loaded.

genes (RIP targets_HC) (Table 3). In both cases, when running the CPE prediction algorithm (Piqué et al., 2008), the two datasets were highly enriched in genes containing CPE motifs (UUUUUA$_{1-2}$U) in their 3'UTRs compare to whole transcriptome (Figure 25B).

Gene ontology of the high-confidence RIP-targets showed that CPEB2 binds mRNAs involved in polarity (*Dorso-ventral axis formation* and *Hedgehog signaling*), stemness (*Wnt signaling*), malignancy (*Pancreatic cancer*, *Pathways in cancer* and *Ras signaling*) and rapid signaling downstream receptors via G proteins (*PI3K-Akt signaling*, *Rap1 signaling* and *cGMP-PKG signaling*) (Figure 25C). Notably, many of the aforementioned pathways also appeared as significant categories when interrogating the broader dataset of RIP target genes (Figure 25D). Interestingly, the group of high-confidence CPEB2-target genes (Table 3) included transcripts for ephrin ligands (such as *Efna1*, *Efnb1* and *Efnb2*) that, besides their important role in tissue architecture (Merlos-Suárez & Batlle, 2008) , have been suggested to influence luminal cell fate in the mammary gland (Kaenel et al., 2012a). Moreover, *Wnt5a* (a non-canoninal Wnt ligand that regulates branching downstream TGF-β (Roarty & Serra, 2007)) and *Kit* (a marker for luminal progenitors) were also identified as high-confidence target mRNAs of CPEB2 in MECs. Nonetheless, we decided to examine other targets directly linked to proliferation in the mammary gland.

8 CPEB2 regulates translation of *Rankl* mRNA

Remarkably, one of the top enriched CPEB2-target genes was *Ccnd1* (CyclinD1); which is a key mediator of proliferation downstream progesterone receptor. Indeed, integrated genomic viewer (IGV), we could appreciate that reads for *Ccnd1* were clearly enriched in RIP_WT compared to RIP_KO (Figure 26A). To further investigate the possibility of CPEB2 regulating the translation of *Ccnd1*, we assessed its mRNA and protein expression in absence of CPEB2. Western-blot analysis suggested that CyclinD1 protein amount might be decreased in CPEB2-KO samples compared to WT. In both isolated MECs or in whole mammary gland tissue, we could observe a tendency in CPEB2-KO mice to have lower levels of CyclinD1 protein (Figure26B). Regarding mRNA expression, *Ccnd1* was diminished only in myoepithelial cells but not in other epithelial compartments (Figure 26C), or in the whole mammary tissue (Figure 24B). Therefore, CPEB2 could be responsible for *Ccnd1* translational activation; nevertheless, more experiments are needed to confirm this hypothesis and, additionally, expression changes due to transcription cannot be completely excluded.

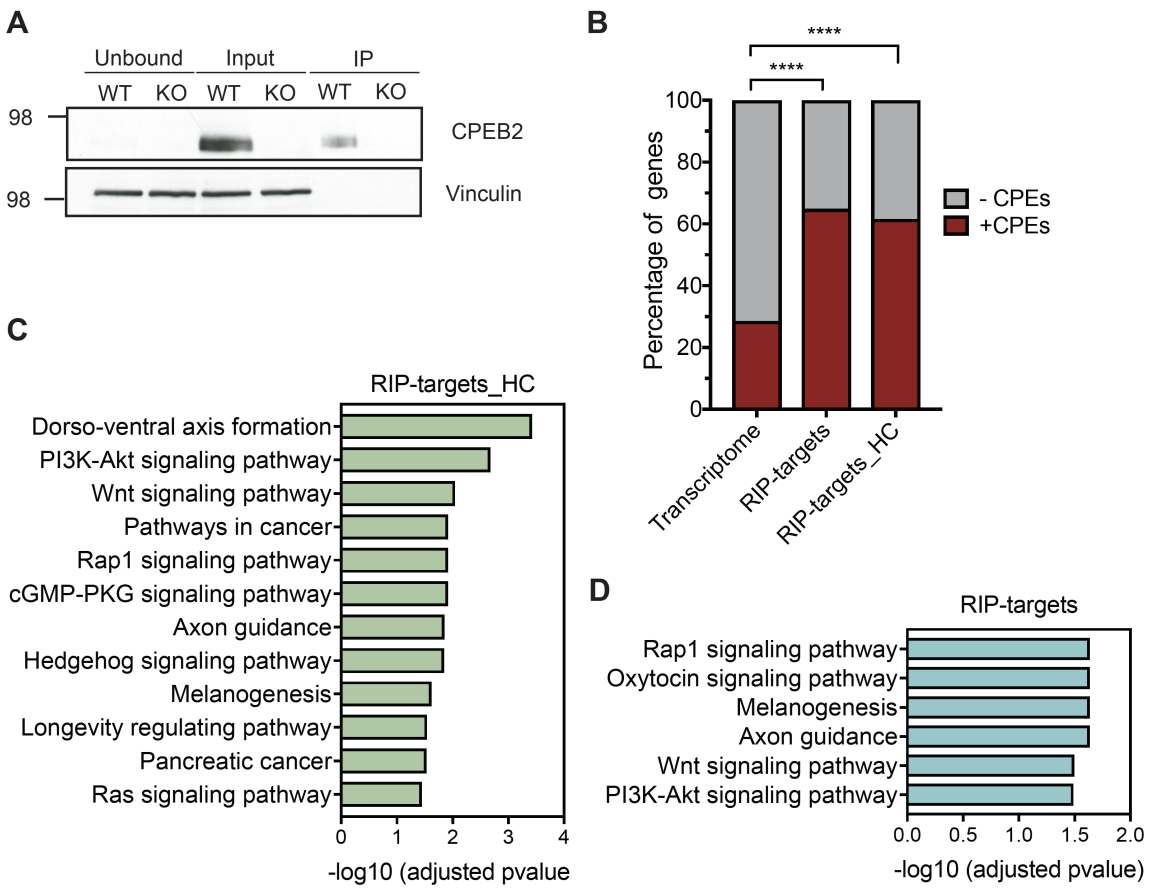

Figure 25: CPEB2-bound mRNAs are involved in polarity, stemness, malignancy and rapid signaling to hormones. (A) Western blot for CPEB2 and Vinculin as a control from unbound, input and immunoprecipitated fractions with anti-CPEB2 antibody in WT and CPEB2-KO MECs. (B) Percentage of genes with (+CPEs, red) or without (-CPEs, grey) in the 3'UTR, comparing RIP-targets *vs.* the mouse transcriptome. Statistics with Fisher's exact test, ****p<0.0001. (C) Significantly enriched KEGG pathways (adjusted p-value<0.05) based on high-confidence (HC) RIP-targets analyzed by Enrichr tool (D) Significantly enriched KEGG pathways (adjusted p-value<0.05) based on the broader group of RIP-targets analyzed by Enrichr tool.

When exploring the possibility of other master effectors of hormone-driven proliferation being regulated by CPEB2, we found out that *Rankl* mRNA (*Tnfsf11*) could be a potential CPEB-target gene since its 3'UTR harbors a nice arrangement of CPE motifs (Figure 27A). Although *Rankl* was enriched in RIP_WT *vs.* RIP_KO, it was excluded from our RIP-Seq analysis because of presenting a low number of reads. Hence, we checked by RIP-qPCR whether *Rankl* mRNA was bound by CPEB2. Remarkably, *Rankl* was immunoprecipitated with the specific anti-CPEB2 antibody only in WT conditions, meaning that the binding was CPEB2-specific (Figure 27B). The levels of *Rankl* mRNA remained unchanged comparing WT and CPEB2-KO epithelial cells (Figure 27C); same results were appreciated in whole mammary gland tissue (Figure 24B). Strikingly, RANKL protein levels were greatly decreased in ab-

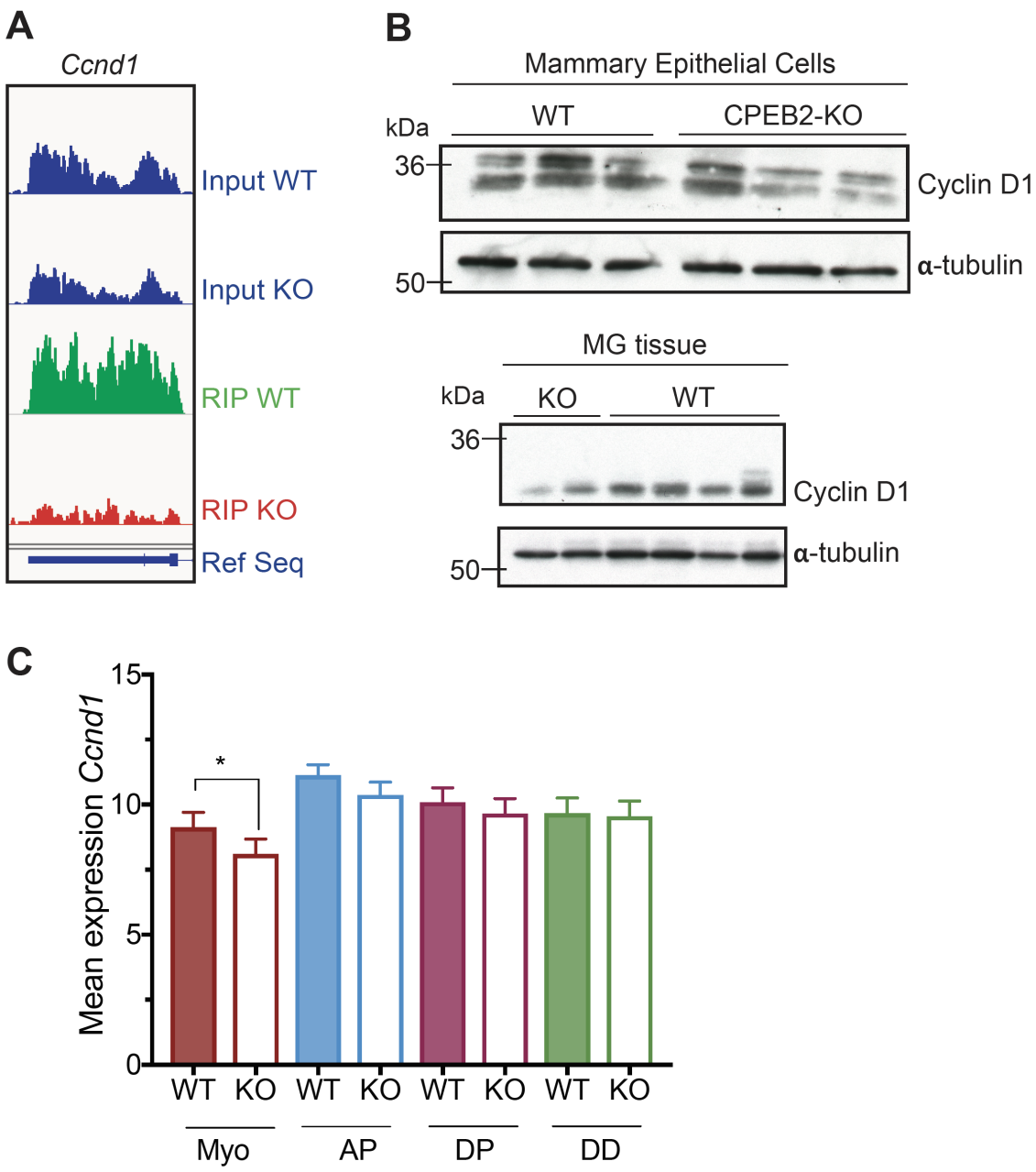

Figure 26: *Ccnd1* mRNA as a potential target of CPEB2. (A) Snapshot of RIP-Seq data for *Ccnd1* 3'UTR depicts normalized RIP-seq coverage for Inputs (blue), WT RIP (green) and KO RIP (red). Image obtained using the integrated genomic viewer (IGV). (B) Western Blot images for CyclinD1 and α-tubulin as a control. Same amounts of protein lysates from either isolated mammary epithelial cells (upper panel) or total adult mammary gland tissue (lower panel) from the indicated genotypes were loaded. KO, CPEB2-KO. (C) Expression of *Ccnd1* mRNA in myoepithelial cells and luminal subpopulations (array data), *pvalue<0.01 (see Methods).

sence of CPEB2 (Figure 27D). Therefore, our results demonstrated that *Rankl* was indeed a bona fide CPEB2-target mRNA and that CPEB2 acted as a translational activator of *Rankl* in mammary epithelial cells. Nicely, lack of CPEB2 lessened RANKL levels only in mammary epithelial cells but not in the immune cells present in the mammary lymph node (Figure

27E).

Additionally, an extra layer of regulation might be occurring upon acute activation of the progesterone receptor. It has been previously reported that RANKL expression is highly induced by the progesterone derivative MPA (Gonzalez-Suarez et al., 2010; Schramek et al., 2010); however, treatment with MPA did not increase *Rankl* levels in epithelial-specific CPEB2-KO (Figure 27F).

9 *Cpeb2* in breast cancer patients

Thus far, we have revealed that CPEB2-KO mammary epithelial cells showed aberrant ductal lineage commitment, and that CPEB2 is a novel key mediator of the paracrine response to progesterone. Remarkably, both of these processes are of paramount relevance for breast cancer development (Brisken, 2013; Visvader & Stingl, 2014). Thence, we decided to investigate a potential role of CPEB2 in breast cancer.

As a starting point, we analyzed the expression of *Cpeb2* mRNA in breast tumors classified by PAM50 molecular subtype (Parker et al., 2009), using both TCGA and Metabric cohorts (Curtis et al., 2012; Cerami et al., 2012). First, the TCGA RNA-seq dataset allowed us to examine tumor samples as well as the adjacent healthy tissue. With this analysis, we observed that, in most breast cancer subtypes, *Cpeb2* was differentially expressed comparing normal (healthy, H) to cancerous (tumor, T) samples. Notably, *Cpeb2* levels displayed facing patterns; CPEB2 expression was decreased in basal-like and Her2 tumors, while it was enhanced in Luminal A tumors (Figure 28A). Similarly, the same conclusion was evident when interrogating the Metabric dataset (Figure 28B). Analysis of *Cpeb2* expression in distinct breast cancer subtypes compared to the Normal-like subtype, which exhibits a normal breast tissue expression profiling (Perou et al., 2000), showed declined *Cpeb2* levels in Basal-like (pvalue<2.22e-16) and HER2 (pvalue=1.50e-13) subtypes, but increased expression for Luminal A (pvalue=8.21e-15) and Luminal B (pvalue=1.15e-13).

Furthermore, we also analyzed whether *Cpeb2* expression could influence overall survival of breast cancer patients. Given that breast cancer profiles included in TCGA possess too little information about death events, we used the Metabric cohorts for our survival analysis. We observed that, for basal-like breast cancer, low levels of CPEB2 correlated with poor prognosis (Figure 29A). On the contrary, for Luminal A tumors, there was a trend as-

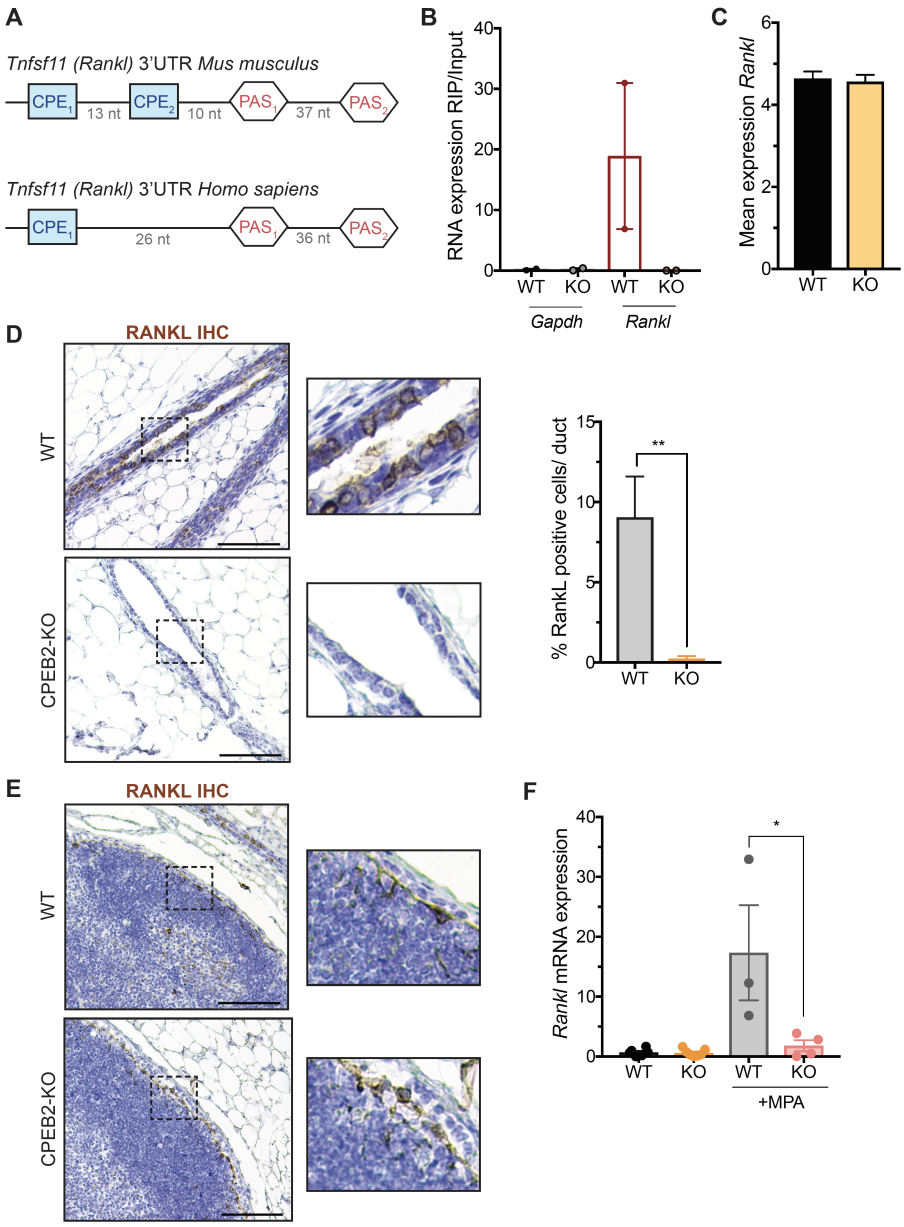

Figure 27: CPEB2 controls synthesis of RANKL. (A) Schematic representation of the endings of the 3'UTR of *Tnfsf11* (mRNA for RANKL) in mouse and human. Canonical cytoplasmic polyadenylation elements (CPEs) and polyadenylation signals (PAS) are depicted, as well as the distance in nucleotides (nt) between such motifs. (B) RIP-qPCR results showing the RIP values normalized by each Input (n=2 animals, each point is an average of 3 experimental replicates per sample). *Gapdh* mRNA and RIP in CPEB2-KO MECs are used as negative controls for enrichment in RIP *vs.* Input . (C) Expression of *Rankl* mRNA in MECs (array data). (D) Representative images and manual quantification of RANKL positive cells by IHC in adult virgin mammary gland WT and CPEB2-KO (n=6, average of 5 fields per animal). Scale bar, 50 μm. (E) Representative images of RANKL positive cells by IHC in lymph nodes, same samples as in (D) are shown. Scale bar, 50 μm. (F) *Rankl* mRNA levels normalized to *Gapdh* in untreated animals or injected with MPA. Not-injected animals (n=7), WT+MPA (n=3), KO+MPA (n=4). KO, CPEB2-KO. For the MPA injection experiment: WT, WT$^{\mathrm{CK14-Cre}}$ and KO, CPEB2-KO$^{\mathrm{CK14-Cre}}$.

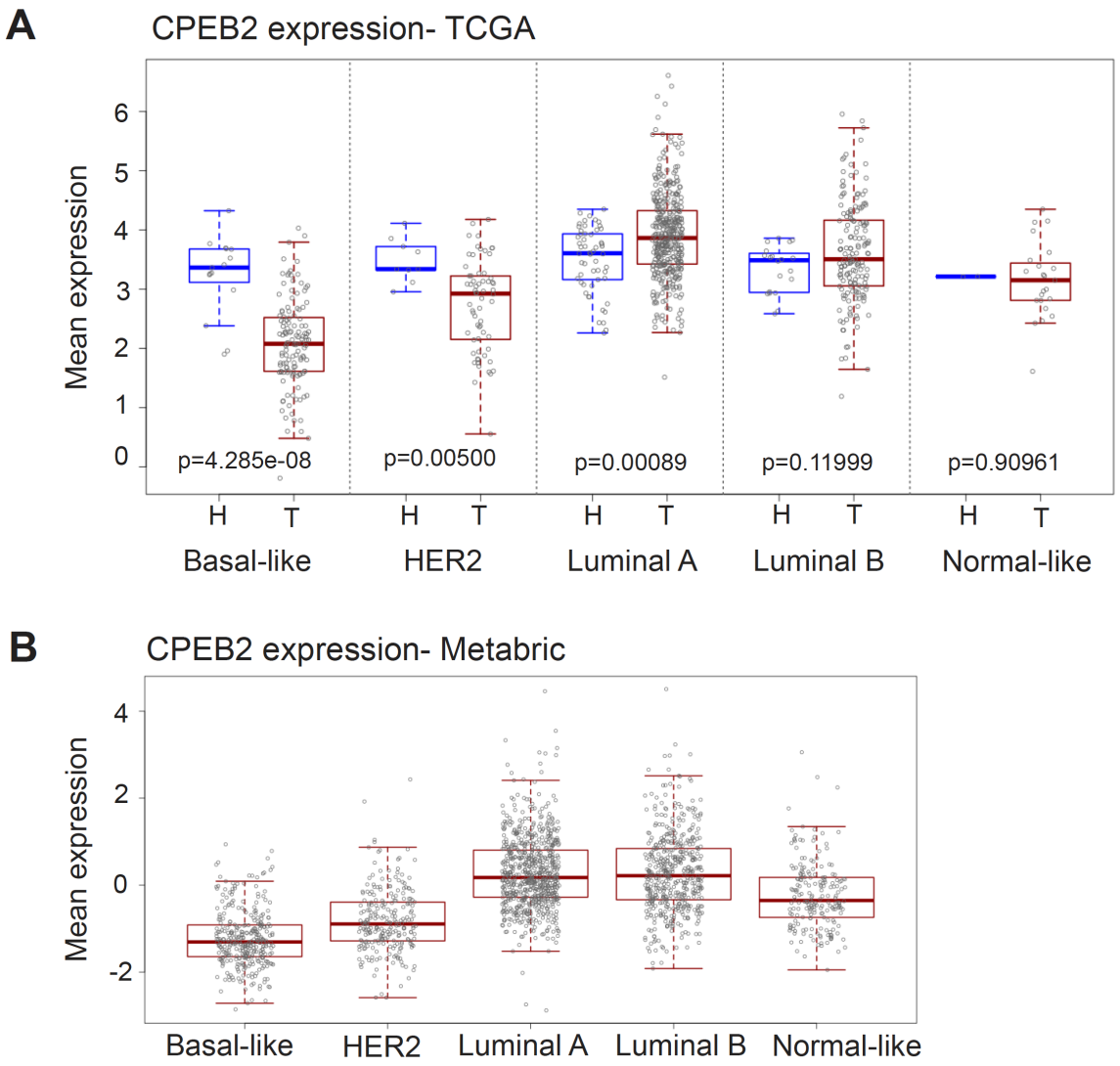

Figure 28: CPEB2 presents opposite expression patterns in different breast cancer subtypes. (A) Box plots for mean RNA expression of CPEB2 in the PAM50 subtypes, analysis with TCGA dataset (Genomic Data Commons). H, adjacent healthy tissue. T, tumor sample. p-values indicated in the graph. (B) Box plots for mean RNA expression of CPEB2 in the PAM50 subtypes, analysis with Metabric dataset (CBioportal).

sociating low expression of CPEB2 with better survival (Figure 29B). Notably, these results fit with the expression profiles of CPEB2 in breast cancer patients (Figure 28); indicating that basal-like and luminal A tumor progression require low and high levels of CPEB2, respectively. Accordingly, there was a strong correlation between *Cpeb2* and *Esr1* (Figure 29C), suggesting a dependence of ER^+ tumors on CPEB2. Nonetheless, luminal B tumors exhibit an opposite behavior compared to luminal A, since they seem to express high *Cpeb2* levels (Figure 28B) but increased *Cpeb2* correlates with good prognosis (Figure 29D). On the other hand, there was no association between *Cpeb2* mRNA and overall survival in either HER2 (Figure 29E) or normal-like (Figure 29F) subtypes.

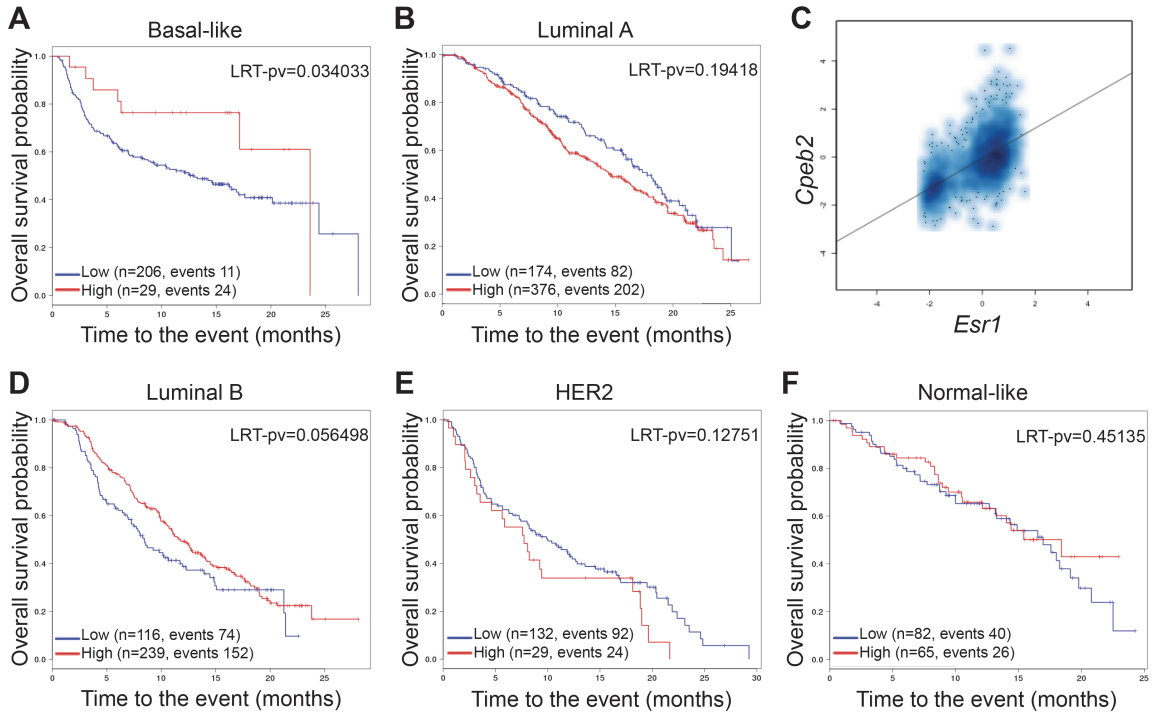

Figure 29: High *Cpeb2* levels correlate with good and poor prognosis in Basal-like and Luminal A breast cancer, respectively. (A) Kaplan-Meier survival curves for basal-like breast cancer. (B) Kaplan-Meier survival curves for Luminal A breast cancer. (C) Correlation of *Cpeb2* with *Esr1* in the Metabric cohort. p-value<2.22e-16. (D) Kaplan-Meier survival curves for Luminal B breast cancer. (E) Kaplan-Meier survival curves for HER2-positive breast cancer. (F) Kaplan-Meier survival curves for normal-like breast cancer. Low, low expression of *Cpeb2* (blue line). High, high expression of *Cpeb2* (red line).

10 CPEB2-KO mice are highly protected against luminal breast cancer

The differential expression of *Cpeb2* in breast cancer, as well as the correlation with prognosis, prompted us to explore the function of CPEB2 in breast tumorigenesis *in vivo*. Taking into account the role of CPEB2 in mediating an effective signaling downstream steroid hormones (Figures 24 and 27), we focused our attention on the study of luminal tumor progression. For this purpose, we initiated a chemical-induced breast cancer model that combined the action of the synthetic progestin medroxyprogesterone (MPA), plus the effect of the mutagenic agent 7,12-dimethylbenz(a)anthracene (DMBA) (Aldaz et al., 1996; Wan et al., 2014). Compared to DMBA alone, the action of MPA, enhancing proliferation of the mammary epithelium, shrinks tumor latency and prevents complications due to non-mammary tumor related mortality (Aldaz et al., 1996). Because most of our data pointed to an epithelial cell-autonomous phenotype (Figures 15E, 22, 24C, 27D and 27E), and in order to solely assess the contribution to carcinogenesis of CPEB2 in the mammary epithelia, we

chose to perform the *in vivo* breast tumorigenesis protocol using the CK14-Cre model.

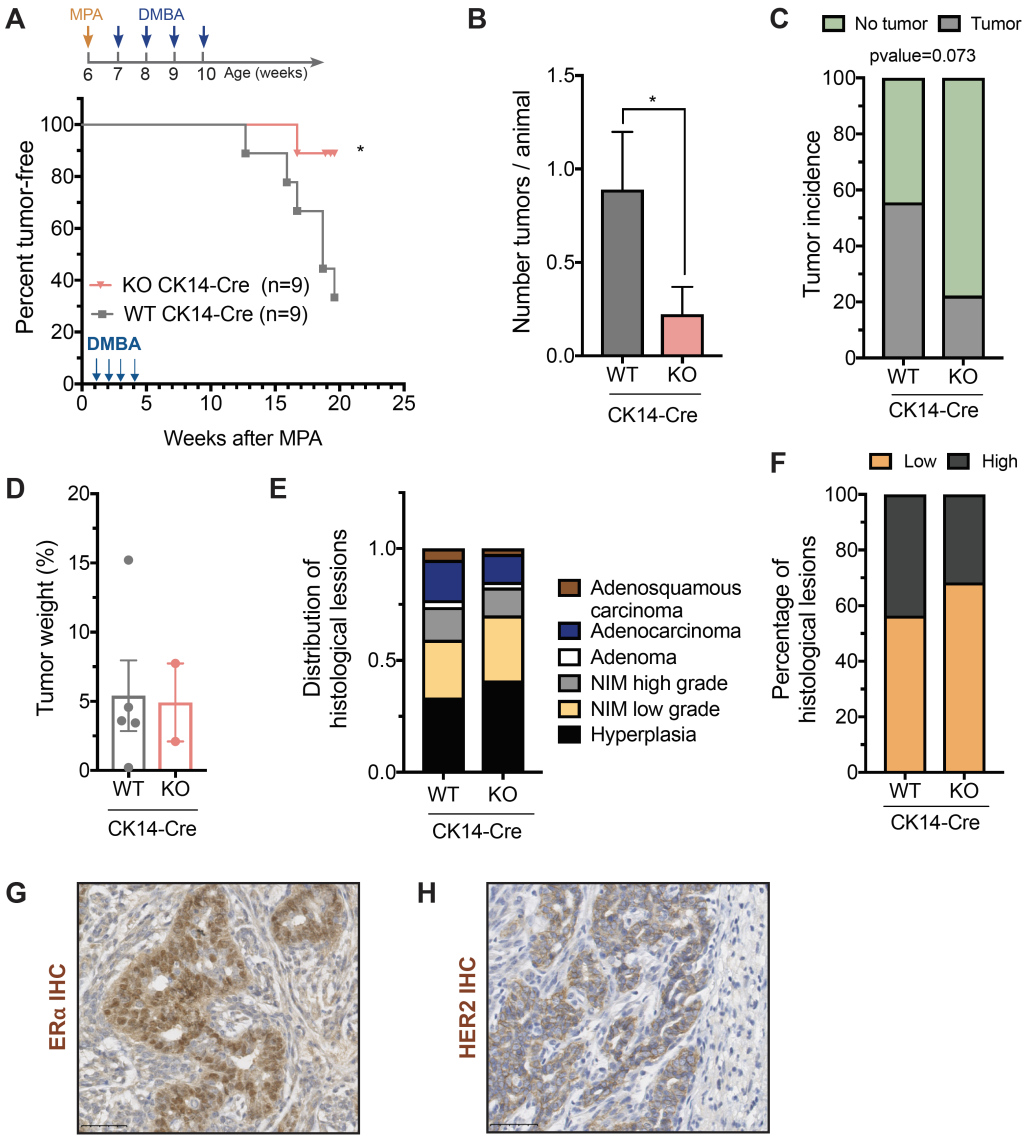

Figure 30: CPEB2 absence protects against luminal breast cancer. (A) Schematic representation of the chemical-induced breast cancer model (see Methods) and kinetics of mammary tumor onset in mice with the indicated genotype treated with MPA and DMBA as indicated. Statistics with Log-rank test, *p<0.05. (B) Number of macroscopic tumors per animal at time of sacrifice (16 weeks after MPA) in $WT^{CK14-Cre}$ (n=9) and $CPEB2^{CK14-Cre}$ (n=9). Statistics with two-tailed unpaired Student's *t*-test, *p<0.05. (C) Tumor incidence in $WT^{CK14-Cre}$ (n=9) and $CPEB2^{CK14-Cre}$ (n=9). Statistics with Chi-square test. (D) Normalized tumor weight in $WT^{CK14-Cre}$ (n=5) and $CPEB2^{CK14-Cre}$ (n=2). (E) Distribution of histological lesions in $WT^{CK14-Cre}$ (n=9) and $CPEB2^{CK14-Cre}$ (n=9) classified according to *Annapolis* nomenclature. MIN, mammary intra-epithelial neoplasia. (F) Percentage of histological lesions in $WT^{CK14-Cre}$ (n=9) and $CPEB2^{CK14-Cre}$ (n=9) grouped as low grade and high grade. (G) Representative image of ERα staining in $WT^{CK14-Cre}$ tumors. Scale bar, 50 μm; minor ticks, 10 μm. (H) Representative image of HER2 staining in $WT^{CK14-Cre}$ tumors. Scale bar, 50 μm; minor ticks, 10 μm.

During the experiment, tumor onset was monitored by weekly palpation and we observed that tumors appeared later in CPEB2-KO$^{CK14-Cre}$ (Figure 30A). Moreover, the number of tumors at the end of the experiment was significantly decreased in CPEB2-KO$^{CK14-Cre}$ compared to WT$^{CK14-Cre}$ (Figure 30B). Consequently, CPEB2-KO$^{CK14-Cre}$ exhibited diminished tumor incidence (Figure 30C). However, tumor size was comparable in CPEB2-KO$^{CK14-Cre}$ and WT$^{CK14-Cre}$ (Figure 30D). Histological analysis of the mammary lesions revealed the existence of hyperplasias and neoplasias, as well as of adenomas, adenocarcinomas and adenosquamouscarcinomas, as previously published (Yin et al., 2005). We observed slight differences between the type of lesions displayed by CPEB2-KO$^{CK14-Cre}$ *v.s.* WT$^{CK14-Cre}$ mammary glands; with enhanced appearance of neoplasias but attenuated occurrence of adenocarcinomas in CPEB2-KO$^{CK14-Cre}$ animals (Figure 30E). When histological lesions were grouped as low grade (including hyperplasisas, neoplasias and adenomas) *v.s.* high grade (adenocarcinomas and adenosquamouscarcinomas), data indicated a trend towards more benign lesions (low grade) being present in CPEB2-KO$^{CK14-Cre}$ (Figure 30F). In addition, as formerly described (Lanari et al., 2009), the resulting WT mammary tumors possessed characteristics of the luminal breast cancer subtype, with high ER and mild HER2 expression (Figures 30G and 30H). Therefore, our *in vivo* data supported the patient data on luminal A tumors (Figures 28 and 29B), where low levels of CPEB2 correlated with good prognosis.

In addition, we measured the weight of the mice weekly during the experiment, and we observed a tendency in CPEB2-KO$^{CK14-Cre}$ females to gain more weight than their WT$^{CK14-Cre}$ counterparts (Figure 31A). This was not the case for untreated CPEB2-KO and WT females from the same age (Figure 31B). Interestingly, it has been formerly described that DMBA treatment causes a decline in body weight *Qing1997*; thus, our results could suggest that WT$^{CK14-Cre}$ mice suffered a drop in body weight as a consequence of the action of the DMBA, while CPEB2-KO$^{CK14-Cre}$ females did not. Furthermore, it has been suggested that MPA exposure accelerates carcinogenesis partially by generating and immunosuppressive tumor microenvironment (Abba et al., 2016). In this regard, we did not observe any difference in lymphocytic infiltration by histological analysis. Besides, levels in blood of lymphocytes (Figure 31C), monocytes (Figure 31D) and granulocytes (mainly neutrophils) (Figure 31E) were the same in WT$^{CK14-Cre}$ and CPEB2-KO$^{CK14-Cre}$ mice at the end of the experiment.

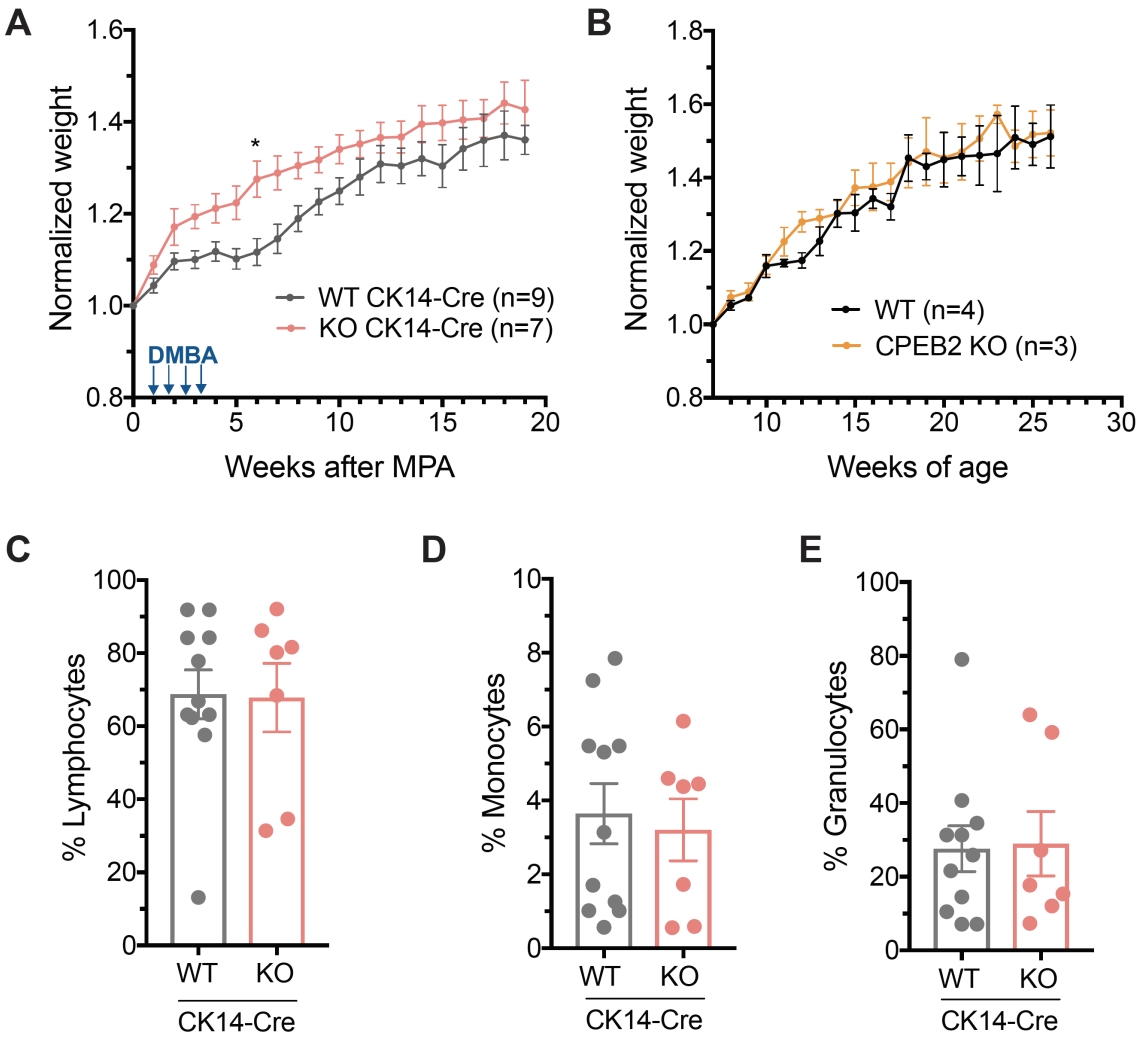

Figure 31: Weight and blood cell counts for animals subjected to chemical-induced breast tumorigenesis. (A) Kinetics of weight of $WT^{CK14-Cre}$ (n=9) and $CPEB2^{CK14-Cre}$ (n=7) animals throughout the experiment, normalized to the weight at the time of MPA injection. Statistics with 2way ANOVA, *p<0.05 (A) Kinetics of weight of WT (n=4) and CPEB2-KO (n=3) not treated mice that were age-paired to animals in (A). X axis starting at 7 weeks of age. (C) Percentage of lymphocytes in blood in $WT^{CK14-Cre}$ and $CPEB2^{CK14-Cre}$ mice. (D) Percentage of monocytes in blood in $WT^{CK14-Cre}$ and $CPEB2^{CK14-Cre}$ mice. (E) Percentage of granulocytes in blood in $WT^{CK14-Cre}$ and $CPEB2^{CK14-Cre}$ mice.

Discussion

1 The CPEB-network

The four components of the CPEB-family share the same RNA-binding domains and consequently they can recognize the same RNAs. Nevertheless, member-specific functions exist because CPEB proteins have various expression patterns and, additionally, their activation is triggered by different stimuli and respond to distinct molecular mechanisms.

Here we have presented a situation where absence of CPEB2 might be compensated by enhanced expression of CPEB4 (Figure 18E). In virgin adult CPEB2-KO mammary gland, the expression of the other CPEB proteins did not change; whereas in lactating mammary gland there was a significant increase of *Cpeb4* mRNA levels when CPEB2 was absent. Accordingly, phenotypic differences in CPEB2-KO glands were observed in virgin adult but not in lactating mammary glands. Therefore, we hypothesized that CPEB4 may compensate for the lack of CPEB2 in lactating but not in virgin mammary gland, underscoring the relevance of breast-feeding.

Concerning the role of CPEB proteins in lactating mammary gland, it has been already suggested that cytoplasmic polyadenylation might be a key mechanism mediating translation and stabilization of milk transcripts (Rhoads & Grudzien-Nogalska, 2007). Indeed, alveolar progenitors already express high level of milk-transcripts (Shehata et al., 2012), suggesting that these mRNAs could be stored dormant until activation by cytoplasmic polyadenylation takes place. The lactation stage is established thanks to the action of lactogenic hormones (such as prolactin) and it requires a great amount of remodeling, expansion and differentiation; thus, the action of the CPEBs might be to allow for rapid and efficient translation of mRNAs involved in growth, alveolar differentiation and milk production. In this regard, RANKL is not only the major responsible of progesterone-driven proliferation but it is also essential for the formation of lobulo-alveolar structures required for lactation (Fata et al., 2000). Then, one could speculate that CPEB4 might be binding and activating RANKL mRNA during lactogenic differentiation in absence of CPEB2.

Unpublished data generated as part of my PhD together with other members of the laboratory, suggested that compensations between CPEB-members are occurring in many other scenarios. For instance, while CPEB2 and CPEB4 single KO mice were viable, the constitutive double CPEB2,4 KO model was embryonically lethal. This data indicated that during embryonic development CPEB2 performed essential roles that were replaced by CPEB4

in CPEB2-KO and vice versa. Beyond CPEB2 and CPEB4, we investigated the deletion of the whole CPEB2-4 subfamily. We observed that triple CPEB2,3,4 KO mice induced by tamoxifen (*Cpeb1*+/+ *Cpeb2*lox/lox *Cpeb3*lox/lox *Cpeb4*lox/lox UBC-Cre-ERT2 T/+; *T* denotes transgene and + indicates *wild type* allele) only survived for one week. Interestingly, lethality did not occur in any combination of the double inducible KO models; indicating that, even in inducible models, compensation between CPEB members occurs at some extend.

So far, a systematic study of common and unique targets for the different CPEB proteins in a given context has never been performed. Therefore, the information obtained by comparing target genes identified by different RIP-Seq experiments is limited because the majority of target mRNAs will differ among cell types. Besides, the amount of false negative genes also hinders the comparison. As an example, the overlap between CPEB4-targets in keratinocytes and CPEB4-targets in hepatocytes was around 35 %; close to the 25 % overlap when comparing CPEB2-targets in MECs and CPEB4-targets in hepatocytes. In our case, the group of CPEB2-targets did not include previously described target genes like *Vegfa* (Calderone et al., 2016) or *Txnip* (Maillo et al., 2017).

Interestingly, zo-1 mRNA (*Tjp1*), which has been described to be bound by CPEB1 in a breast epithelial cell line (Nagaoka et al., 2012), appeared as CPEB2-target in MECs. Nagaoka et al showed that CPEB1 was required for apical localization of zo-1 mRNA; nonetheless, they did not observe differences in total levels of zo-1 protein. Hence, one hypothetical scenario could be that CPEB1 is responsible for the transport of *Tjp1* in a deadenylated state and then CPEB2 is in charge of its translational activation in the apical side. Indeed, CPEB2 target genes were enriched in membrane raft and membrane microdomain compartments (Enrichr gene ontology, data not shown); indicating a possible role in activation of local translation of mRNAs related to polarity or rapid signaling downstream receptors. Ideally, proximity-specific ribosome profiling, which has been used to shed light into endoplasmic reticulum and mitochondria translational dynamics in yeast (Jan et al., 2014; Williams et al., 2014; Costa et al., 2018), could be performed in a 3D culture model to evaluate such questions. In addition, it is worthy to briefly mention that *Tjp1* was included in the group of RIP-targets but not in the reduced list of high confidence RIP-targets (Figure 32). Moreover, although 80 % of short-listed high confidence RIP-targets overlapped with the extended list of RIP-targets, 32 new target genes appeared when taking into account the expression in the Inputs (Figure 32). Thus, we need to carefully interrogate the data and understand that, as for any high throughput analysis, there is a risk for false positive

and false negative hits; so potential targets should be further validated.

In summary, all these examples illustrate how CPEB proteins form a complex network that include proteins and mRNAs and how, in certain situations, the lack of one or two CPEBs can be compensated by other members of the CPEB-family.

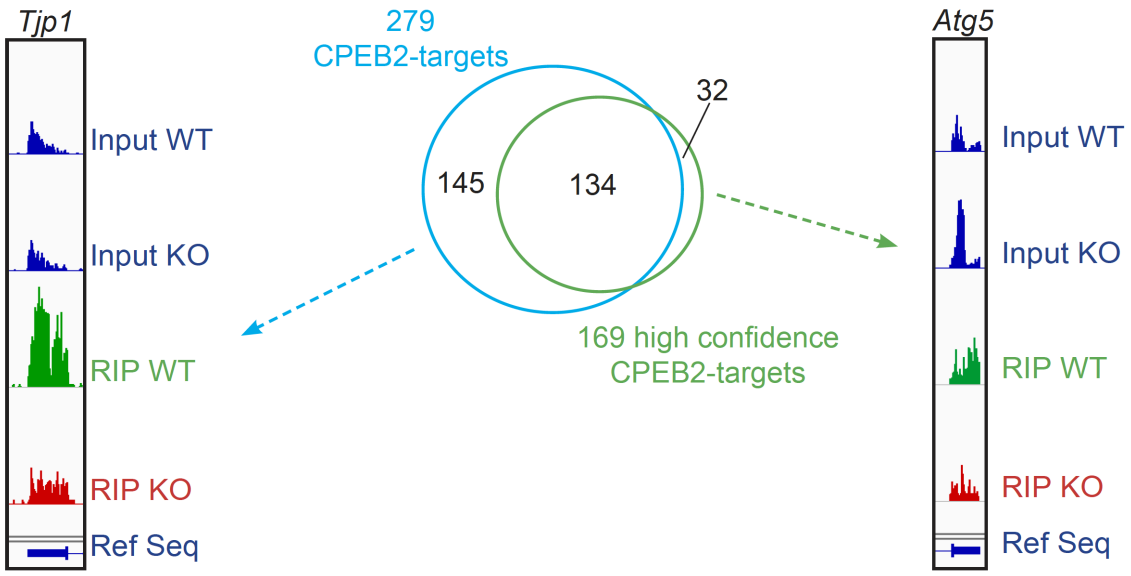

Figure 32: CPEB2 RIP-target genes in MECs. Venn diagram for CPEB2-target genes (279; DESeq2, BHp-value<0.05 and FC>2) and high confidence CPEB2-target genes (169; DESeq2, interaction BH-pvalue<0.1) (Table 3). Also snapshots exemplifying RIP-Seq data for 3'UTRs only included in one of these groups. Normalized RIP-seq coverage for Inputs (blue), WT RIP (green) and KO RIP (red) are depicted. Snapshot images obtained using the integrated genomic viewer (IGV).

2 CPEB2 and estrogen signaling

During puberty, the ductal tree greatly elongates and branches invading the fat pad and becoming a mature mammary gland; the main trigger of this dramatic remodeling is estrogen which signals through the ER (Macias & Hinck, 2012). Interestingly, ductal extension was delayed in CPEB2-KO compared to WT at mid-puberty (Figure 18A), indicating a deficient response to estrogen.

Moreover, our results showed that the number of ER positive cells were increased, as well as the levels of *Pgr*; however, downstream effectors of this pathway were not enhanced, also suggesting a defect in ER signaling (Figure 24). In addition, we also observed decreased

protein levels of PBX1 (Figure 33). PBX1 is a pioneer factor, like AP2γ or FOXA1, that provides increased accessibility for ER recruitment (Jozwik & Carroll, 2012; Magnani et al., 2011; Manavathi et al., 2014). Thus, it is possible that CPEB2 regulates PBX1 expression (directly or indirectly) and that, in absence of CPEB2, ER transcriptional activity is hampered.

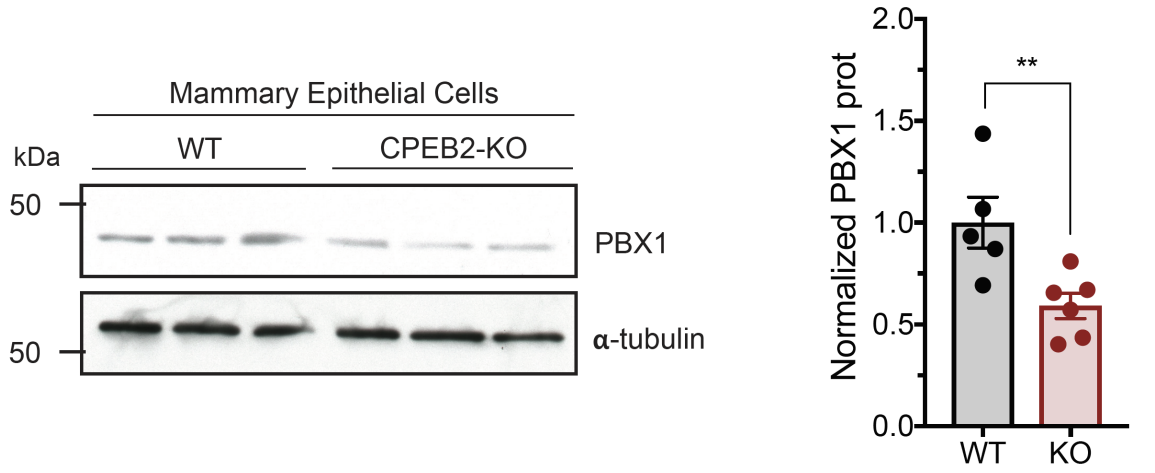

Figure 33: Decreased PBX1 expression in CPEB2-KO MECs. Western Blot images and quantification for PBX1 and α-tubulin as a control. Same amounts of protein lysates from isolated mammary epithelial cells from the indicated genotypes were loaded. KO, CPEB2-KO

Furthermore, CPEB2-target genes were enriched in key mediators of rapid signaling downstream estrogen (such as *Creb1* or *Gnai1*). Besides from the classical nuclear signaling, where estrogen promotes dimerization and conformational change of ER allowing its binding to estrogen responsive elements in the DNA (Jozwik & Carroll, 2012); ER also orchestrate a rapid extranuclear signaling. Membrane-localized ER can bind estrogen and subsequent signal transduction occurs through the physical interaction of ER with G proteins and kinases (such as PI3K-Akt and Src); inducing downstream signaling events (such as calcium flux) that further increases signal propagation (Levin & Hammes, 2016). Although the mechanism is less characterized, PR is also localized at the plasma membrane and it regulates signals like ERK and PI3K-Akt too (Levin & Hammes, 2016). Thus, sex steroid receptors localized in the membrane can associate and cooperate in signal transduction. Both genomic and non-genomic actions are tightly integrated with modulatory impact on gene transcription. Based on the potential RIP-targets, CPEB2 could be an important player in response to ovarian hormones by influencing translation of mediators involved in the ER extranuclear signaling.

3 CPEB2 regulates translation of *Rankl*

The work presented here demonstrated that synthesis of RANKL in mammary epithelial cells requires CPEB2 (Figures 27 and 34). This finding has very relevant implications in the understanding of mammary gland biology because it places CPEB2 upstream the utmost potent mediator of hormone-induced proliferation in the mammary gland (Grimm et al., 2016). As a result, CPEB2-KO mice reproduced the breast-related phenotypes already described for RANKL depletion, such as decreased proliferation (Figure 23) and attenuated tumorigenesis (Figure 30) (Gonzalez-Suarez et al., 2010; Schramek et al., 2010). Furthermore, in a murine breast cancer model, recent work showed that blockade of RANKL/RANK signaling led to an increment in $Sca1^{high}$ cells, which showed a lower tumor-initiating ability (Yoldi et al., 2016). Accordingly, the reduced number of RANKL positive cells in absence of CPEB2 could account for the changes in Sca1 expression observed in the CPEB2-KO mammary glands (Figures 20D and 20E). Moreover, RANKL has been shown to enhance expression of *Rspo1* (Joshi et al., 2015), which was diminished in absence of CPEB2 (Figure 22E). In conclusion, most of the mammary gland phenotypes described for CPEB2-KO animals might be driven by the loss of RANKL. Thence, it is tempting to speculate that the effects derived from CPEB2-loss could be rescued by enhancing RANKL/RANK signaling. In this regard, in order to overexpress RANKL, injection of recombinant RANKL has been used in other contexts, like in central nervous system (Hanada et al., 2009) or in lung metastasis (Tan et al., 2011). Then, available protocols might be adapted to investigate mammary gland biology in a scenario with no CPEB2 but physiological levels of RANKL. In any case, it is important to bear in mind that CPEB2 is probably regulating other mRNAs in addition to RANKL, and, thus, the observed phenotypes may be a consequence of the combined effects driven by the modulation of several CPEBB2-bound mRNAs. For instance, *Ccnd1* was a promising CPEB2-target that acts downstream RANKL (Figure 26); as a consequence, it might be that even when the levels of RANKL are rescued, the entire pathway is not restored. Moreover, it is not surprising that CPEB2 regulates mRNAs with linked biological functions, since it has already been described that RBPs could bind functionally related mRNAs that represent the so-called "RNA regulons" (Morris et al., 2010).

Beyond its function in mammary gland, RANKL plays also pivotal roles in bone and immune system that might be compromised in absence of CPEB2 too. In bone, RANKL, which is expressed in osteoblasts and other stromal cells, is bound by RANK receptor present in osteoclast precursors (Boyce & Xing, 2007). Upon binding, RANKL/RANK signaling en-

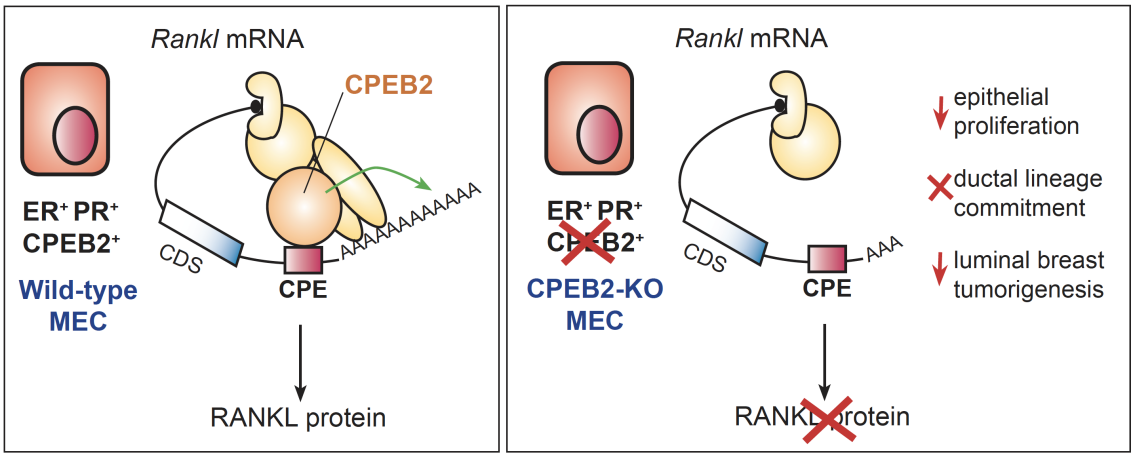

Figure 34: Working model for the function of CPEB2 in mammary epithelial cells. Here we show how CPEB2 is expressed in hormone-sensing cells, where it mediates translation of RANKL by binding the cytoplasmic polyadenylation element (CPE) in its 3'UTR and promoting cytoplasmic polyadenylation. In absence of CPEB2, RANKL is not effectively synthesized and we observed decreased mammary epithelial proliferation, a partial differentiation in the ductal lineage and diminished luminal tumor incidence.

hances osteoclast differentiation promoting bone loss. When this process is perturbed in absence of either RANKL or RANK, the bone cannot be remodeled normally because of deficient osteoclast differentiation, resulting in osteoporosis and severe skeletal abnormalities (Dougall et al., 1999; Yun Kong et al., 1999). Although we did not observe any evident bone- or tooth-related phenotype in CPEB2-KO mice, experiments should be done to address mild alterations that could be occurring in CPEB2-KO animals.

Regarding the immune system, RANKL appears to play multiple roles in immunity (González-Suárez & Sanz-Moreno, 2016; Rao et al., 2017), from organogenesis of the lymph node system (Yun Kong et al., 1999) to the establishment of functional interactions between T-cells and dendritic cells (Anderson et al., 1997); yet the underlying mechanisms remain largely elusive. Even though *Cpeb2* mRNA is highly expressed in the immune compartment ($CD45^+$ cells), we did not observe any major difference in complete blood counts from CPEB2-KO mice compared to WT (data not shown). The IHC for RANKL in mammary glands (Figure 27E) further supports this data, since absence of CPEB2 only ablates the expression of RANKL in mammary epithelial cells but not in lymph nodes; either suggesting that CPEB2 does not regulate RANKL expression in the immune compartment or that other members of the CPEB-family are compensating for the lack of CPEB2 in immune cells.

In sum, it seems that CPEB2-KO mice only phenocopies the RANKL-KO model with re-

spect to the mammary epithelium. Additionally, in the mammary gland, CPEB2 seemed to be required for the rise of *Rankl* mRNA upon MPA injection (Figure 27F). It has already been published that *Rankl* levels greatly elevate upon MPA stimulation (Gonzalez-Suarez et al., 2010; Schramek et al., 2010; Abba et al., 2016); however, this increase did not take place in CPEB2-KO$^{CK14-Cre}$. This piece of data could indicate that, upon acute progestin stimulation, CPEB2 may be also necessary to mediate *Rankl* mRNA stability. In fact, it has been shown that the increase of *Rankl* mRNA downstream PR signaling occurs via mRNA stabilization, rather than at the transcriptional level (Tanos et al., 2013). Experiments treating WT and CPEB2-KO MECs with actinomycin D, which inhibits transcription, would shed light into this new potential function of CPEB2. On the contrary, another possibility would be that, instead of regulating mRNA stability, CPEB2 is regulating a factor upstream RANKL. For instance, it has been shown that Stat5a, a transcription factor downstream of the Jak2 tyrosine kinase, is essential for the induction of *Rankl* and other PR-target genes upon progesterone treatment (Obr et al., 2013). Nevertheless, Stat5a levels remained unchanged upon CPEB2 depletion (Figure 24B). Interestingly, the 3'UTR of Stat5b, the homologue of Stat5a, harbors CPEs and it could be potentially bound by CPEB2. Similar to Stat5a, Stat5b has been described to play a role in lactogenic differentiation in the mammary gland (Teglund et al., 1998) yet its impact on *Rankl* transcription remains unexplored.

4 CPEB2 is required for development of luminal breast cancer

This study reveals that loss of CPEB2 in the mammary epithelium confers an advantage to prevent luminal breast tumor establishment and/or progression (Figure 30). Notably, this result nicely fits with the patient data from luminal A breast cancer, where having low levels of *Cpeb2* confers good prognosis (Figure 29B). However, the molecular mechanisms that are orchestrated by CPEB2 during luminal oncogenic development are still poorly understood.

On the one hand, the most obvious explanation for the lack of CPEB2 being protective against luminal breast cancer is linked to the abrogation of RANKL synthesis. As explained in the previous section, a decrease on RANKL levels compromises mammary epithelial proliferation and, thus, hinders hormone-driven breast cancer (Gonzalez-Suarez et al., 2010; Schramek et al., 2010). Interestingly, RANKL inhibition also attenuates mammary tumor progression in the MMTV-neu transgenic model, that develops breast tumor spontaneously (Gonzalez-Suarez et al., 2010). In fact, a recent publication, that also made

use of a spontaneous breast cancer model (mouse mammary tumor virus-Polyoma Middle T, MMTV-PyMT), suggests that RANKL inhibition also promotes differentiation of tumor initiating cells (Yoldi et al., 2016). Authors showed that pharmacological inhibition of RANKL, with RANK-Fc blocking antibody, induced the expression of milk proteins genes (like β-casein), and they relate this phenotype to the reduced capacity of tumor-initiation upon RANKL ablation (Yoldi et al., 2016). Consequently, in CPEB2-KO animals, the curtailment of RANKL protein levels may result in both decreased proliferation and increased epithelial differentiation, hampering oncogenic development.

On the other hand, we have shown that the absence of CPEB2 perturbs commitment in the ductal lineage (Figure 22). Thence, one appeling possibility is that CPEB2 deletion influences breast cancer outcome by modifying the cell of origin for luminal breast cancer. It has been proposed that different breast cancer subtypes may arise from distinct epithelial differentiation stages and lineages (Visvader & Stingl, 2014). So far, it has been shown that basal-like breast tumors initiate from an aberrant luminal progenitor (Lim et al., 2009) and that MaSC/basal signature comparable to that displayed by tumors included in the claudin-low cancer subtype (Prat & Perou, 2011). Nonetheless, the population originating luminal tumorigenesis has not been yet identified. Even when the profile for luminal breast cancer is most concordant with the signature of mature luminal cells, it is presumed that a small progenitor subset that expresses differentiation markers is the likely cell of origin for this subtype (Visvader & Stingl, 2014). Thus, the population of ductal progenitors, which has clonogenic capacity but expresses high levels of markers of mature luminal cells like ER, PR, Gata3 or Foxa1 (Asselin-Labat et al., 2007; Kouros-Mehr et al., 2006; Shehata et al., 2012), is a suitable candidate for being cell of origin for luminal breast cancer. Interestingly, loss of CPEB2 has profound effects specifically in the ductal compartment and in the transition from ductal progenitors to ductal differentiated cells (Figures 20 and 22). Hence, the intermediate ductal population arising in CPEB2-KO animals could give rise to altered tumor-initiating cells (TICs) that establish luminal breast tumorigenesis in a less efficient manner.

In this latter regard, as mentioned earlier, loss of CPEB2 (similar to lack of RANKL) causes an increase of Sca1$^{\text{high}}$ cells (Figure 20), which showed a decreased tumor-initiating capacity *in vitro* and *in vivo* (Yoldi et al., 2016). Furthermore, high confidence RIP-target 3'UTRs (Table 3) include genes involved in Wnt signaling (Figure 25C); for instance, main components of the Wnt surface receptors (*Fzd2* and *Lrp6*) and Wnt-target genes such as eprhin ligands (*Efnb1*, *Efna1* and *Efnb2*). The Wnt/β-catenin signaling pathway is a mas-

ter regulator of stem cell maintenance and morphogenesis in multiple tissues (Nusse & Clevers, 2017). Concerning the mammary gland, the Wnt/β-catenin signaling pathway has been implicated in branching morphogenesis and alveolar bud formation (Brisken et al., 2000; Macias et al., 2011; Sreekumar et al., 2017; Teuliere et al., 2005), as well as in breast cancer (Khramtsov et al., 2010; Zardawi et al., 2009). Specifically, the role of ephrin receptors (Ephs) and ligands has been related to the regulation of the stem cell niche identity and lineage specification by regulating cell-transition and differentiation, mostly in the intestine and nervous system (Batlle et al., 2002; Merlos-Suárez & Batlle, 2008; Nomura et al., 2010). Even though little is known about the role of ephrins in the mammary gland and breast cancer (Kaenel et al., 2012b), we could speculate that a potential modulation of the Wnt-ephrin signaling pathway by CPEB2 might be important for ductal luminal specification. Then, deletion of CPEB2 could lead to an aberrant signaling downstream ephrin receptors, which in turn could trigger the appearance of an intermediate ductal population (Figure 22) and a subsequent modified cell of origin for luminal breast cancer.

Our results in breast carcinogenesis suggested that CPEB2 could be required for the initiation of ER^+ tumors, rather than for growth of these tumors. Evidences supporting this idea are that a reduced number of CPEB2-$KO^{CK14-Cre}$ mice developed tumors compared to $WT^{CK14-Cre}$ animals (Figures 30A, 30B and 30C), while the tumor burden (evaluated in those animals with tumors) was the same (Figure 30D). Nonetheless, the low number of CPEB2-$KO^{CK14-Cre}$ females developing tumors limited our analysis, making hard to draw any conclusion. In order to further investigate the tumors arising in CPEB2-$KO^{CK14-Cre}$ mice, we could extend the time until sacrifice or use a different strain rather than C57BL/6 animals. It has already been published that the C57BL/6 strain is more resistance to carcinogenesis (Abel et al., 2011); similarly, MPA alone fails to induce mammary carcinomas in C57BL/6 while it does in BALB/c mice (Montero Girard et al., 2007). Thus, a higher tumor incidence is expected in other backgrounds. Moreover, we have to take into account, that all the herein presented cancer data comes from a chemical-induced breast cancer model. Compared to other widely used breast cancer models, like the MMTV-PyMT model, the combined treatment MPA/DMBA has a larger latency that permits a more physiological epithelial transformation, which is useful when evaluating primary tumor rather than metastasis. However, other breast cancer models (Fantozzi & Christofori, 2006; Herschkowitz & Lubet, 2010) could be used in order to broaden our analysis.

Hitherto, we have commented on why CPEB2 might be required for luminal breast can-

cer initiation and progression. However, according to the available patient data, CPEB2 might play an opposite role in basal-like breast cancer, where it would act as an oncogenic brake (Figures 28 and 29A). Which could be the role of CPEB2 in basal-like breast cancer? Contrary to the patient data, the function of CPEB2 as a pivotal regulator of RANKL synthesis (Figure 27) suggests that CPEB2 ablation would be beneficial in basal-like breast cancer, since $RANK^+$ cells are highly proliferative and accumulate DNA damage in the context of *Brca1* mutation (Nolan et al., 2016; Sau et al., 2016). Then, there might be other mechanisms accounting for the effects of CPEB2 in basal-like breast cancer patients.

5 Clinical implications of the study

Our work indicated that lack of CPEB2 may benefit luminal breast cancer patients (Figures 29B, 30A, 30B and 30C), while did not affect fitness or impaired mammary gland functionality (Figures 10D, 18C and 18E). Thus, the depletion of CPEB2 by targeted approaches, such small-molecule inhibitors, might be an attractive possibility to improve luminal breast cancer therapy exploiting a novel mechanism of action. Nonetheless, a stronger, and more definitive, proof for the clinical impact of CPEB2 attenuation would be to investigate its therapeutic inhibition *in vivo*; that is to say, to mimic the patient scenario to some extend, and study the deletion of CPEB2 once breast tumors have been formed.

Luminal tumors represent nearly 80 % of all breast cancer cases (Syed, 2015). Because luminal tumors are ER^+, luminal breast cancer patients are treated with endocrine therapy that targets the estrogen receptor pathway. Tamoxifen, which is an estrogen antagonist that competes for binding to ER, has been the "therapy of choice" in ER^+ breast cancer for more than 30 years (Musgrove & Sutherland, 2009). Even though adjuvant therapy with tamoxifen has made a significant contribution to the 25-30 % decrease in breast cancer mortality in the past years (EBCTCG, 2005), its efficacy is limited by intrinsic and acquired therapeutic resistance. The intrinsic resistance to tamoxifen could be caused by either defects in tamoxifen metabolism or by alterations in pathways related to ER, growth factors, cell cycle and apoptosis (Musgrove & Sutherland, 2009). Notably, some of the individual candidate genes that are associated with tamoxifen resistance *in vitro* appear as candidate CPEB2 target-genes, like *Ccnd1*). Therefore, and despite the limited information available, it might be relevant to analyze whether *Cpeb2* is included in any of the signatures predicting response to endocrine therapies (Musgrove & Sutherland, 2009). Moreover, in order to evaluate the potential of CPEB2 as a novel biomarker for tamoxifen resistance in luminal

breast cancer, we could assess the effects of CPEB2 attenuation in ER^+ breast cancer cell lines regarding tamoxifen response.

Furthermore, given the pleiotropic functions of RANKL, inhibition of CPEB2 also holds potential interest for osteoporosis and bone-metastasis treatment. For instance, after menopause, decreased estrogen levels are associated to low OPG expression (which is the soluble decoy receptor for RANKL), and subsequent raise in RANKL activity (Walsh & Choi, 2003). As a consequence, the resulting osteoclast activity leads to diminished bone mass and osteoporosis, which is characterized by compromised bone strength and increased risk of bone fracture (William J. Boyle et al., 2003). Interestingly, this mechanism, that links age and bone-loss occurrence, would likely account for the high incidence of osteoporosis in older women (Wada et al., 2006). In fact, denosumab (Kostenuik et al., 2009), a human monoclonal RANKL-blocking antibody, was approved for the treatment of osteoporosis in post-menopausal women in 2010 (Lacey et al., 2012). Furthermore, RANKL also influences bone metastatic disease, which occurs at highest rates in prostate and breast cancer (Croucher et al., 2016). Tumor cells secret cytokines that enhance production of RANKL by bone stromal cells, leading to osteoclast activation; concomitantly, bone destruction releases growth factors that sustain tumor activity and metastatic colonization. This harmful crosstalk, between bone microenvironment and cancer cells, that self-amplifies is often termed the "vicious cycle" of bone metastasis (Croucher et al., 2016; González-Suárez & Sanz-Moreno, 2016). In this regard, denosumab therapy translates into clinical benefit for treating skeletal-related events in cancer, such as bone metastasis in advanced cancer patients (Lacey et al., 2012). Therefore, CPEB2 inhibition, alone or in combination, could be a promising tool for treating both luminal breast cancer and for preventing bone loss.

6 CPEB2, the great unknown

It is relevant to highlight that very little is known about CPEB2. In fact, the role of CPEB2 in mammals has been only studied in neurons, where very recent studies reported that CPEB2 was important for parasympathetic signaling, neuronal long-term potentiation and memory (Lai et al., 2016; Lu et al., 2017b). This is the first time, to our knowledge, that a role in growth and differentiation *in vivo* was demonstrated for CPEB2. Therefore, our work opens the door to future studies investigating the function of CPEB2 in other proliferative and cell-fate decision programs operating in different organs; notably, CPEB2 is highly expressed in the skin (*biogps.org*), which has a high turnover rate (Solanas & Benitah, 2013).

Moreover, nothing is known in regard to the mechanisms by which CPEB2 is activated. Unpublished data, from our laboratory in *Xenopus Laevis* oocytes, indicated that CPEB2 is phosphorylated upon progesterone stimulation. In a similar way to CPEB1 (Mendez et al., 2000a,b), we could hypothesize that CPEB2 phosphorylation is linked to its activation state. Thus, in an analogous manner in mammary epithelial cells, progesterone would phosphorylate and activate CPEB2, that would drive efficient translation of downstream target-mRNAs and orchestrate a proper response to progesterone in the mammary gland. A function of CPEB2 as a repressor of translation of bound-mRNAs is a plausible, yet unexplored, mechanism of action.

Further underscoring the relevance of this study, the biology of the mammary gland has been mainly described in terms of transcriptional circuits (Hennighausen & Robinson, 2005; Kouros-Mehr et al., 2006; Asselin-Labat et al., 2007) and the majority of the proposed post-transcriptional mechanisms are related to the the microRNA machinery (Gigli & Maizon, 2013). Herein, we have unveiled a novel mechanism of translational regulation mediated by the RNA-binding protein CPEB2 in mammary epithelial cells. Remarkably, this CPEB2-driven regulation controls pivotal functions in mammary gland homeostasis and breast cancer (Figure 34).

Conclusions

The present study identifies CPEB2 as a novel regulator of the ductal (ER^+) compartment of the mammary gland. Herein, we have unraveled that CPEB2 is required for mediating a correct response to steroid hormones in the mammary epithelium. Furthermore, we have demonstrated that absence of CPEB2 has relevant consequences *in vivo* for proliferation, cell-fate and tumorigenesis in the mammary gland.

The main conclusions of our work are the following:

- CPEB2 is the only CPEB-member that regulates mammary gland homeostasis.
- Absence of CPEB2 leads to decrease epithelial branching in adult mammary gland in a cell-autonomous manner.
- CPEB2-KO mice showed an unbalance between the two main mammary epithelial cell types: luminal and myoepithelial populations.
- Deletion of CPEB2 causes a delay in ductal expansion during puberty.
- CPEB2 is dispensable for breast-feeding.
- Ablation of CPEB2 leads to an increase in $Sca1^{high}$ cells.
- *Cpeb2* is mostly expressed in the ductal (ER^+) populations (both progenitors and differentiated).
- CPEB2 regulates cell-fate in the ductal compartment.
- CPEB2 is required for hormone-driven proliferation.
- CPEB2 controls translation of *Rankl* mRNA.
- *Cpeb2* behaves differently in basal-like and luminal A subtypes.
- Loss of CPEB2 highly protects against luminal breast cancer.

References

Abba, M. C., Zhong, Y., Lee, J., Kil, H., Lu, Y., Takata, Y., Simper, M. S., Gaddis, S., Shen, J., & Aldaz, C. M. (2016). DMBA induced mouse mammary tumors display high incidence of activating Pik3caH1047 and loss of function Pten mutations. *Oncotarget*, *7*(39).

Abel, E. L., Angel, J. M., Kiguchi, K., & Digiovanni, J. (2011). Fundamentals and applications. *Methods*, *4*(9), 1350–1362.

Afroz, T., Skrisovska, L., Belloc, E., Guillén-Boixet, J., Méndez, R., & Allain, F. H. T. (2014). A fly trap mechanism provides sequence-specific RNA recognition by CPEB proteins. *Genes and Development*, *28*(13), 1498–1514.

Aguilera, A. (2005). Cotranscriptional mRNP assembly: From the DNA to the nuclear pore. *Current Opinion in Cell Biology*, *17*(3), 242–250.

Aldaz, C. M., Liao, Q. Y., LaBate, M., & Johnston, D. a. (1996). Medroxyprogesterone acetate accelerates the development and increases the incidence of mouse mammary tumors induced by dimethylbenzanthracene. *Carcinogenesis*, *17*(9), 2069–2072.

Amrani, N., Ghosh, S., Mangus, D. A., & Jacobson, A. (2008). Translation factors promote the formation of two states of the closed-loop mRNP. *Nature*, *453*(7199), 1276–1280.

Anderson, D. M., Maraskovsky, E., Billingsley, W. L., Dougall, W. C., Tometsko, M. E., Roux, E. R., Teepe, M. C., DuBose, R. F., Cosman, D., & Galibert, L. (1997). A homologue of the TNF receptor and its ligand enhance T-cell growth and dendritic-cell function. *Nature*, *390*(6656), 175–179.

Asselin-Labat, M.-L., Sutherland, K. D., Barker, H., Thomas, R., Shackleton, M., Forrest, N. C., Hartley, L., Robb, L., Grosveld, F. G., van der Wees, J., Lindeman, G. J., & Visvader, J. E. (2007). Gata-3 is an essential regulator of mammary-gland morphogenesis and luminal-cell differentiation. *Nature cell biology*, *9*(2), 201–9.

Asselin-Labat, M.-L., Sutherland, K. D., Vaillant, F., Gyorki, D. E., Wu, D., Holroyd, S., Breslin, K., Ward, T., Shi, W., Bath, M. L., Deb, S., Fox, S. B., Smyth, G. K., Lindeman, G. J., & Visvader, J. E. (2011). Gata-3 Negatively Regulates the Tumor-Initiating Capacity of Mammary Luminal Progenitor Cells and Targets the Putative Tumor Suppressor Caspase-14. *Molecular and Cellular Biology*, *31*(22), 4609–4622.

Asselin-Labat, M.-L., Vaillant, F., Sheridan, J. M., Pal, B., Wu, D., Simpson, E. R., Yasuda, H., Smyth, G. K., Martin, T. J., Lindeman, G. J., & Visvader, J. E. (2010). Control of mammary stem cell function by steroid hormone signalling. *Nature*, *465*(June), 798–802.

Batlle, E., Henderson, J. T., Beghtel, H., Van den Born, M. M., Sancho, E., Huls, G., Meeldijk, J., Robertson, J., Van de Wetering, M., Pawson, T., & Clevers, H. (2002). β-catenin and TCF mediate cell positioning in the intestinal epithelium by controlling the expression of EphB/EphrinB. *Cell*, *111*(2), 251–263.

Bava, F.-A., Eliscovich, C., Ferreira, P. G., Miñana, B., Ben-Dov, C., Guigó, R., Valcárcel, J., & Méndez, R. (2013). CPEB1 coordinates alternative 3'-UTR formation with translational regulation. *Nature*, *495*(7439), 121–5.

Beleut, M., Rajaram, R. D., Caikovski, M., Ayyanan, A., Germano, D., Choi, Y., Schneider, P., & Brisken, C. (2010). Two distinct mechanisms underlie progesterone-induced proliferation in the mammary gland. *Proceedings of the National Academy of Sciences*, *107*(7), 2989–2994.

Belloc, E., & Méndez, R. (2008). A deadenylation negative feedback mechanism governs meiotic metaphase arrest. *Nature*, *452*(7190), 1017–21.

Berkovits, B. D., & Mayr, C. (2015). Alternative 3′ UTRs act as scaffolds to regulate membrane protein localization. *Nature*, *8*.

Bertolin, K., & Murphy, B. D. (2014). Reproductive Tract Changes During the Mouse Estrous Cycle. *The Guide to Investigation of Mouse Pregnancy*, (pp. 85–94).

Bocchinfuso, W. P., & Korach, K. S. (1997). Mammary gland development and tumorigenesis in estrogen receptor knockout mice. *Journal of mammary gland biology and neoplasia*, *2*(4), 323–34.

Boussemart, L., Malka-Mahieu, H., Girault, I., Allard, D., Hemmingsson, O., Tomasic, G., Thomas, M., Basmadjian, C., Ribeiro, N., Thuaud, F., Mateus, C., Routier, E., Kamsu-Kom, N., Agoussi, S., Eggermont, A. M., Désaubry, L., Robert, C., & Vagner, S. (2014). eIF4F is a nexus of resistance to anti-BRAF and anti-MEK cancer therapies. *Nature*, *513*(7516), 105–109.

Boyce, B. F., & Xing, L. (2007). Biology of RANK, RANKL, and osteoprotegerin. *Arthritis Research and Therapy*, *9*(SUPPL.1).

Brisken, C. (2013). Progesterone signalling in breast cancer: a neglected hormone coming into the limelight. *Nature Reviews Cancer*, *13*(6), 385–396.

Brisken, C., Heineman, A., Chavarria, T., Brisken, C., Heineman, A., Chavarria, T., Elenbaas, B., Tan, J., Dey, S. K., Mcmahon, J. A., Mcmahon, A. P., & Weinberg, R. A. (2000). Essential function of Wnt-4 in mammary gland development downstream of progesterone signaling Essential function of Wnt-4 in mammary gland development downstream of progesterone signaling. *Genes & development*, *14*(617), 650–654.

Brisken, C., Kaur, S., Chavarria, T. E., Binart, N., Sutherland, R. L., Weinberg, R. A., Kelly, P. A., & Ormandy, C. J. (1999). Prolactin Controls Mammary Gland Development via Direct and Indirect Mechanisms. *Developmental biology*, *210*(1), 96–106.

Brisken, C., & O'Malley, B. (2010). Hormone action in the mammary gland. *Cold Spring Harbor perspectives in biology*, *2*(a003178), 1–15.

Bruna, A., Rueda, O. M., Greenwood, W., Batra, A. S., Callari, M., Batra, R. N., Pogrebniak, K., Sandoval, J., Cassidy, J. W., Tufegdzic-Vidakovic, A., Sammut, S. J., Jones, L., Provenzano, E., Baird, R., Eirew, P., Hadfield, J., Eldridge, M., McLaren-Douglas, A., Barthorpe, A., Lightfoot, H., O'Connor, M. J., Gray, J., Cortes, J., Baselga, J., Marangoni, E., Welm, A. L., Aparicio, S., Serra, V., Garnett, M. J., & Caldas, C. (2016). A Biobank of Breast Cancer Explants with Preserved Intra-tumor Heterogeneity to Screen Anticancer Compounds. *Cell*, *167*(1), 260–274.e22.

Burns, D. M., & Richter, J. D. (2008). CPEB regulation of human cellular senescence , energy metabolism , and p53 mRNA translation. *Genes & development*, *22*, 3449–3460.

Byers, S. L., Wiles, M. V., Dunn, S. L., & Taft, R. A. (2012). Mouse estrous cycle identification tool and images. *PLoS ONE*, *7*(4), 2–6.

Caldeira, J., Simões-Correia, J., Paredes, J., Pinto, M. T., Sousa, S., Corso, G., Marrelli, D., Roviello, F., Pereira, P. S., Weil, D., Oliveira, C., Casares, F., & Seruca, R. (2012). CPEB1, a novel gene silenced in gastric cancer: a Drosophila approach. *Gut*, *61*(8), 1115–23.

Calderone, V., Gallego, J., Fernandez-Miranda, G., Garcia-Pras, E., Maillo, C., Berzigotti, A., Mejias, M., Bava, F. A., Angulo-Urarte, A., Graupera, M., Navarro, P., Bosch, J., Fernandez, M., & Mendez, R. (2016). Sequential Functions of CPEB1 and CPEB4 Regulate Pathologic Expression of Vascular Endothelial Growth Factor and Angiogenesis in Chronic Liver Disease. *Gastroenterology*, *150*(4), 982–997.e30.

Cao, Y., Bonizzi, G., Seagroves, T. N., Greten, F. R., Johnson, R., Schmidt, E. V., & Karin, M. (2001). IKKα provides an essential link between RANK signaling and cyclin D1 expression during mammary gland development. *Cell*, *107*(6), 763–775.

Cardiff, R. D., Anver, M. R., Gusterson, B. a., Hennighausen, L., Jensen, R. a., Merino, M. J., Rehm, S., Russo, J., Tavassoli, F. a., Wakefield, L. M., Ward, J. M., & Green, J. E. (2000). The mammary pathology of genetically engineered mice: the consensus report and recommendations from the Annapolis meeting. *Oncogene*, *19*(8), 968–988.

Carvalho, B. S., & Irizarry, R. A. (2010). A framework for oligonucleotide microarray preprocessing. *Bioinformatics*, *26*(19), 2363–2367.

Cerami, E., Gao, J., Dogrusoz, U., Gross, B. E., Sumer, S. O., Aksoy, B. A., Jacobsen, A., Byrne, C. J., Heuer, M. L., Larsson, E., Antipin, Y., Reva, B., Goldberg, A. P., Sander, C., & Schultz, N. (2012). The cBio Cancer Genomics Portal: An open platform for exploring multidimensional cancer genomics data. *Cancer Discovery*, *2*(5), 401–404.

Chabot, B., & Shkreta, L. (2016). Defective control of pre-messenger RNA splicing in human disease. *Journal of Cell Biology*, *212*(1), 13–27.

Chang, Y.-T. (2014). Gene expression profile of peripheral blood in colorectal cancer. *World Journal of Gastroenterology*, *20*(39), 14463.

Chao, H.-W., Tsai, L.-Y., Lu, Y.-L., Lin, P.-Y., Huang, W.-H., Chou, H.-J., Lu, W.-H., Lin, H.-C., Lee, P.-T., & Huang, Y.-S. (2013). Deletion of CPEB3 Enhances Hippocampus-Dependent Memory via Increasing Expressions of PSD95 and NMDA Receptors. *The Journal of neuroscience : the official journal of the Society for Neuroscience*, *33*(43), 17008–22.

Cheang, M. C., Chia, S. K., Voduc, D., Gao, D., Leung, S., Snider, J., Watson, M., Davies, S., Bernard, P. S., Parker, J. S., Perou, C. M., Ellis, M. J., & Nielsen, T. O. (2009). Ki67 index, HER2 status, and prognosis of patients with luminal B breast cancer. *Journal of the National Cancer Institute*, *101*(10), 736–750.

Chen, E. Y., Tan, C. M., Kou, Y., Duan, Q., Wang, Z., Meirelles, G. V., Clark, N. R., & Ma'ayan, A. (2013). Enrichr: Interactive and collaborative HTML5 gene list enrichment analysis tool. *BMC Bioinformatics*, *14*.

Chen, P.-J., & Huang, Y.-S. (2012). CPEB2-eEF2 interaction impedes HIF-1α RNA translation. *The EMBO journal*, *31*(4), 959–71.

Choi, K. M., Barash, I., & Rhoads, R. E. (2004). Insulin and prolactin synergistically stimulate beta-casein messenger ribonucleic acid translation by cytoplasmic polyadenylation. *Molecular endocrinology (Baltimore, Md.)*, *18*(7), 1670–1686.

Ciarloni, L., Mallepell, S., & Brisken, C. (2007). Amphiregulin is an essential mediator of estrogen receptor function in mammary gland development. *Proceedings of the National Academy of Sciences*, *104*(13), 5455–5460.

Clarke, B., Potten, S., Howell, A., Potten, C., & Anderson, E. (1997). Dissociation between Steroid Receptor Expression and Cell Proliferation in the Human Breast. *Cancer Research*, *Volume 57*(22), 4987–4991.

Costa, E. A., Subramanian, K., Nunnari, J., & Weissman, J. S. (2018). Defining the physiological role of SRP in protein-targeting efficiency and specificity. *Science*, *359*(6376), 689–692.

Cowin, P., & Wysolmerski, J. (2017). Mammary Gland Development. *Cold Spring Harbor Perspectives in Biology*, *2*(a003251), 1–14.

Crick, F. (1958). On Protein Synthesis. *The Symposia of the Society for Experimental Biology*, (pp. 138–166).

Crick, F. H. C. (1970). Central Dogma of Molecular Biology. *Nature*, *227*(5258), 561–563.

Crook, T., Brooks, L. a., Crossland, S., Osin, P., Barker, K. T., Waller, J., Philp, E., Smith, P. D., Yulug, I., Peto, J., Parker, G., Allday, M. J., Crompton, M. R., & Gusterson, B. a. (1998). p53 mutation with frequent novel condons but not a mutator phenotype in BRCA1- and BRCA2-associated breast tumours. *Oncogene*, *17*, 1681–1689.

Croucher, P. I., McDonald, M. M., & Martin, T. J. (2016). Bone metastasis: The importance of the neighbourhood. *Nature Reviews Cancer*, *16*(6), 373–386.

Curtis, C., Shah, S. P., Chin, S. F., Turashvili, G., Rueda, O. M., Dunning, M. J., Speed, D., Lynch, A. G., Samarajiwa, S., Yuan, Y., Gräf, S., Ha, G., Haffari, G., Bashashati, A., Russell, R., McKinney, S., Aparicio, S., Brenton, J. D., Ellis, I., Huntsman, D., Pinder, S., Murphy, L., Bardwell, H., Ding, Z., Jones, L., Liu, B., Papatheodorou, I., Sammut, S. J., Wishart, G., Chia, S., Gelmon, K., Speers, C., Watson, P., Blamey, R., Green, A., MacMillan, D., Rakha, E., Gillett, C., Grigoriadis, A., De Rinaldis, E., Tutt, A., Parisien, M., Troup, S., Chan, D., Fielding, C., Maia, A. T., McGuire, S., Osborne, M., Sayalero, S. M., Spiteri, I., Hadfield, J., Bell, L., Chow, K., Gale, N., Kovalik, M., Ng, Y., Prentice, L., Tavaré, S., Markowetz, F., Langerød, A., Provenzano, E., Purushotham, A., Børresen-Dale, A. L., & Caldas, C. (2012). The genomic and transcriptomic architecture of 2,000 breast tumours reveals novel subgroups. *Nature*, *486*(7403), 346–352.

Dai, X., Li, T., Bai, Z., Yang, Y., Liu, X., Zhan, J., & Shi, B. (2015). Breast cancer intrinsic subtype classification, clinical use and future trends. *Am J Cancer Res*, *5*(10), 2929–2943.

D'Ambrogio, A., Nagaoka, K., & Richter, J. D. (2013). Translational control of cell growth and malignancy by the CPEBs. *Nature reviews. Cancer*, *13*(4), 283–90.

Daniel, C. W., Deome, K. B., Young, J. T., Blair, P. B., & Faulkin, L. J. (1968). The in vivo life span of normal and preneoplastic mouse mammary glands: a serial transplantation study. *Proc Natl Acad Sci U S A*, *61*(1), 53–60.

Daniel, C. W., Silberstein, G. B., & Strickland, P. (1987). Direct Action of 17 / 3-Estradiol on Mouse Mammary Ducts Analyzed by Sustained Release Implants and Steroid Autoradiography1. *Cancer Research*, *47*, 6052–6057.

DeLigio, J. T., Lin, G., Chalfant, C. E., & Park, M. A. (2017). Splice variants of cytosolic polyadenylation element– binding protein 2 (CPEB2) differentially regulate pathways linked to cancer metastasis. *Journal of Biological Chemistry*, *292*(43), 17909–17918.

DeOme, K. B., Faulkin, L. J., Bern, H. A., & Blair, P. B. (1959). Development of mammary tumors from hyperplastic alveolar nodules transplanted into gland-free mammary fat pads of female C3H mice. *Cancer research*, *19*(5), 515–20.

Desantis, C., Ma, J., Bryan, L., & Jemal, A. (2014). Breast Cancer Statistics , 2013. *CA Cancer Journal for Clinicians*, *64*(1), 52–62.

Dever, T. E., & Green, R. (2015). Phases of Translation in Eukaryotes. *Cold Spring Harbor Perspectives in Biology*, *4*(a013706), 1–16.

Di Giammartino, D. C., Nishida, K., & Manley, J. L. (2011). Mechanisms and Consequences of Alternative Polyadenylation. *Molecular Cell*, *43*(6), 853–866.

Dias, K., Dvorkin-Gheva, A., Hallett, R. M., Wu, Y., Hassell, J., Pond, G. R., Levine, M., Whelan, T., & Bane, A. L. (2017). Claudin-low breast cancer; clinical & pathological characteristics. *PLoS ONE*, *12*(1), 1–17.

Dougall, W. C., Glaccum, M., Charrier, K., Rohrbach, K., Brasel, K., De Smedt, T., Daro, E., Smith, J., Tometsko, M. E., Maliszewski, C. R., Armstrong, A., Shen, V., Bain, S., Cosman, D., Anderson, D., Morrissey, P. J., Peschon, J. J., & Schuh, J. A. (1999). RANK is essential for osteoclast and lymph node development. *Genes and Development*, *13*(18), 2412–2424.

Drisaldi, B., Colnaghi, L., Fioriti, L., Rao, N., Myers, C., Snyder, A., Metzger, D., Tarasoff, J., Konstantinov, E., Fraser, P. E., Manley, J., & Kandel, E. (2015). SUMOylation Is an Inhibitory Constraint that Regulates the Prion-like Aggregation and Activity of CPEB3. *Cell Reports*, (pp. 1–9).

EBCTCG, E. B. C. T. C. G. (2005). Effects of chemotherapy and hormonal therapy for early breast cancer on recurrence and 15-year survival: an overview of the randomised trials. *Lancet*, *365*(9472), 1687–717.

Eliscovich, C., Peset, I., Vernos, I., & Méndez, R. (2008). Spindle-localized CPE-mediated translation controls meiotic chromosome segregation. *Nature cell biology*, *10*(7), 858–65.

Fantozzi, A., & Christofori, G. (2006). Mouse models of breast cancer metastasis. *Breast Cancer Research*, *8*(4).

Fata, J., Chaudhary, V., & Khokha, R. (2001). Cellular Turnover in the Mammary Gland Is Correlated with Systemic Levels of Progesterone and Not 17??-Estradiol During the Estrous Cycle. *Biology of reproduction*, *65*, 680–688.

Fata, J. E., Kong, Y.-Y., Li, J., Sasaki, T., Irie-Sasaki, J., Moorehead, R. A., Elliott, R., Scully, S., Voura, E. B., Lacey, D. L., Boyle, W. J., Khokha, R., & Penninger, J. M. (2000). The Osteoclast Differentiation Factor Osteoprotegerin-Ligand Is Essential for Mammary Gland Development. *Cell*, *103*(1), 41–50.

Feeley, L. P., Mulligan, A. M., Pinnaduwage, D., Bull, S. B., & Andrulis, I. L. (2014). Distinguishing luminal breast cancer subtypes by Ki67, progesterone receptor or TP53 status provides prognostic information. *Modern Pathology*, *27*(4), 554–561.

Fernández-Miranda, G., & Méndez, R. (2012). The CPEB-family of proteins, translational control in senescence and cancer. *Ageing research reviews*, *11*(4), 460–72.

Fioriti, L., Myers, C., Huang, Y. Y., Li, X., Stephan, J. S., Trifilieff, P., Colnaghi, L., Kosmidis, S., Drisaldi, B., Pavlopoulos, E., & Kandel, E. R. (2015). The Persistence of Hippocampal-Based Memory Requires Protein Synthesis Mediated by the Prion-like Protein CPEB3. *Neuron*, *86*(6), 1433–1448.

Fong, S. W., Lin, H. C., Wu, M. F., Chen, C. C., & Huang, Y. S. (2016). CPEB3 deficiency elevates TRPV1 expression in dorsal root ganglia neurons to potentiate thermosensation. *PLoS ONE*, *11*(2), 1–19.

Forsyth, I. A., & Neville, M. C. (2009). Introduction: The myoepithelial cell and milk letdown; entrance to the multifunctional role of oxytocin. *Journal of Mammary Gland Biology and Neoplasia*, *14*(3), 221–222.

Gebauer, F., & Hentze, M. W. (2004). Molecular mechanisms of translational control. *Nature Reviews Molecular Cell Biology*, *5*(10), 827–835.

Gentleman, R., Carey, V., Bates, D., Bolstad, B., Dettling, M., Dudoit, S., Ellis, B., Gautier, L., Ge, Y., Gentry, J., Hornik, K., Hothorn, T., Huber, W., Iacus, S., Irizarry, R., Leisch, F., Li, C., Maechler, M., Rossini, A., Sawitzki, G., Smith, C., Smyth, G., Tierney, L., Yang, J., & Zhang, J. (2004). Bioconductor: open software development for computational biology and bioinformatics. *Genome Biology*, *5*(10), R80.

Giangarrà, V., Igea, A., Castellazzi, C. L., Bava, F.-A., & Mendez, R. (2015). Global Analysis of CPEBs Reveals Sequential and Non-Redundant Functions in Mitotic Cell Cycle. *Plos One*, *10*(9), e0138794.

Gigli, I., & Maizon, D. O. (2013). microRNAs and the mammary gland: A new understanding of gene expression. *Genetics and Molecular Biology*, *36*(4), 465–474.

Giraddi, R. R., Shehata, M., Gallardo, M., Blasco, M. A., Simons, B. D., & Stingl, J. (2015). Stem and progenitor cell division kinetics during postnatal mouse mammary gland development. *Nature communications*, *6*, 8487.

Gjorevski, N., & Nelson, C. M. (2010). Endogenous patterns of mechanical stress are required for branching morphogenesis. *Integrative Biology*, *2*(9), 424.

Gjorevski, N., & Nelson, C. M. (2011). Integrated morphodynamic signalling of the mammary gland. *Nature Reviews Molecular Cell Biology*, *12*(9), 581–593.

Glisovic, T., Bachorik, J. L., Yong, J., & Dreyfuss, G. (2008). RNA-binding proteins and post-transcriptional gene regulation. *FEBS Letters*, *582*(14), 1977–1986.

Gonzalez-Suarez, E., Jacob, A. P., Jones, J., Miller, R., Roudier-Meyer, M. P., Erwert, R., Pinkas, J., Branstetter, D., & Dougall, W. C. (2010). RANK ligand mediates progestin-induced mammary epithelial proliferation and carcinogenesis. *Nature*, *468*(7320), 103–107.

González-Suárez, E., & Sanz-Moreno, A. (2016). RANK as a therapeutic target in cancer. *The FEBS journal*, *283*(11), 2018–2033.

Gradishar, W. J. (2012). HER2 Therapy — An Abundance of Riches. *New England Journal of Medicine*, *366*(2), 176–178.

Gray, N. K., & Wickens, M. (1998). Control of translation initiation in animals. *Annual Review of Cell and Developmental Biology*, *14*, 399–458.

Grimm, S. L., Hartig, S. M., & Edwards, D. P. (2016). Progesterone Receptor Signaling Mechanisms. *Journal of Molecular Biology*, *428*(19), 3831–3849.

Groisman, I., Ivshina, M., Marin, V., Kennedy, N. J., Davis, R. J., & Richter, J. D. (2006). Control of cellular senescence by CPEB. *Genes & development*, *20*, 2701–2712.

Groppo, R., & Richter, J. D. (2011). CPEB control of NF-kappaB nuclear localization and interleukin-6 production mediates cellular senescence. *Molecular and cellular biology*, *31*(13), 2707–14.

Guillén-Boixet, J., Buzon, V., Salvatella, X., & Méndez, R. (2016). CPEB4 is regulated during cell cycle by ERK2/Cdk1-mediated phosphorylation and its assembly into liquid-like droplets. *eLife*, *5*(NOVEMBER2016), 1–26.

Hägele, S., Kühn, U., Böning, M., & Katschinski, D. M. (2009). Cytoplasmic polyadenylation-element-binding protein (CPEB)1 and 2 bind to the HIF-1alpha mRNA 3'-UTR and modulate HIF-1alpha protein expression. *The Biochemical journal*, *417*(1), 235–246.

Halbeisen, R. E., Galgano, A., Scherrer, T., & Gerber, A. P. (2008). Post-transcriptional gene regulation:From genome-wide studies to principles. *Cellular and Molecular Life Sciences*, *65*, 798–813.

Hanada, R., Leibbrandt, A., Hanada, T., Kitaoka, S., Furuyashiki, T., Fujihara, H., Trichereau, J., Paolino, M., Qadri, F., Plehm, R., Klaere, S., Komnenovic, V., Mimata, H., Yoshimatsu, H., Takahashi, N., Von Haeseler, A., Bader, M., Kilic, S. S., Ueta, Y., Pifl, C., Narumiya, S., & Penninger, J. M. (2009). Central control of fever and female body temperature by RANKL/RANK. *Nature*, *462*(7272), 505–509.

Hanahan, D., & Weinberg, R. A. (2011). Hallmarks of cancer: The next generation. *Cell*, *144*(5), 646–674.

Hansen, C. N., Ketabi, Z., Rosenstierne, M. W., Palle, C., Boesen, H. C., & Norrild, B. (2009). Expression of CPEB, GAPDH and U6snRNA in cervical and ovarian tissue during cancer development. *Apmis*, *117*(1), 53–59.

Hennighausen, L., & Robinson, G. W. (2005). Information networks in the mammary gland. *Nature reviews. Molecular cell biology*, *6*(9), 715–725.

Hentze, M. W., Castello, A., Schwarzl, T., & Preiss, T. (2018). A brave new world of RNA-binding proteins. *Nature Reviews Molecular Cell Biology*.

Herschkowitz, J. I., & Lubet, R. (2010). Mouse models of triple negative [basal-like/claudin low] breast cancer. *Breast Disease*, *32*(1-2), 63–71.

Herschkowitz, J. I., Simin, K., Weigman, V. J., Mikaelian, I., Usary, J., Hu, Z., Rasmussen, K. E., Jones, L. P., Assefnia, S., Chandrasekharan, S., Backlund, M. G., Yin, Y., Khramtsov, A. I., Bastein, R., Quackenbush, J., Glazer, R. I., Brown, P. H., Green, J. E., Kopelovich, L., Furth, P. A., Palazzo, J. P., Olopade, O. I., Bernard, P. S., Churchill, G. A., Van Dyke, T., & Perou, C. M. (2007). Identification of conserved gene expression features between murine mammary carcinoma models and human breast tumors. *Genome Biology*, *8*(5), 1–17.

Hosoda, N., Funakoshi, Y., Hirasawa, M., Yamagishi, R., Asano, Y., Miyagawa, R., Ogami, K., Tsujimoto, M., & Hoshino, S. I. (2011). Anti-proliferative protein Tob negatively regulates CPEB3 target by recruiting Caf1 deadenylase. *EMBO Journal*, *30*(7), 1311–1323.

Hovey, R. C., Trott, J. F., & Vonderhaar, B. K. (2002). Establishing a framework for the functional mammary gland: From endocrinology to morphology. *Journal of Mammary Gland Biology and Neoplasia*, *7*(1), 17–38.

Hu, W., Yuan, B., & Lodish, H. (2014). Cpeb4-Mediated Translational Regulatory Circuitry Controls Terminal Erythroid Differentiation. *Developmental Cell*, *30*(6), 660–672.

Huang, Y.-S., Carson, J. H., Barbarese, E., & Richter, J. D. (2003). Facilitation of dendritic mRNA transport by CPEB. *Genes & development*, *17*(5), 638–53.

Igea, A., & Méndez, R. (2010). Meiosis requires a translational positive loop where CPEB1 ensues its replacement by CPEB4. *The EMBO journal*, *29*(13), 2182–93.

Ihmels, J., Friedlander, G., Bergmann, S., Sarig, O., Ziv, Y., & Barkai, N. (2002). Revealing modular organization in the yeast transcriptional network. *Nature Genetics*, *31*(4), 370–377.

Ilic, N., Utermark, T., Widlund, H. R., & Roberts, T. M. (2011). PI3K-targeted therapy can be evaded by gene amplification along the MYC-eukaryotic translation initiation factor 4E (eIF4E) axis. *Proceedings of the National Academy of Sciences*, *108*(37), E699–E708.

Ismail, P. M., DeMayo, F. J., Amato, P., & Lydon, J. P. (2004). Progesterone induction of calcitonin expression in the murine mammary gland. *Journal of Endocrinology*, *180*(2), 287–295.

Ivshina, M., Lasko, P., & Richter, J. D. (2014). Cytoplasmic Polyadenylation Element Binding Proteins in Development, Health, and Disease. *Annual Review of Cell and Developmental Biology*, *30*(1), 393–415.

Jahchan, N. S., You, Y. H., Muller, W. J., & Luo, K. (2010). Transforming growth factor-?? regulator SnoN modulates mammary gland branching morphogenesis, postlactational involution, and mammary tumorigenesis. *Cancer Research*, *70*(10), 4204–4213.

Jamieson, P. R., Dekkers, J. F., Rios, A. C., Fu, N. Y., Lindeman, G. J., & Visvader, J. E. (2017). Derivation of a robust mouse mammary organoid system for studying tissue dynamics. *Development*, *144*(6), 1065–1071.

Jan, C. H., Williams, C. C., & Weissman, J. S. (2014). Principles of ER cotranslational translocation revealed by proximity- specific ribosome profiling. *Science*, *346*(6210), 748–751.

Johnson, R. M., Vu, N. T., Griffin, B. P., Gentry, A. E., Archer, K. J., Chalfant, C. E., & Park, M. A. (2015). The alternative splicing of cytoplasmic polyadenylation element binding protein 2 drives anoikis resistance and the metastasis of triple negative breast cancer. *Journal of Biological Chemistry*, *290*(42), 25717–25727.

Joshi, P. A., Jackson, H. W., Beristain, A. G., Di Grappa, M. A., Mote, P. A., Clarke, C. L., Stingl, J., Waterhouse, P. D., & Khokha, R. (2010). Progesterone induces adult mammary stem cell expansion. *Nature*, *465*(7299), 803–807.

Joshi, P. A., Waterhouse, P. D., Kannan, N., Narala, S., Fang, H., Di Grappa, M. A., Jackson, H. W., Penninger, J. M., Eaves, C., & Khokha, R. (2015). RANK Signaling Amplifies WNT-Responsive Mammary Progenitors through R-SPONDIN1. *Stem Cell Reports*, *5*(1), 31–44.

Jozwik, K. M., & Carroll, J. S. (2012). Pioneer factors in hormone-dependent cancers. *Nature Reviews Cancer*, *12*(6), 381–385.

Kaenel, P., Antonijevic, M., Richter, S., Küchler, S., Sutter, N., Wotzkow, C., Strange, R., & Andres, A. C. (2012a). Deregulated ephrin-B2 signaling in mammary epithelial cells alters the stem cell compartment and interferes with the epithelial differentiation pathway. *International Journal of Oncology*, *40*(2), 357–369.

Kaenel, P., Mosimann, M., & Andres, A. C. (2012b). The multifaceted roles of Eph-ephrin signaling in breast cancer. *Cell Adhesion and Migration*, *6*(2), 138–147.

Kan, M.-C., Oruganty-Das, A., Cooper-Morgan, A., Jin, G., Swanger, S. a., Bassell, G. J., Florman, H., van Leyen, K., & Richter, J. D. (2010). CPEB4 is a cell survival protein retained in the nucleus upon ischemia or endoplasmic reticulum calcium depletion. *Molecular and cellular biology*, *30*(24), 5658–71.

Kennecke, H., Yerushalmi, R., Woods, R., Cheang, M. C. U., Voduc, D., Speers, C. H., Nielsen, T. O., & Gelmon, K. (2010). Metastatic behavior of breast cancer subtypes. *Journal of Clinical Oncology*, *28*(20), 3271–3277.

Khokha, R., & Werb, Z. (2011). Mammary gland reprogramming: Metalloproteinases couple form with function. *Cold Spring Harbor Perspectives in Biology*, *3*(4), 1–19.

Khramtsov, A. I., Khramtsova, G. F., Tretiakova, M., Huo, D., Olopade, O. I., & Goss, K. H. (2010). Wnt/β-catenin pathway activation is enriched in basal-like breast cancers and predicts poor outcome. *American Journal of Pathology*, *176*(6), 2911–2920.

Kiechl, S., Schramek, D., Widschwendter, M., Fourkala, E.-O., Zaikin, A., Jones, A., Jaeger, B., Rack, B., Janni, W., Scholz, C., Willeit, J., Weger, S., Mayr, A., Teschendorff, A., Rosenthal, A., Fraser, L., Philpott, S., Dubeau, L., Keshtgar, M., Roylance, R., Jacobs, I. J., Menon, U., Schett, G., & Penninger, J. M. (2017). Aberrant regulation of RANKL/OPG in women at high risk of developing breast cancer. *Oncotarget*, *8*(3), 3811–3825.

Kim, J. H., & Richter, J. D. (2006). Opposing Polymerase-Deadenylase Activities Regulate Cytoplasmic Polyadenylation. *Molecular Cell*, *24*(2), 173–183.

Kordon, E. C., & Smith, G. H. (1998). An entire functional mammary gland may comprise the progeny from a single cell. *Development*, *125*(10), 1921–1930.

Koren, S., Reavie, L., Couto, J. P., De Silva, D., Stadler, M. B., Roloff, T., Britschgi, A., Eichlisberger, T., Kohler, H., Aina, O., Cardiff, R. D., & Bentires-Alj, M. (2015). PIK3CAH1047Rinduces multipotency and multi-lineage mammary tumours. *Nature*, *525*(7567), 114–118.

Kostenuik, P. J., Nguyen, H. Q., McCabe, J., Warmington, K. S., Kurahara, C., Sun, N., Chen, C., Li, L., Cattley, R. C., Van, G., Scully, S., Elliott, R., Grisanti, M., Morony, S., Hong, L. T., Asuncion, F., Li, X., Ominsky, M. S., Stolina, M., Dwyer, D., Dougall, W. C., Hawkins, N., Boyle, W. J., Simonet, W. S., & Sullivan, J. K. (2009). Denosumab, a fully human monoclonal antibody to RANKL, inhibits bone resorption and increases BMD in knock-in mice that express chimeric (murine/human) RANKL. *Journal of Bone and Mineral Research*, *24*(2), 182–195.

Kouros-Mehr, H., Slorach, E. M., Sternlicht, M. D., & Werb, Z. (2006). GATA-3 Maintains the Differentiation of the Luminal Cell Fate in the Mammary Gland. *Cell*, *127*(5), 1041–1055.

Kuleshov, M. V., Jones, M. R., Rouillard, A. D., Fernandez, N. F., Duan, Q., Wang, Z., Koplev, S., Jenkins, S. L., Jagodnik, K. M., Lachmann, A., McDermott, M. G., Monteiro, C. D., Gundersen, G. W., & Ma'ayan, A. (2016). Enrichr: a comprehensive gene set enrichment analysis web server 2016 update. *Nucleic acids research*, *44*(W1), W90–W97.

Kuraishi, T., Sun, Y., Aoki, F., Imakawa, K., & Sakai, S. (2000). The poly(A) tail length of casein mRNA in the lactating mammary gland changes depending upon the accumulation and removal of milk. *The Biochemical journal*, *347*(Pt 2), 579–83.

Lacey, D. L., Boyle, W. J., Simonet, W. S., Kostenuik, P. J., Dougall, W. C., Sullivan, J. K., Martin, J. S., & Dansey, R. (2012). Bench to bedside: Elucidation of the OPG-RANK-RANKL pathway and the development of denosumab. *Nature Reviews Drug Discovery*, *11*(5), 401–419.

Lai, Y.-T., Su, C.-K., Jiang, S.-T., Chang, Y.-J., Lai, A. C.-Y., & Huang, Y.-S. (2016). Deficiency of CPEB2-Confined ChAT Expression in the Dorsal Motor Nucleus of Vagus Causes Hyperactivated Parasympathetic Signaling-Associated Bronchoconstriction. *The Journal of Neuroscience*, (pp. 0557–16).

Lanari, C., Lamb, C. A., Fabris, V. T., Helguero, L. A., Soldati, R., Bottino, M. C., Giulianelli, S., Cerliani, J. P., Wargon, V., & Molinolo, A. (2009). The MPA mouse breast cancer model: Evidence for a role of progesterone receptors in breast cancer. *Endocrine-Related Cancer*, *16*(2), 333–350.

Langmead, B., & Salzberg, S. L. (2012). Fast gapped-read alignment with Bowtie 2. *Nature Methods*, *9*(4), 357–359.

Langmead, B., Trapnell, C., Pop, M., & Salzberg, S. L. (2009). Ultrafast and memory-efficient alignment of short DNA sequences to the human genome. *Genome Biology*, *10*(3).

Leppek, K., Das, R., & Barna, M. (2017). Functional 5′ UTR mRNA structures in eukaryotic translation regulation and how to find them. *Nature Reviews Molecular Cell Biology*, *19*(3), 158–174.

Levin, E. R., & Hammes, S. R. (2016). Nuclear receptors outside the nucleus: extranuclear signalling by steroid receptors. *Nature Reviews Molecular Cell Biology*, *17*(12), 783–797.

Lim, E., Vaillant, F., Wu, D., Forrest, N. C., Pal, B., Hart, A. H., Asselin-Labat, M.-L., Gyorki, D. E., Ward, T., Partanen, A., Feleppa, F., Huschtscha, L. I., Thorne, H. J., Fox, S. B., Yan, M., French, J. D., Brown, M. A., Smyth, G. K., Visvader, J. E., & Lindeman, G. J. (2009). Aberrant luminal progenitors as the candidate target population for basal tumor development in BRCA1 mutation carriers. *Nature medicine*, *15*(8), 907–13.

Lim, E., Wu, D., Pal, B., Bouras, T., Asselin-Labat, M.-L., Vaillant, F., Yagita, H., Lindeman, G. J., Smyth, G. K., & Visvader, J. E. (2010). Transcriptome analyses of mouse and human mammary cell subpopulations reveal multiple conserved genes and pathways. *Breast Cancer Research*, *12*(2), R21.

Lin, S., & Gregory, R. I. (2015). MicroRNA biogenesis pathways in cancer. *Nature Reviews Cancer*, *15*(6), 321–333.

Lo, P.-K., Kanojia, D., Liu, X., Singh, U. P., Berger, F. G., Wang, Q., & Chen, H. (2012). CD49f and CD61 identify Her2/neu-induced mammary tumor-initiating cells that are potentially derived from luminal progenitors and maintained by the integrin–TGFβ signaling. *Oncogene*, *31*(21), 2614–2626.

Love, M. I., Huber, W., & Anders, S. (2014). Moderated estimation of fold change and dispersion for RNA-seq data with DESeq2. *Genome Biology*, *15*(12), 1–21.

Lu, R., Zhou, Z., Yu, W., Xia, Y., & Zhi, X. (2017a). CPEB4 promotes cell migration and invasion via upregulating Vimentin expression in breast cancer. *Biochemical and Biophysical Research Communications*, *489*(2), 135–141.

Lu, W.-H., Yeh, N.-H., & Huang, Y.-S. (2017b). CPEB2 Activates GRASP1 mRNA Translation and Promotes AMPA Receptor Surface Expression, Long-Term Potentiation, and Memory. *Cell Reports*, *21*(7), 1783–1794.

Macias, H., & Hinck, L. (2012). Mammary gland development.

Macias, H., Moran, A., Samara, Y., Moreno, M., Compton, J. E., Harburg, G., Strickland, P., & Hinck, L. (2011). SLIT/ROBO1 signaling suppresses mammary branching morphogenesis by limiting basal cell number. *Developmental Cell*, *20*(6), 827–840.

Magnani, L., Ballantyne, E. B., Zhang, X., & Lupien, M. (2011). PBX1 genomic pioneer function drives ERα signaling underlying progression in breast cancer. *PLoS Genetics*, *7*(11), 1–15.

Maillo, C., Martin, J., Sebastian, D., Hernandez-Alvarez, M., Garcia-Rocha, M., Reina, O., Zorzano, A., Fernandez, M., & Mendez, R. (2017). Circadian- and UPR-dependent control of CPEB4 mediates a translational response to counteract hepatic steatosis under ER stress. *Nat Cell Biol, advance on*.

Manavathi, B., Samanthapudi, V. S. K., & Gajulapalli, V. N. R. (2014). [ERa] Estrogen receptor coregulators and pioneer factors: the orchestrators of mammary gland cell fate and development. *Frontiers in cell and developmental biology*, *2*(August), 34.

Maningat, P., Sen, P., & Rijnkels, M. (2009). Gene expression in the human mammary epithelium during lactation: the milk fat globule transcriptome. *Physiological …*, *77030*, 12–22.

Mayr, C. (2016). Evolution and Biological Roles of Alternative 3'UTRs. *Trends in Cell Biology*, *26*(3), 227–237.

Mayr, C., & Bartel, D. P. (2009). Widespread Shortening of 3′UTRs by Alternative Cleavage and Polyadenylation Activates Oncogenes in Cancer Cells. *Cell*, *138*(4), 673–684.

Meier-Abt, F., Milani, E., Roloff, T., Brinkhaus, H., Duss, S., Meyer, D. S., Klebba, I., Balwierz, P. J., van Nimwegen, E., & Bentires-Alj, M. (2013). Parity induces differentiation and reduces Wnt/Notch signaling ratio and proliferation potential of basal stem/progenitor cells isolated from mouse mammary epithelium. *Breast Cancer Research*, *15*(2).

Mendez, R., Barnard, D., & Richter, J. D. (2002). Differential mRNA translation and meiotic progression require Cdc2-mediated CPEB destruction. *EMBO Journal*, *21*(7), 1833–1844.

Mendez, R., Hake, L. E., Andresson, T., Littlepage, L. E., Ruderman, J. V., & Richter, J. D. (2000a). Phosphorylation of CPE binding factor by Eg2 regulates translation of c- mos mRNA. *Nature*, *404*(6775), 302–307.

Mendez, R., Murthy, K. G., Ryan, K., Manley, J. L., & Richter, J. D. (2000b). Phosphorylation of CPEB by Eg2 mediates the recruitment of CPSF into an active cytoplasmic polyadenylation complex. *Molecular Cell*, *6*(5), 1253–1259.

Mendez, R., & Richter, J. D. (2001). Translational control by CPEB: a means to the end. *Nature reviews. Molecular cell biology*, *2*(7), 521–9.

Merlos-Suárez, A., & Batlle, E. (2008). Eph-ephrin signalling in adult tissues and cancer. *Current Opinion in Cell Biology*, *20*(2), 194–200.

Mohammed, H., Russell, I. A., Stark, R., Rueda, O. M., Hickey, T. E., Tarulli, G. A., Serandour, A. A., Birrell, S. N., Bruna, A., Saadi, A., Menon, S., Hadfield, J., Pugh, M., Raj, G. V., Brown, G. D., D'Santos, C., Robinson, J. L., Silva, G., Launchbury, R., Perou, C. M., Stingl, J., Caldas, C., Tilley, W. D., & Carroll, J. S. (2015). Progesterone receptor modulates ERα action in breast cancer. *Nature*, *523*(7560), 313–317.

Molyneux, G., Geyer, F. C., Magnay, F. A., McCarthy, A., Kendrick, H., Natrajan, R., MacKay, A., Grigoriadis, A., Tutt, A., Ashworth, A., Reis-Filho, J. S., & Smalley, M. J. (2010). BRCA1 basal-like breast cancers originate from luminal epithelial progenitors and not from basal stem cells. *Cell Stem Cell*, *7*(3), 403–417.

Montero Girard, G., Vanzulli, S. I., Cerliani, J. P., Bottino, M. C., Bolado, J., Vela, J., Becu-Villalobos, D., Benavides, F., Gutkind, S., Patel, V., Molinolo, A., & Lanari, C. (2007). Association of estrogen receptor-α and progesterone receptor A expression with hormonal mammary carcinogenesis: Role of the host microenvironment. *Breast Cancer Research*, *9*(2), 1–16.

Moore, M. J. (2005). From birth to death: The complex lives of eukaryotic mRNAs. *Science*, *309*(5740), 1514–1518.

Morris, A. R., Mukherjee, N., & Keene, J. D. (2010). Systematic analysis of posttranscriptional gene expression. *Wiley Interdisciplinary Reviews: Systems Biology and Medicine*, *2*(2), 162–180.

Mukherjee, A., Soyal, S. M., Li, J., Ying, Y., He, B., DeMayo, F. J., & Lydon, J. P. (2010). Targeting RANKL to a specific subset of murine mammary epithelial cells induces ordered branching morphogenesis and alveologenesis in the absence of progesterone receptor expression. *The FASEB Journal*, *24*(11), 4408–4419.

Musgrove, E. A., & Sutherland, R. L. (2009). Biological determinants of endocrine resistance in breast cancer. *Nature Reviews Cancer*, *9*(9), 631–643.

Nagaoka, K., Fujii, K., Zhang, H., Usuda, K., Watanabe, G., Ivshina, M., & Richter, J. D. (2015). CPEB1 mediates epithelial-to-mesenchyme transition and breast cancer metastasis. *Oncogene*, *35*(22), 2893–2901.

Nagaoka, K., Udagawa, T., & Richter, J. D. (2012). CPEB-mediated ZO-1 mRNA localization is required for epithelial tight-junction assembly and cell polarity. *Nature communications*, *3*, 675.

Nagata, Y., Lan, K. H., Zhou, X., Tan, M., Esteva, F. J., Sahin, A. A., Klos, K. S., Li, P., Monia, B. P., Nguyen, N. T., Hortobagyi, G. N., Hung, M. C., & Yu, D. (2004). PTEN activation contributes to tumor inhibition by trastuzumab, and loss of PTEN predicts trastuzumab resistance in patients. *Cancer Cell*, *6*(2), 117–127.

Nairismägi, M.-L., Vislovukh, a., Meng, Q., Kratassiouk, G., Beldiman, C., Petretich, M., Groisman, R., Füchtbauer, E.-M., Harel-Bellan, a., & Groisman, I. (2012). Translational control of TWIST1 expression in MCF-10A cell lines recapitulating breast cancer progression. *Oncogene*, *31*(47), 4960–6.

Nelson, C. M., VanDuijn, M. M., Inman, J. L., Fletcher, D. A., & Bissell, M. J. (2006). Tissue geometry determines sites of mammary branching morphogenesis in organotypic cultures. *Science*, *314*(5797), 298–300.

Nguyen-Ngoc, K.-V., Shamir, E. R., Huebner, R. J., Beck, J. N., Cheung, K. J., & Ewald, A. J. (2014). *Tissue Morphogenesis: Methods and Protocols*. Springer US.

Nolan, E., Vaillant, F., Branstetter, D., Pal, B., Giner, G., Whitehead, L., Lok, S. W., Mann, G. B., Rohrbach, K., Huang, L.-Y., Soriano, R., Smyth, G. K., Dougall, W. C., Visvader, J. E., & Lindeman, G. J. (2016). RANK ligand as a potential target for breast cancer prevention in BRCA1-mutation carriers. *Nature Medicine*, *22*(8), 933–939.

Nomura, T., Göritz, C., Catchpole, T., Henkemeyer, M., & Frisén, J. (2010). EphB signaling controls lineage plasticity of adult neural stem cell niche cells. *Cell Stem Cell*, *7*(6), 730–743.

Novoa, I., Gallego, J., Ferreira, P. G., & Mendez, R. (2010). Mitotic cell-cycle progression is regulated by CPEB1 and CPEB4-dependent translational control. *Nature cell biology*, *12*(5), 447–56.

Nusse, R., & Clevers, H. (2017). Wnt/β-Catenin Signaling, Disease, and Emerging Therapeutic Modalities. *Cell*, *169*(6), 985–999.

Oakes, S. R., Naylor, M. J., Blazek, K. D., Hilton, H. N., Kazlauskas, M., Pritchard, M. a., Chodosh, L. a., Peter, L., Lindeman, G. J., Visvader, J. E., Ormandy, C. J., Gardiner-garden, M., & Pfeffer, P. L. (2008). The Ets transcription factor Elf5 specifies mammary alveolar cell fate service The Ets transcription factor Elf5 specifies mammary alveolar cell fate. *Genes & development*, *22*, 581–586.

Obr, A. E., Grimm, S. L., Bishop, K. a., Pike, J. W., Lydon, J. P., & Edwards, D. P. (2013). Progesterone receptor and Stat5 signaling cross talk through RANKL in mammary epithelial cells. *Molecular endocrinology (Baltimore, Md.)*, *27*(November 2013), 1808–24.

Orphanides, G. (2002). A Unified Theory of Gene Expression. *Cell*, *108*, 439–451.

Ortiz-Zapater, E., Pineda, D., Martínez-Bosch, N., Fernández-Miranda, G., Iglesias, M., Alameda, F., Moreno, M., Eliscovich, C., Eyras, E., Real, F. X., Méndez, R., & Navarro, P. (2012). Key contribution of CPEB4-mediated translational control to cancer progression. *Nature medicine*, *18*(1), 83–90.

Papasaikas, P., & Valcárcel, J. (2016). The Spliceosome: The Ultimate RNA Chaperone and Sculptor. *Trends in Biochemical Sciences*, *41*(4), 386.

Parker, J. S., Mullins, M., Cheung, M. C., Leung, S., Voduc, D., Vickery, T., Davies, S., Fauron, C., He, X., Hu, Z., Quackenhush, J. F., Stijleman, I. J., Palazzo, J., Matron, J. S., Nobel, A. B., Mardis, E., Nielsen, T. O., Ellis, M. J., Perou, C. M., & Bernard, P. S. (2009). Supervised risk predictor of breast cancer based on intrinsic subtypes. *Journal of Clinical Oncology*, *27*(8), 1160–1167.

Parsyan, A., Svitkin, Y., Shahbazian, D., Gkogkas, C., Lasko, P., Merrick, W. C., & Sonenberg, N. (2011). MRNA helicases: The tacticians of translational control. *Nature Reviews Molecular Cell Biology*, *12*(4), 235–245.

Pasquale, P., Alex, C., Marta Ines, G., William, D. C., Purificaci??n, M., Miguel Angel, P., & Eva, G. S. (2013). Constitutive activation of RANK disrupts mammary cell fate leading to tumorigenesis. *Stem Cells*, *31*(9), 1954–1965.

Pavlopoulos, E., Trifilieff, P., Chevaleyre, V., Fioriti, L., Zairis, S., Pagano, A., Malleret, G., & Kandel, E. R. (2011). Neuralized1 activates CPEB3: A function for nonproteolytic ubiquitin in synaptic plasticity and memory storage. *Cell*, *147*(6), 1369–1383.

Peaker, M. (2002). The mammary gland in mammalian evolution: A brief commentary on some of the concepts. *Journal of Mammary Gland Biology and Neoplasia*, *7*(3), 347–353.

Peng, S. C., Lai, Y. T., Huang, H. Y., Huang, H. D., & Huang, Y. S. (2010). A novel role of CPEB3 in regulating EGFR gene transcription via association with Stat5b in neurons. *Nucleic Acids Research*, *38*(21), 7446–7457.

Pérez-Guijarro, E., Karras, P., Cifdaloz, M., Martínez-Herranz, R., Cañón, E., Graña, O., Horcajada-Reales, C., Alonso-Curbelo, D., Calvo, T. G., Gómez-López, G., Bellora, N., Riveiro-Falkenbach, E., Ortiz-Romero, P. L., Rodríguez-Peralto, J. L., Maestre, L., Roncador, G., de Agustín Asensio, J. C., Goding, C. R., Eyras, E., Megías, D., Méndez, R., & Soengas, M. S. (2016). Lineage-specific roles of the cytoplasmic polyadenylation factor CPEB4 in the regulation of melanoma drivers. *Nature Communications*, *7*, 13418.

Perou, C. M., Sùrlie, T., Eisen, M. B., Rijn, M. V. D., Jeffrey, S. S., Rees, C. A., Pollack, J. R., Ross, D. T., Johnsen, H., Akslen, L. A., Fluge, I., Pergamenschikov, A., Williams, C., Zhu, S. X., Lùnning, P. E., Brown, P. O., Botstein, D., & Grant, S. (2000). Molecular portraits of human breast tumours. *Nature*, *533*(May), 747–752.

Piqué, M., López, J. M., Foissac, S., Guigó, R., & Méndez, R. (2008). A combinatorial code for CPE-mediated translational control. *Cell*, *132*(3), 434–48.

Polyak, K., & Kalluri, R. (2010). The role of the microenvironment in mammary gland development and cancer. *Cold Spring Harb Perspect Biol*, *2*(11), a003244.

Prat, A., & Perou, C. M. (2011). Deconstructing the molecular portraits of breast cancer. *Molecular Oncology*, *5*(1), 5–23.

Prater, M., Shehata, M., Watson, C. J., & Stingl, J. (2012). *Methods in Molecular Biology*, vol. 531. Springer US.

Proudfoot, N. J. (2011). Ending the message : poly (A) signals then and now. *Genes & development*, *25*, 1770–1782.

Rajaram, R. D., Buric, D., Caikovski, M., Ayyanan, A., Rougemont, J., Shan, J., Vainio, S. J., Yalcin-Ozuysal, O., & Brisken, C. (2015). Progesterone and Wnt4 control mammary stem cells via myoepithelial crosstalk. *The EMBO journal*, *34*(5), 641–52.

Rao, S., Cronin, S. J., Sigl, V., & Penninger, J. M. (2017). RANKL and RANK: From Mammalian Physiology to Cancer Treatment. *Trends in Cell Biology*, *28*(3), 213–223.

Regan, J. L., Kendrick, H., Magnay, F. A., Vafaizadeh, V., Groner, B., & Smalley, M. J. (2012). C-Kit is required for growth and survival of the cells of origin of Brca1-mutation-associated breast cancer. *Oncogene*, *31*(7), 869–883.

Reverte, C. G., Ahearn, M. D., & Hake, L. E. (2001). CPEB degradation during Xenopus oocyte maturation requires a PEST domain and the 26S proteasome. *Developmental Biology*, *231*(2), 447–458.

Rhoads, R. E., & Grudzien-Nogalska, E. (2007). Translational regulation of milk protein synthesis at secretory activation. *Journal of Mammary Gland Biology and Neoplasia*, *12*(4), 283–292.

Rios, A. C., Fu, N. Y., Lindeman, G. J., & Visvader, J. E. (2014). In situ identification of bipotent stem cells in the mammary gland. *Nature*, *506*(7488), 322–7.

Ritchie, M. E., Phipson, B., Wu, D., Hu, Y., Law, C. W., Shi, W., & Smyth, G. K. (2015). Limma powers differential expression analyses for RNA-sequencing and microarray studies. *Nucleic Acids Research*, *43*(7), e47.

Roarty, K., & Serra, R. (2007). Wnt5a is required for proper mammary gland development and TGF-beta-mediated inhibition of ductal growth. *Development (Cambridge, England)*, *134*(21), 3929–3939.

Russo, J., Ao, X., Grill, C., & Russo, I. H. (1999). Pattern of distribution of cells positive for estrogen receptor a and progesterone receptor in relation to proliferating cells in the mammary gland. *Breast Cancer Research and Treatment*, *53*(3), 217–227.

Sachs, A. B., Sarnow, P., & Hentze, M. W. (1997). Starting at the beginning, middle, and end: Translation initiation in eukaryotes. *Cell*, *89*(6), 831–838.

Sarink, D., Schock, H., Johnson, T., Overvad, K., Holm, M., Tjønneland, A., Boutron-Ruault, M. C., His, M., Kvaskoff, M., Boeing, H., Lagiou, P., Papatesta, E. M., Trichopoulou, A., Palli, D., Pala, V., Mattiello, A., Tumino, R., Sacerdote, C., Bueno-De-Mesquita, H. B., Van Gils, C. H., Peeters, P. H., Weiderpass, E., Agudo, A., Sánchez, M. J., Chirlaque, M. D., Ardanaz, E., Amiano, P., Khaw, K. T., Travis, R., Dossus, L., Gunter, M., Rinaldi, S., Merritt, M., Riboli, E., Kaaks, R., & Fortner, R. T. (2017). Circulating RANKL and RANKL/OPG and breast cancer risk by ER and PR subtype: Results from the EPIC cohort. *Cancer Prevention Research*, *10*(9), 525–534.

Sau, A., Lau, R., Cabrita, M., Nolan, E., Crooks, P., Visvader, J., & Pratt, M. (2016). Persistent Activation of NF-κB in BRCA1-Deficient Mammary Progenitors Drives Aberrant Proliferation and Accumulation of DNA Damage. *Cell Stem Cell*, (pp. 1–14).

Schedin, P. (2006). Pregnancy-associated breast cancer and metastasis. *Nature Reviews Cancer*, *6*(4), 281–291.

Schramek, D., Leibbrandt, A., Sigl, V., Kenner, L., Pospisilik, J. A., Lee, H. J., Hanada, R., Joshi, P. A., Aliprantis, A., Glimcher, L., Pasparakis, M., Khokha, R., Ormandy, C. J., Widschwendter, M., Schett, G., & Penninger, J. M. (2010). Osteoclast differentiation factor RANKL controls development of progestin-driven mammary cancer. *Nature*, *468*(7320), 98–102.

Segal, E., Shapira, M., Regev, A., Pe'er, D., Botstein, D., Koller, D., & Friedman, N. (2003). Module networks: Identifying regulatory modules and their condition-specific regulators from gene expression data. *Nature Genetics*, *34*(2), 166–176.

Sendoel, A., Dunn, J. G., Rodriguez, E. H., Naik, S., Gomez, N. C., Hurwitz, B., Levorse, J., Dill, B. D., Schramek, D., Molina, H., Weissman, J. S., & Fuchs, E. (2017). Translation from unconventional 5′ start sites drives tumour initiation. *Nature*, *541*(7638), 494–499.

Senkus, E., Kyriakides, S., Ohno, S., Penault-Llorca, F., Poortmans, P., Rutgers, E., Zackrisson, S., & Cardoso, F. (2015). Primary breast cancer: ESMO Clinical Practice Guidelines for diagnosis, treatment and follow-up. *Annals of Oncology*, *26*(November), v8–v30.

Shackleton, M., Vaillant, F., Simpson, K. J., Stingl, J., Smyth, G. K., Asselin-Labat, M.-L., Wu, L., Lindeman, G. J., & Visvader, J. E. (2006). Generation of a functional mammary gland from a single stem cell. *Nature*, *439*(7072), 84–88.

Shehata, M., Teschendorff, A., Sharp, G., Novcic, N., Russell, I. A., Avril, S., Prater, M., Eirew, P., Caldas, C., Watson, C. J., & Stingl, J. (2012). Phenotypic and functional characterisation of the luminal cell hierarchy of the mammary gland. *Breast Cancer Res*, *14*(5), R134.

Sigl, V., Owusu-Boaitey, K., Joshi, P. A., Kavirayani, A., Wirnsberger, G., Novatchkova, M., Kozieradzki, I., Schramek, D., Edokobi, N., Hersl, J., Sampson, A., Odai-Afotey, A., Lazaro, C., Gonzalez-Suarez, E., Pujana, M. A., Heyn, H., Vidal, E., Cruickshank, J., Berman, H., Sarao, R., Ticevic, M., Uribesalgo, I., Tortola, L., Rao, S., Tan, Y., Pfeiler, G., Lee, E. Y., Bago-Horvath, Z., Kenner, L., Popper, H., Singer, C., Khokha, R., Jones, L. P., & Penninger, J. M. (2016). RANKL/RANK control Brca1 mutation-driven mammary tumors. *Cell Research*, *26*(7), 761–774.

Sleeman, K. E., Kendrick, H., Ashworth, A., Isacke, C. M., & Smalley, M. J. (2005). CD24 staining of mouse mammary gland cells defines luminal epithelial, myoepithelial/basal and non-epithelial cells. *Breast Cancer Research*, *8*(1), 6–11.

Sleeman, K. E., Kendrick, H., Robertson, D., Isacke, C. M., Ashworth, A., & Smalley, M. J. (2007). Dissociation of estrogen receptor expression and in vivo stem cell activity in the mammary gland. *The Journal of cell biology*, *176*(1), 19–26.

Solanas, G., & Benitah, S. A. (2013). Regenerating the skin: a task for the heterogeneous stem cell pool and surrounding niche. *Nature reviews. Molecular cell biology*, *14*(11), 737–48.

Sonenberg, N., & Hinnebusch, A. G. (2009). Regulation of Translation Initiation in Eukaryotes: Mechanisms and Biological Targets. *Cell*, *136*(4), 731–745.

Sreekumar, A., Toneff, M. J., Toh, E., Roarty, K., Creighton, C. J., Belka, G. K., Lee, D. K., Xu, J., Chodosh, L. A., Richards, J. A. S., & Rosen, J. M. (2017). WNT-Mediated Regulation of FOXO1 Constitutes a Critical Axis Maintaining Pubertal Mammary Stem Cell Homeostasis. *Developmental Cell*, *43*(4), 436–448.e6.

Stebbins-Boaz, B., Cao, Q., De Moor, C. H., Mendez, R., & Richter, J. D. (1999). Maskin is a CPEB-associated factor that transiently interacts with eIF-4E. *Molecular Cell*, *4*(6), 1017–1027.

Stephan, J. S., Fioriti, L., Lamba, N., Colnaghi, L., Karl, K., Derkatch, I. L., & Kandel, E. R. (2015). The CPEB3 Protein Is a Functional Prion that Interacts with the Actin Cytoskeleton. *Cell Reports*, *11*(11), 1772–1785.

Stingl, J., Eaves, C. J., Zandieh, I., & Emerman, J. T. (2001). Characterization of bipotent mammary epithelial progenitor cells in normal adult human breast tissue. *Breast Cancer Res. Treat.*, *67*(2), 93–109.

Stingl, J., Eirew, P., Ricketson, I., Shackleton, M., Vaillant, F., Choi, D., Li, H. I., & Eaves, C. J. (2006). Purification and unique properties of mammary epithelial stem cells. *Nature*, *439*(7079), 993–997.

Subramanian, A., Tamayo, P., Mootha, V. K., Mukherjee, S., Ebert, B. L., Gillette, M. A., Paulovich, A., Pomeroy, S. L., Golub, T. R., Lander, E. S., & Mesirov, J. P. (2005). Gene set enrichment analysis: A knowledge-based approach for interpreting genome-wide expression profiles. *Proceedings of the National Academy of Sciences*, *102*(43), 15545–15550.

Sun, H.-T., Wen, X., Han, T., Liu, Z.-H., Li, S.-B., Wang, J.-G., & Liu, X.-P. (2015). Expression of CPEB4 in invasive ductal breast carcinoma and its prognostic significance. *OncoTargets and therapy*, *8*, 3499–3506.

Syed, B. A. (2015). The breast cancer market. *Nature Reviews Drug Discovery*, *14*(4), 233–234.

Tan, W., Zhang, W., Strasner, A., Grivennikov, S., Cheng, J. Q., Hoffman, R. M., & Karin, M. (2011). Tumour-infiltrating regulatory T cells stimulate mammary cancermetastasis through RANKL-RANK signalling. *Nature*, *470*(7335), 548–553.

Tanos, T., Sflomos, G., Echeverria, P. C., Ayyanan, A., Delaloye, J.-f., Raffoul, W., Fiche, M., Dougall, W., Schneider, P., Yalcin-ozuysal, O., & Brisken, C. (2013). Supplementary Materials for Progesterone / RANKL Is a Major Regulatory Axis in the Human Breast. *Breast cancer*, *55*(April).

Tarun, S., & Sachs, A. (1995). A common function for mRNA 5'and 3'ends in translation initiation in yeast. *Genes & development*, *9*(23), 2997.

Tay, J., & Richter, J. D. (2001). Germ Cell Differentiation and Synaptonemal Complex Formation Are Disrupted in CPEB Knockout Mice. *Developmental Cell*, *1*(2), 201–213.

Teglund, S., McKay, C., Schuetz, E., Van Deursen, J. M., Stravopodis, D., Wang, D., Brown, M., Bodner, S., Grosveld, G., & Ihle, J. N. (1998). Stat5a and Stat5b proteins have essential and nonessential, or redundant, roles in cytokine responses. *Cell*, *93*(5), 841–850.

Teuliere, J., Faraldo, M. M., Deugnier, M.-A., Shtutman, M., Ben-Ze'ev, A., Thiery, J. P., & Glukhova, M. a. (2005). Targeted activation of -catenin signaling in basal mammary epithelial cells affects mammary development and leads to hyperplasia. *Development*, *132*(2), 267–277.

Theis, M., Si, K., & Kandel, E. R. (2003). Two previously undescribed members of the mouse CPEB family of genes and their inducible expression in the principal cell layers of the hippocampus. *Proceedings of the National Academy of Sciences of the United States of America*, *100*(16), 9602–9607.

Thévenaz, P., & Unser, M. (2007). User-Friendly Semiautomated Assembly of Accurate Image Mosaics in Microscopy. *Microscopy Research and Technique*, *70*(3), 135–146.

Topisirovic, I., Svitkin, Y. V., Sonenberg, N., & Shatkin, A. J. (2011). Cap and cap-binding proteins in the control of gene expression. *Wiley interdisciplinary reviews. RNA*, *2*(2), 277–98.

Tremont, A., Lu, J., & Cole, J. T. (2017). Endocrine therapy for early breast cancer. *Expert Review of Anticancer Therapy*, *4*(5), 877–888.

Truitt, M. L., & Ruggero, D. (2016). New frontiers in translational control of the cancer genome. *Nature Reviews Cancer*, *16*(5), 288–304.

Turner, N., Tutt, A., & Ashworth, A. (2004). Hallmarks of 'BRCAness' in sporadic cancers. *Nature Reviews Cancer*, *4*(10), 814–819.

Uchida, N., ichi Hoshino, S., Imataka, H., Sonenberg, N., & Katada, T. (2002). A novel role of the mammalian GSPT/eRF3 associating with poly(A)-binding protein in cap/poly(A)-dependent translation. *Journal of Biological Chemistry*, *277*(52), 50286–50292.

Van Amerongen, R., Bowman, A. N., & Nusse, R. (2012). Developmental stage and time dictate the fate of Wnt/β-catenin- responsive stem cells in the mammary gland. *Cell Stem Cell*, *11*(3), 387–400.

Van Der Groep, P., Bouter, A., Van Der Zanden, R., Siccama, I., Menko, F. H., Gille, J. J. P., Van Kalken, C., Van Der Wall, E., Verheijen, R. H. M., & Van Diest, P. J. (2006). Distinction between hereditary and sporadic breast cancer on the basis of clinicopathological data. *Journal of Clinical Pathology*, *59*(6), 611–617.

Van Keymeulen, A., Fioramonti, M., Centonze, A., Bouvencourt, G., Achouri, Y., & Blanpain, C. (2017). Lineage-Restricted Mammary Stem Cells Sustain the Development, Homeostasis, and Regeneration of the Estrogen Receptor Positive Lineage. *Cell Reports*, *20*(7), 1525–1532.

Van Keymeulen, A., Lee, M. Y., Ousset, M., Brohée, S., Rorive, S., Giraddi, R. R., Wuidart, A., Bouvencourt, G., Dubois, C., Salmon, I., Sotiriou, C., Phillips, W. A., & Blanpain, C. (2015). Reactivation of multipotency by oncogenic PIK3CA induces breast tumour heterogeneity. *Nature*, *525*(7567), 119–123.

Van Keymeulen, A., Rocha, A. S., Ousset, M., Beck, B., Bouvencourt, G., Rock, J., Sharma, N., Dekoninck, S., & Blanpain, C. (2011). Distinct stem cells contribute to mammary gland development and maintenance. *Nature*, *479*(7372), 189–193.

Villanueva, E., Navarro, P., Rovira-Rigau, M., Sibilio, A., Méndez, R., & Fillat, C. (2017). Translational reprogramming in tumour cells can generate oncoselectivity in viral therapies. *Nature Communications*, *8*.

Visvader, J. E., & Stingl, J. (2014). Mammary stem cells and the differentiation hierarchy: current status and perspectives. *Genes & Development*, *28*(11), 1143–1158.

Wada, T., Nakashima, T., Hiroshi, N., & Penninger, J. M. (2006). RANKL-RANK signaling in osteoclastogenesis and bone disease. *Trends in Molecular Medicine*, *12*(1), 17–25.

Wahle, E., & Rüegsegger, U. (1999). 3'-End processing of pre-mRNA in eukaryotes. *FEMS Microbiology Reviews*, *23*(3), 277–295.

Walsh, M. C., & Choi, Y. (2003). Biology of the TRANCE axis. *Cytokine and Growth Factor Reviews*, *14*(3-4), 251–263.

Wan, L., Lu, X., Yuan, S., Wei, Y., Guo, F., Shen, M., Yuan, M., Chakrabarti, R., Hua, Y., Smith, H. A., Blanco, M. A., Chekmareva, M., Wu, H., Bronson, R. T., Haffty, B. G., Xing, Y., & Kang, Y. (2014). MTDH-SND1 Interaction Is Crucial for Expansion and Activity of Tumor-Initiating Cells in Diverse Oncogene- and Carcinogen-Induced Mammary Tumors. *Cancer Cell*, *26*(1), 92–105.

Watson, C. J. (2006). Key stages in mammary gland development Involution: Apoptosis and tissue remodelling that convert the mammary gland from milk factory to a quiescent organ. *Breast Cancer Research*, *8*(2), 1–5.

Weill, L., Belloc, E., Bava, F.-A., & Méndez, R. (2012). Translational control by changes in poly(A) tail length: recycling mRNAs. *Nature structural & molecular biology*, *19*(6), 577–85.

Widschwendter, M., Burnell, M., Fraser, L., Rosenthal, A. N., Philpott, S., Reisel, D., Dubeau, L., Cline, M., Pan, Y., Yi, P. C., Gareth Evans, D., Jacobs, I. J., Menon, U., Wood, C. E., & Dougall, W. C. (2015). Osteoprotegerin (OPG), The Endogenous Inhibitor of Receptor Activator of NF-κB Ligand (RANKL), is Dysregulated in BRCA Mutation Carriers. *EBioMedicine*, *2*(10), 1331–1339.

Wild, P., Rupp, N., Buhmann, J., Schüffler, P., Fuchs, T., & Ong, C. (2013). TMARKER: A free software toolkit for histopathological cell counting and staining estimation. *Journal of Pathology Informatics*, *4*(2), 2.

William J. Boyle, W. Scott Simonet, & David L. Lacey (2003). Osteoclast differentiation and activation. *Nature*, *423*(May), 337–342.

Williams, C. C., Jan, C. H., & Weissman, J. S. (2014). Targeting and plasticity of mitochondrial proteins revealed by proximity-specific ribosome profiling. *Science*, *346*(6210), 748–752.

Wolfe, A. L., Singh, K., Zhong, Y., Drewe, P., Rajasekhar, V. K., Sanghvi, V. R., Mavrakis, K. J., Jiang, M., Roderick, J. E., Van der Meulen, J., Schatz, J. H., Rodrigo, C. M., Zhao, C., Rondou, P., de Stanchina, E., Teruya-Feldstein, J., Kelliher, M. A., Speleman, F., Porco, J. A., Pelletier, J., Rätsch, G., & Wendel, H. G. (2014). RNA G-quadruplexes cause eIF4A-dependent oncogene translation in cancer. *Nature*, *513*(7516), 65–70.

Wurth, L., & Gebauer, F. (2015). RNA-binding proteins, multifaceted translational regulators in cancer. *Biochimica et Biophysica Acta - Gene Regulatory Mechanisms*, *1849*(7), 881–886.

Wurth, L., Papasaikas, P., Olmeda, D., Bley, N., Calvo, G. T., Guerrero, S., Cerezo-Wallis, D., Martinez-Useros, J., García-Fernández, M., Hüttelmaier, S., Soengas, M. S., & Gebauer, F. (2016). UNR/CSDE1 Drives a Post-transcriptional Program to Promote Melanoma Invasion and Metastasis. *Cancer Cell*, *30*(5), 694–707.

Yin, Y., Bai, R., Russell, R. G., Beildeck, M. E., Xie, Z., Kopelovich, L., & Glazer, R. I. (2005). Characterization of medroxyprogesterone and DMBA-induced multilineage mammary tumors by gene expression profiling. *Molecular Carcinogenesis*, *44*(1), 42–50.

Yoldi, G., Pellegrini, P., Trinidad, E. M., Cordero, A., Gomez-Miragaya, J., Serra-Musach, J., Dougall, W. C., Muñoz, P., Pujana, M. A., Planelles, L., & González-Suárez, E. (2016). RANK signaling blockade reduces breast cancer recurrence by inducing tumor cell differentiation. *Cancer Research*, *76*(19), 5857–5869.

Yun Kong, Y., Yoshida, H., Boyle, W. J., & Penniger, J. M. (1999). OPGL is a key regulator of osteoclastogenesis, lymphocyte development and lymph-node organogenesis. *Nature*, *397*(6717), 315–323.

Zardawi, S. J., O'Toole, S. A., Sutherland, R. L., & Musgrove, E. A. (2009). Dysregulation of Hedgehog, Wnt and Notch signalling pathways in breast cancer. *Histology and Histopathology*, *24*(3), 385–398.

Zhong, X., Xiao, Y., Chen, C., Wei, X., Hu, C., Ling, X., & Liu, X. (2015). MicroRNA-203-mediated posttranscriptional deregulation of CPEB4 contributes to colorectal cancer progression. *Biochemical and Biophysical Research Communications*, (pp. 4–11).

Zudaire, E., Gambardella, L., Kurcz, C., & Vermeren, S. (2011). A computational tool for quantitative analysis of vascular networks. *PLoS ONE*, *6*(11), 1–12.

Appendix

Appendix 1. Southern Blot probes

Southern Blot 3'probe

GGGCTTTGGTTAGGAAAAGGAAACACGCAACACATACACATTTTCCTAAATGCACCCTGACGCT
GAAGTAGTCATTCTCATAATAAATTTGGAAACTTAATATTTTATTTTATCACATAGCTACTCAG
AACTGAGTTTATGGAAGTACAACTTACACGACTTTGGACTTGTGTTCTCAGTGAGAGGATCTAC
AGTCTAAAGGGGAAGGAGACAACTCTGTGGAAGTTCTTGTCAGAGAAAACTTACTTGAACTAA
AACACCAGTAGAGATTTGAAAGTCTTATTTCTTTACAGGTAGCTGTCTCTGTCAATAGCAGTAT
TTGAGAGCATGGATGCCCTTATTTCCTTTAGGCATCTTTGATTATTTAGGCAAATTCTTGAATT
ATAACACTAGAACTTCATTTTTCAAAACCAAAGCCTTTATCATACAGAAATTACAGTGCATTTG
TGCCAATTCAGATACATAATATTATTTTGAAAGTCACTTCATATCTTTCTTGTGATTTAAAGTA
GAAGTTTTTATCTCTGAAAGTGGACAATTTAATAAATTCTTATATATAGCATACATCTCATACA
TAATTTATAACGCTAAAATGAAGTACTTGGGAATATTTGGTATATAAATTTTGGCTTATATGA
GGAGCAGTATCTTAGAATTTTTCCTTCAAAAGCATATTTAATCTCTTAAAGTATTTTCCATCAT
AGAAAGCCTTTACTCATTAATGGAAAACTAGAAACGTAAATTTTAATACCACCAGCAGTAATG
CAAA

Southern Blot 5'probe

GCCGGAACATCCAGAATAGACCAGGTAGGCTGCACAGTAGTGTATGTTTCTCAGGATCGCGGCT
AGGAGTTTAGTATTTACATTATGAGTAGGAGTGAACACTTGCGTTTCACTTATGCCATTTAAGC
ATATGTCGGAGATTATTAAAGCAATTTGAGTTTTTCAATATCGTTTGATCTAAACTCTTCAATA
TGTTTCTGTTCAAATTTAAAAGATTTGTAGTCATATTTTGAAATCATAACAAATGTGTTTATTA
CAATGAGTTATATATCCAAGAGCACCTGACTTTAAACATCATTCAAACTAAACAGATACTGTCT
TTCTTTCAGAATTATCTGCATTTAAAATACAGCCTCATATGTTTATTTAACATCCAGCTTTACA
TTTAATGTTTTAAGAAATCTTCCAGTCAATGTTTGTCATGAAGTTTGATGCATTTGTTTTGCAG
TATATCTCTGAATAGCTCCTTTTTTTTTATTGTTTTTTAAACTTTTATAAAAAAGCCTTATAGCA
TAGTATTTTTACTCTACATTTTATTATTGCTTTTATCCTACAACTTATCTTCAGTATATTTGTGA
TTTAGAATGCTAAATCTGTCTTTCTGCAGACTGAATTTGAGTGTATACCGGTCCCAGGTGATGA
GGATTAATAAAGGAGGGCGTAGAAACCTCAGGTCTTACATAAGAGGGAGGGGCTTTTCCTATA
GATCCCAAGTCTGACCTTCATTTGTAAGTTAAGTGAGTGGATCTTTGTAATCCATAGCTAAGGC
TCTTCCTCAAGGAATGTAGCAGCGTGA

Appendix 2. Tables

Table 1: Sequence of the primers used for *Cpeb2* genotyping

Name	Sequence
Minus_Fw1	tttttctgtcttccaggatcg
Minus_Fw2	aaggcagttctcagttgggg
Minus_Rv	tgtcttgactccccttgtga
Lox_Fw	ggatatgggaatgtgagcacct
Lox_Rv	acacattttcagttgcttcaca

Table 2: Primers used for qPCR

	Fw	Rv
Cpeb1	CGCTGCAAAGAGGTACAGGT	CAAGGCACCAACAAACACC
Cpeb2	GCTTGAATATGCACTCTCTGGAAAA	GCTCAGACGACCCTTGAGAG
Cpeb3	CGTTTGTACGGTGGTGTTTG	CCGTTTGTCAATGTCGTTGT
Cpeb4	CCAGAATGGGGAGAGAGTGG	CGGAAACTAGCTGTGATCTCATCT
Gapdh	CTTCACCACCATGGAGGAGGC	GGCATGGACTGTGGTCATGAG
Pgr	ATGGTCCTTGGAGGTCGTAAG	AGAGCAACACCGTCAAGGG
Esr1	TGGCTACCATTATGGGGTCTG	AACTCTTCCTCCGGTTCTTGTC
Tnfsf11	CAGCCATTTGCACACCTCAC	AGAGGACAGAGTGACTTTATGGG
Wnt4	AGGCCATCTTGACACACATG	ACGTCTTTACCTCGCAGGAG
Ccnd1	CTGCAAATGGAACTGCTTCTGGTGA	AGCAGGAGAGGAAGTTGTTGGGGCT
Stat5a	TTGACTCTCCGGACCGAAAC	CCAGGGACCGAATGGAGAAA

Table 3: High confidence RIP-targets

symbol	padj	symbol	padj	symbol	padj	symbol	padj
Prkar2b	9,19E-06	*Aplnr*	0,0128	*Cdh5*	0,0347	*Etl4*	0,0530
Plxna2	1,65E-05	*Dapk1*	0,0146	*Gfod1*	0,0347	*Rgs2*	0,0530
Cmip	5,10E-04	*Jag1*	0,0148	*Nfya*	0,0347	*Fli1*	0,0530
Creb1	5,10E-04	*Aqp7*	0,0167	*Ppp2r5e*	0,0347	*Klhl12*	0,0530
Atp2b4	5,10E-04	*Csnk1g2*	0,0173	*Sgms1*	0,0347	*Rad54l2*	0,0546
Brd3	5,10E-04	*Pkn2*	0,0173	*Sox18*	0,0347	*Rnf152*	0,0546
Kras	5,36E-04	*Pdzd2*	0,0175	*Zmpste24*	0,0357	*Lrrc8c*	0,0558
Taf1	5,36E-04	*Adgrl2*	0,0183	*Zmiz1*	0,0366	*Tmem2*	0,0569
Pou3f1	1,01E-03	*Kctd12*	0,0233	*Lrp6*	0,0366	*Helz*	0,0573
Fzd2	1,01E-03	*Tshz1*	0,0233	*Atp2b1*	0,0366	*Ets1*	0,0613
Rbms2	1,02E-03	*Tiparp*	0,0271	*Rala*	0,0377	*Vgll4*	0,0672
Stc1	1,04E-03	*Tm7sf3*	0,0271	*Cpeb3*	0,0377	*Kit*	0,0680
Cpeb2	1,19E-03	*Tnrc18*	0,0272	*Klf11*	0,0377	*Nrarp*	0,0716
Cadm4	1,96E-03	*Thsd7a*	0,0277	*Mef2c*	0,0395	Tmtc1	0,0750
Shank3	2,24E-03	*Insr*	0,0287	*Tob2*	0,0395	Plscr4	0,0750
Ccnd1	2,24E-03	*Ifnlr1*	0,0287	*Cdc40*	0,0398	Zbtb43	0,0774
Efnb1	3,43E-03	*Kcna1*	0,0288	*Foxj2*	0,0405	*Lyve1*	0,0781
Enpp4	3,43E-03	*Zcchc24*	0,0291	*Crebrf*	0,0405	*Secisbp2l*	0,0803
Arhgap19	3,43E-03	*Cux1*	0,0292	*Rpn1*	0,0405	*Nlk*	0,0803
Elovl4	3,57E-03	*Pcdh19*	0,0292	*Rpgrip1*	0,0405	*Mal*	0,0804
Mpz	3,68E-03	*Nectin1*	0,0293	*Sipa1l2*	0,0405	*Megf9*	0,0816
Anp32a	3,68E-03	*Etv6*	0,0293	*Gcnt1*	0,0405	*Chl1*	0,0831
Ankrd12	3,68E-03	*Setd5*	0,0293	*Sp1*	0,0407	*Plekha2*	0,0870
Msl2	3,71E-03	*Adrbk1*	0,0293	*Spop*	0,0407	*Sertad2*	0,0870
Sema6a	3,91E-03	*Kmt2e*	0,0293	*Mef2a*	0,0427	*Efna1*	0,0873
Prdm16	3,91E-03	*Dcp1a*	0,0293	*Cdk6*	0,0429	*Sirpa*	0,0873
Limch1	7,03E-03	*Oraov1*	0,0293	*Ddit4*	0,0453	*Slfn5*	0,0878
Stard4	7,66E-03	*Nova2*	0,0293	*Rbm47*	0,0453	*Efnb2*	0,0882
Flt1	8,61E-03	*Sfmbt1*	0,0293	*Ugcg*	0,0459	*Tmod2*	0,0893
Cadm1	8,61E-03	*Pik3c2b*	0,0293	*Atxn3*	0,0468	*Eif4ebp2*	0,0902
Kctd12b	8,61E-03	*Vangl2*	0,0293	*Efr3a*	0,0475	*Gpm6b*	0,0928
Elk3	9,05E-03	*Sppl3*	0,0306	*Prox1*	0,0490	*Api5*	0,0929
Kdelc2	9,05E-03	*Tmx3*	0,0306	*Ndst1*	0,0492	*Bmp2*	0,0929
Pcdh17	9,05E-03	*She*	0,0306	*F2r*	0,0498	*Wnt5a*	0,0953
Hdac7	0,0100	*Armc10*	0,0306	*Sacm1l*	0,0501	*Ago1*	0,0953
St8sia4	0,0100	*Sostdc1*	0,0306	*4931406P16Rik*	0,0512	*Spcs2*	0,0959
Stard13	0,0107	*Smim15*	0,0309	*Csnk1g3*	0,0514	*Pank3*	0,0959
Glcci1	0,0127	*Gmeb1*	0,0309	*Vasn*	0,0514	*Sc5d*	0,0959
Slc6a6	0,0128	*Nfyb*	0,0309	*Wsb1*	0,0520	*Zmynd8*	0,0959
Igfbp4	0,0128	*Kcnj2*	0,0329	*Fam101b*	0,0527	*Atg5*	0,0989
Tbl1xr1	0,0128	*Supt16*	0,0339	*Ptk7*	0,0527		
Plekhg1	0,0128	*Herpud2*	0,0339	*Vezf1*	0,0530		

Appendix 3. List of publications

Pascual R., Martín J., Salvador F., Reina O., Suñer C., Fernández-Miranda G., Gomis R. and Méndez R. Post-transcriptional regulation of estrogen signaling by the RNA-binding protein CPEB2 controls mammary gland homeostasis and luminal tumor development. Manuscript in preparation.

Segura-Morales C.*, **Pascual R.*** , Bellora N. , Eyras E. and Méndez R. Spindle-localized mRNA translation mediated by CPEB1 and CPEB4 controls mitotic progression. In revision in *Nature Communications*. *Equal contribution.

Doménech E., Maestre C., Esteban-Martínez L., Partida D., **Pascual R.**, Fernández-Miranda G., Seco E., Campos-Olivas R., Pérez M., Megias D., Allen K, López M., Saha A.K., Velasco G., Rial E., Méndez R., Boya P., Salazar-Roa M., Malumbres M. (2015). AMPK and PFKFB3 mediate glycolysis and survival in response to mitophagy during mitotic arrest. *Nat Cell Biol.*